NANOTECHNOLOGY CHARACTERIZATION LABORATORY

Prepared for Dr. Mark Kester, Penn State University

Ceramide Liposomes
NCL200702A
February 2007

Nanotechnology Characterization Laboratory
National Cancer Institute at Frederick
SAIC-Frederick, Inc.
Frederick, MD 21702
(301) 846-6939 • ncl@ncifcrf.gov
http://ncl.cancer.gov

TABLE OF CONTENTS

Executive Summary

The objective of the Penn State University-NCL collaboration was to characterize C6-ceramide liposomes as a drug delivery platform. Ceramide, an endogenous shingolipid derived membrane component, has been shown to have antiproliferative and proapoptotic properties in cancer cell lines. Ceramide has also been reported to have additive anticancer effects when combined with current chemotherapeutics *in vitro*. Liposomal formulation of ceramide was shown to enhance ceramide's potency against cancer cells *in vitro*, and liposomal ceramide has proven anticancer activity in murine breast adenocarcinoma models. The nanomaterials submitted for testing were ghost liposome (NCL48) and ceramide liposome (NCL49). Two batches of these samples were submitted for characterization. NCL studies conducted on the ceramide liposome drug delivery platform can be divided into four main categories: physico-chemical, *in vitro* toxicology, *in vitro* immunological, and *in vivo* ADME toxicology.

Physico-chemical Characterization
Hydrodynamic size as a function of sample concentration, media, temperature, freeze-thaw cycles, lyophilization, and short and long-term stability were measured, as well as zeta potential.

Additionally, fractionation methods, such as Size Exclusion Chromatography (SEC) and Asymmetric Field Flow Fractionation (AFFF), and Atomic Force Microscopy (AFM) were used to determine particle size.

Hydrodynamic sizes for the first batch of liposomes, as measured by batch-mode Dynamic Light Scattering (DLS), were 80 nm and 94 nm for NCL48-1 and NCL49-1, respectively (the number after the hyphen indicates batch number).

The liposome particles in the second batch are approximately 30 nm *larger* in size, as determined by batch-mode DLS, than those in the first batch.

In Vitro Toxicology

The ghost liposome (NCL48-1) was determined to be nontoxic, while the ceramide loaded liposome (NCL49-1) was determined to be moderately toxic to human hepatocarcinoma cells (HEP G2). The IC_{50} of NCL49-1 in the liver cells was 39μg ceramide/mL. NCL49-1 cytotoxicity in liver cells appeared to be caspase 3 independent, while cytotoxicity in LLC-PK1 porcine kidney cells was associated with caspase 3 dependent apoptosis.

In Vitro Immunology

Evaluation of nanoparticle blood contact properties included study of the particle effects on coagulation pathways and the integrity of blood cellular components. Analysis of the first batch of liposomes demonstrated that neither ghost liposome (NCL48-1) nor ceramide loaded liposome (NCL49-1) induced platelet activation (NCL protocol ITA-2) or interfered with collagen induced platelet aggregation at the maximum concentrations tested.

Additionally, NCL48-1 and NCL49-1 did not perturb plasma coagulation, as measured by prothrombin time (PT), activated partial thromboplastin time (APTT), thrombin and reptilase times. Both NCL48-1 and 49-1 where found to be slightly hemolytic at high concentrations (ITA-1).

The second batch of liposomes was compared with the first in terms of hemolysis (ITA-1) and platelet aggregation (ITA-2). NCL48-2 was found to be less hemolytic than NCL48-1 (the first batch). Further studies of complement activation (ITA-5), coagulation (ITA-12), CFU-GM (ITA-3), leukocyte proliferation (ITA-6), oxidative burst (ITA-7), chemotaxis (ITA-8) and phagocytosis (ITA-9) were conducted on this batch of samples at both high and low particle concentrations. NCL48-2 and NCL49-2 were observed to cause complement activation, suppression of CFU-GM formation, inhibition of PHA-M-induced leukocyte proliferation, and a slight reduction of zymosan uptake by macrophages.

In Vivo ADME Toxicology

Acute toxicology studies in rats for the ceramide liposome were negative for all signs of systemic toxicity, at the maximum intravenous dose achievable. No biologically significant changes in mortality, body weight, organ weight, clinical chemistry, hematology, gross pathology, or histology were observed between control and treatment groups.

Nanoparticle Description

The lead therapeutic candidate for this study, NCL49, is a liposome associated with 30% C6-ceramide. NCL48 is a control empty or “ghost” liposome. The liposomes are composed of 1,2-Distearoyl-*sn*-Glycero-3-Phosphocholine (DSPC), 1,2-Dioleoyl-*sn*-Glycero-3-Phosphoethanolamine (DOPE), PEG(2000)- 1,2-Distearoyl-*sn*-Glycero-3-Phosphoethanolamine (DSPE), and PEG(750)-C8.

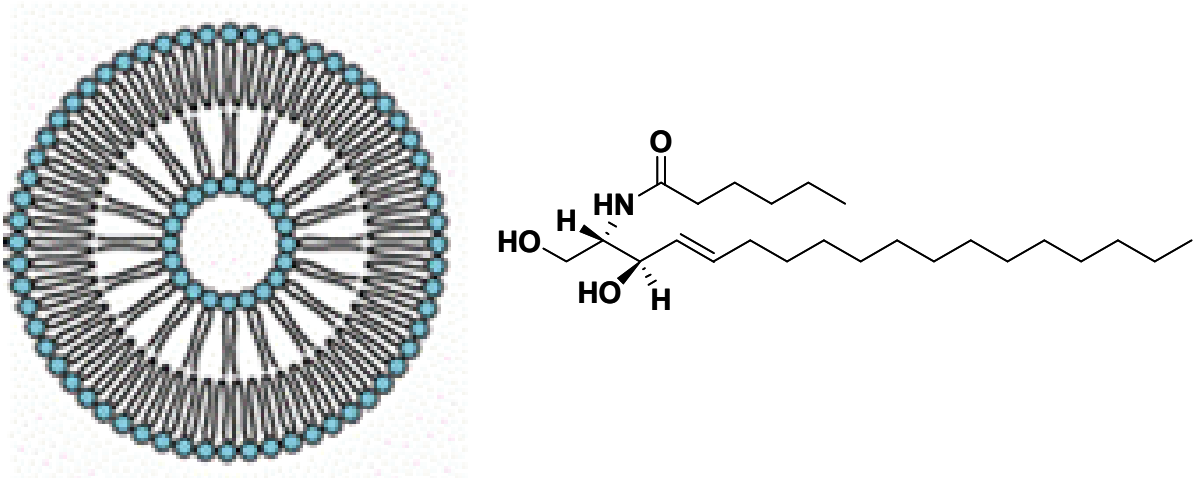

Liposome C6-Ceramide

Figure 1. Schematic illustration of a liposome and the molecular structure of ceramide.

Physico-Chemical Characterization

Section Summary

The lead therapeutic candidate in this project was a ceramide liposome (NCL49). Physical characterization was carried out on this sample along with the corresponding control liposome without ceramide (NCL48). The nominal hydrodynamic diameters, as measured by batch-mode Dynamic Light Scattering (DLS), were 80 nm for NCL48-1 and 94 nm for NCL49-1. Hydrodynamic size as a function of sample concentration, media, temperature, freeze-thaw cycles, lyophilization and short-term storage stability were also measured as well as zeta potential. Additionally, Size Exclusion Chromatography (SEC), Asymmetric Field Flow Fractionation (AFFF), and Atomic Force Microscopy (AFM) were used to determine the size.

A second batch of liposomal ceramide preparation (NCL49-2) along with the corresponding control liposomes without ceramide (NCL48-2) was received and characterized. Physico-chemical characterization was carried out on these samples and compared to the first batch of samples (NCL48-1, NCL49-1) to measure batch-to-batch consistency. The characterization included measuring hydrodynamic size via Dynamic Light Scattering (DLS) as a function of sample concentration, media, temperature, pH, and freeze-thaw cycle. The long-term and short-term stability and zeta potential were also measured with DLS. Additionally, Size Exclusion Chromatography (SEC), a fractionation method, was used and the size of the fractionated sample was measured using a Multi-Angle Laser Light Scattering (MALLS) detector in flow mode.

The main difference between the batches of liposomes was in the DLS-measured hydrodynamic size. Hydrodynamic sizes for the second batch of liposomes, as measured by batch-mode DLS, were 110 nm and 120 nm for NCL48-2 and NCL49-2, respectively. This corresponds to a ~30 nm *increase* in size compared to the first batch.

Hydrodynamic Size/Size Distribution via Dynamic Light Scattering (DLS)

Design and Methods

Hydrodynamic size (diameter) of the liposome samples was measured in aqueous solutions using DLS at 25° C. This measurement included the intensity-weighted average diameter over all size populations (Z-avg), the polydispersity index (PdI), the volume-weighted average diameter over the major volume peak (Vol-Peak), and its percentage of the total population (Vol-Peak %Vol). An instrument with a back scattering detector was used for these measurements in batch mode (i.e. without fractionation). Samples were diluted in either PBS or saline (154 mM NaCl) to a final concentration of 1 mg/mL. For this purpose, 67 or 40 μL stock for the first and second batch, respectively, was brought up to a final volume of 1 mL in the appropriate solvent. A minimum of seven measurements were taken for each sample (as is, no filtration) in a disposable low volume (polystyrene) cuvette.

Results

Table 1. Hydrodynamic sizes in PBS and saline for two batches of NCL48 and NCL49.

Sample	Media	Z-avg	PdI	Vol-Peak	Vol-Peak
		(nm)		(nm)	%Vol
NCL48-1	Saline	99.1 (0.5)	0.174 (0.011)	**80.0 (3.8)**	99.8 (0.4)
NCL48-2	Saline	117.8 (0.9)	0.104 (0.011)	**110.7 (1.5)**	100 (0)
NCL48-1	PBS	99.6 (0.4)	0.174 (0.019)	**77.3 (3.3)**	99.8 (0.7)
NCL48-2	PBS	118.6 (0.8)	0.114 (0.012)	**109.9 (1.4)**	100 (0)
NCL49-1	Saline	109.0 (2.2)	0.168 (0.026)	**93.6 (1.7)**	99.0 (1.1)
NCL49-2	Saline	128.1 (2.2)	0.155 (0.026)	**119.6 (1.8)**	98.0 (2)
NCL49-1	PBS	111.0 (1.4)	0.189 (0.015)	**93.6 (1.4)**	98.4 (1.3)
NCL49-2	PBS	130.5 (2.1)	0.162 (0.017)	**122.6 (3.4)**	100 (0)

Note: The standard deviations (N > 7) are given in parenthesis.

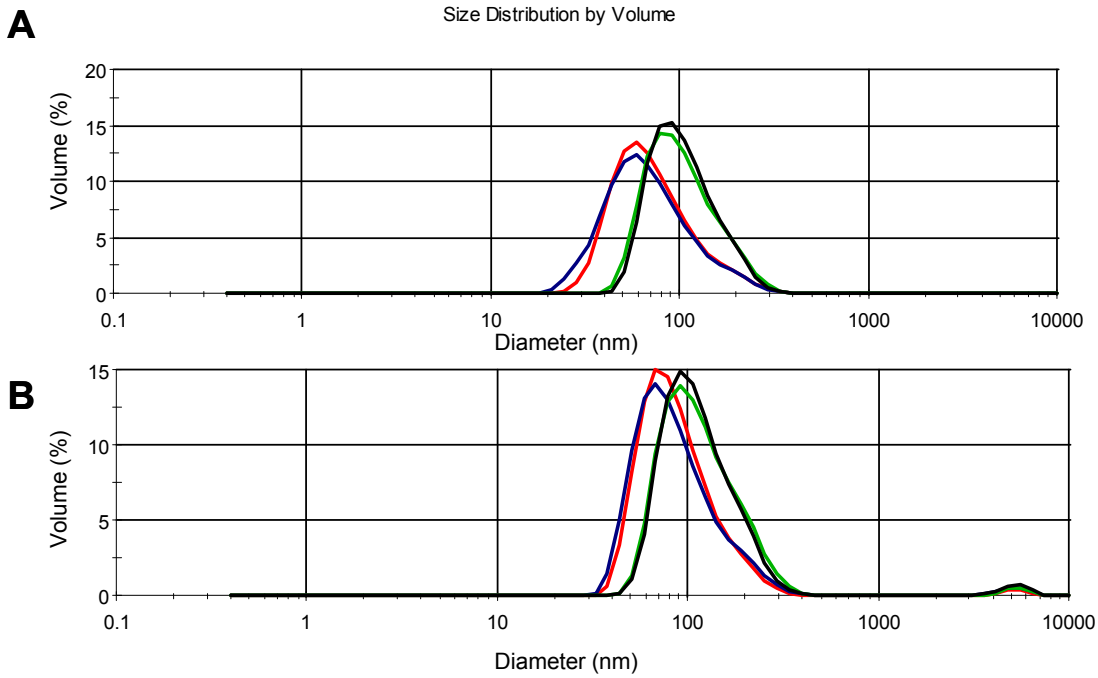

Figure 2. Comparison of particle size of two batches of NCL48 and NCL49. The average size by volume distributions (each line is the average of at least seven measurements) for both batches of (A) NCL48 and (B) NCL49 in PBS and saline (154 mM NaCl).

Analysis and Conclusions

The batches of liposomes differed in initial (i.e. stock) concentration. The first batch was prepared to a stock concentration of 15 mg/mL and the second batch was prepared to a stock concentration of 25 mg/mL. The second batch was prepared to provide a relevant C6-ceramide concentration in a single dose for *in vivo* studies. Both sample batches were prepared in saline. After running both samples through size characterization under similar conditions, the major observed difference between the two sample batches was in the hydrodynamic size of the particles. The particles in the second batch of NCL48 and NCL49 (Table 1, Figure 1), regardless of solvent, are ~30 nm larger than those in the first batch..

As can be observed from a comparison of panels A and B in Figure 2, NCL49 (the ceramide liposome) is approximately 30 nm larger than NCL48 (the ghost liposome).

Hydrodynamic Size vs. Solvent

Design and Methods

The hydrodynamic size (diameter) of the liposome samples was measured in aqueous solutions using batch-mode DLS at 25° C. Samples were diluted either in water, 10 mM NaCl, PBS, or saline (154 mM NaCl) to give final concentrations of 1 mg/mL. A minimum of seven measurements were taken for each sample.

Results

Table 2. Summary of the effect of solvent on the hydrodynamic size for NCL48 and NCL49.

Sample	Media	Z-avg (nm)	PdI	Vol-Peak (nm)	Vol-Peak %Vol
NCL48-1	Saline	99.1 (0.5)	0.174 (0.011)	80.0 (3.8)	99.8 (0.4)
NCL48-1	PBS	99.6 (0.4)	0.174 (0.019)	77.3 (3.3)	99.8 (0.7)
NCL49-1	Saline	109.0 (2.2)	0.168 (0.026)	93.6 (1.7)	99.0 (1.1)
NCL49-1	PBS	111.0 (1.4)	0.189 (0.015)	93.6 (1.4)	98.4 (1.3)
NCL48-2	Water	113.4 (0.9)	0.162 (0.009)	99.8 (3.2)	100 (0)
NCL48-2	10 mM NaCl	112.3 (0.8)	0.149 (0.006)	102.5 (2.0)	100 (0)
NCL48-2	PBS	118.6 (0.8)	0.114 (0.012)	109.9 (1.4)	100 (0)
NCL48-2	Saline	117.8 (0.9)	0.104 (0.011)	110.7 (1.5)	100 (0)
NCL49-2	Water	114.6 (2.6)	0.269 (0.047)	88.7 (2.4)	96 (2)
NCL49-2	10 mM NaCl	115.1 (3.6)	0.233 (0.030)	93.6 (2.3)	98 (2)
NCL49-2	PBS	130.5 (2.1)	0.162 (0.017)	122.6 (3.4)	100 (0)
NCL49-2	Saline	128.1 (2.2)	0.155 (0.026)	119.6 (1.8)	98 (2)

Note: The standard deviations (N > 7) are given in parenthesis.

Analysis and Conclusions

The diameters of the first batch of liposomes (NCL48-1 and NCL49-1) are largely independent of dilution media in PBS and saline (154 mM NaCl). NCL49-1 is slightly larger (~10 nm) than NCL48-1 in both examined media.

For NCL48-2, studied in H_20, 10 mM NaCl, and saline (154 mM NaCl), there is a slight increase in size as the ionic strength increases, though as in the first batch no significant difference in size in PBS and saline is observed. For NCL49-2, the size is relatively constant for the lower ionic strength media (H_20 and 10 mM NaCl) but increases by ~30 nm for the

higher ionic strength media (PBS and saline). NCL49-2 is approximately 10 nm larger than NCL48-2 in all studied media. This size difference between the ceramide liposome and ghost liposome is similar to that observed for the first batch of liposomes. It is interesting to note that a larger-sized population appears and may be liposomal aggregates.

Hydrodynamic Size vs. Concentration

Design and Methods

The effect of concentration on size was studied via batch-mode DLS measurements at 25 °C. Samples were diluted in saline (154 mM NaCl) to give a 0.1, 1, and 10 mg/mL final concentrations of NCL48-1 and NCL49-1, and 0.25, 2.5, and 25 mg/mL final concentrations of NCL48-2 and NCL49-2. A minimum of ten measurements were taken for each sample.

Results

Table 3. Summary of the effect of concentration on hydrodynamic size for NCL48-1 and NCL49-1 in PBS, and NCL48-2 and NCL49-2 in saline.

Sample	Conc.	Z-avg	PdI	Vol-Peak	Vol-Peak
	(mg/mL)	(nm)		(nm)	%Vol
NCL48-1	0.1	101.0 (1.1)	0.181 (0.008)	77.8 (3.9)	100 (0)
NCL48-1	1	99.6 (0.4)	0.174 (0.019)	77.3 (3.3)	99.8 (0.7)
NCL48-1	10	102.0 (0.7)	0.203 (0.005)	72.5 (5.2)	100 (0)
NCL49-1	0.1	110.0 (2.6)	0.178 (0.023)	93.9 (1.5)	98.8 (1.6)
NCL49-1	1	111.0 (1.4)	0.189 (0.015)	93.6 (1.4)	98.4 (1.3)
NCL49-1	10	118.0 (1.2)	0.202 (0.015)	102.0 (3.8)	98.8 (1.4)
NCL48-2	*0.25*	116.8 (0.6)	0.105 (0.014)	109.0 (1.8)	100 (0)
NCL48-2	*2.5*	117.9 (0.5)	0.106 (0.008)	110.6 (1.1)	100 (0)
NCL48-2	*25*	133.2 (0.7)	0.145 (0.011)	128.8 (6.1)	100 (0)
NCL49-2	*0.25*	122.9 (2.5)	0.122 (0.026)	116.0 (1.9)	100 (0)
NCL49-2	*2.5*	127.9 (3.7)	0.142 (0.028)	121.4 (3.2)	100 (0)
NCL49-2	*25*	149.3 (1.8)	0.196 (0.007)	150.1 (6.1)	100 (0)

Note: The standard deviations (N>10) are given in parenthesis.

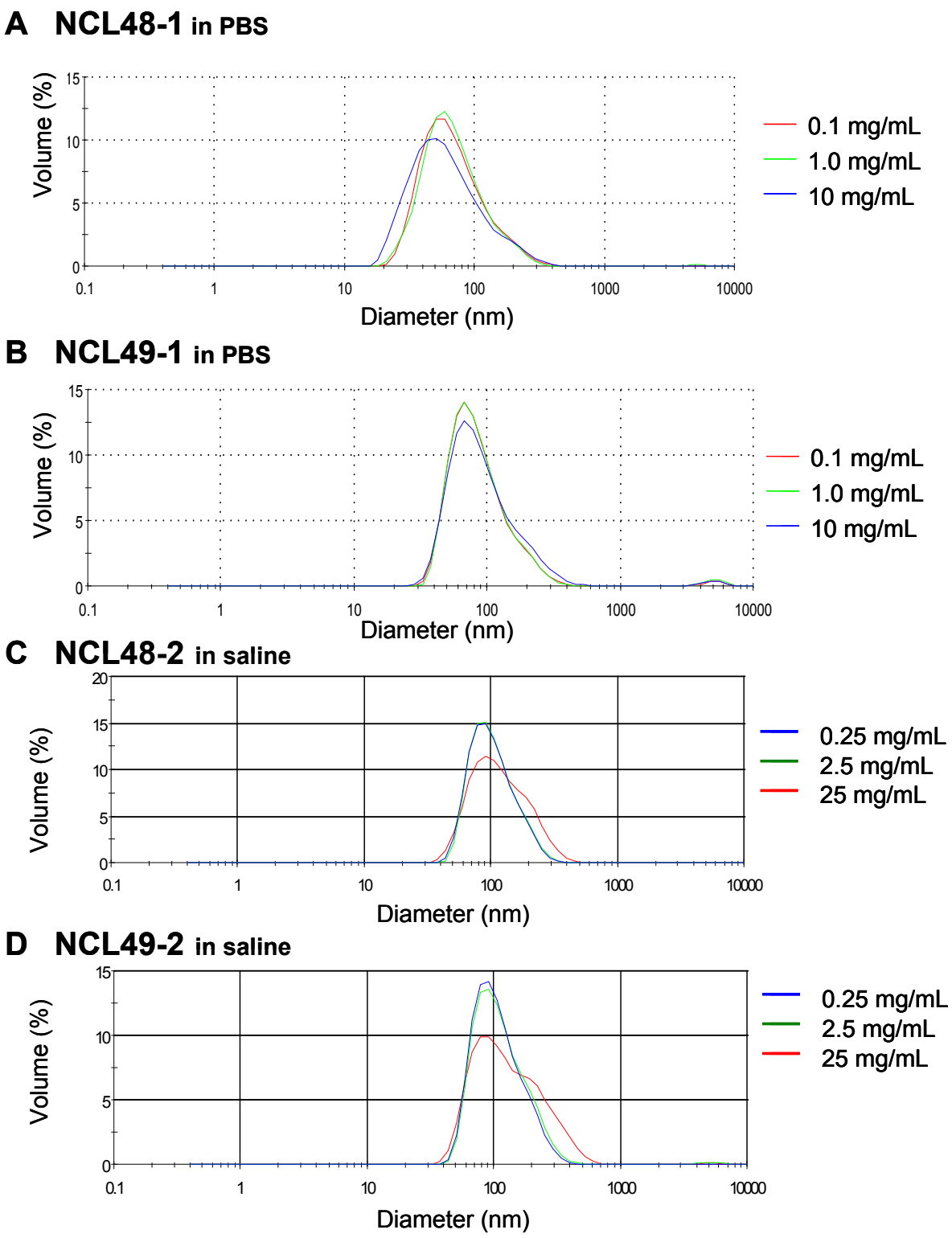

Figure 3. The effect of concentration on hydrodynamic size for NCL48-1 and NCL49-1 in PBS, and NCL48-2 and NCL49-2 in saline. The average size by volume distributions (each line is the average of at least seven measurements) for (A) NCL48-1 and (B) NCL49-1 in PBS, and (C) NCL48-2 and (D) NCL49-2 in saline, all at 3 different concentrations.

Analysis and Conclusions

For NCL48-1, there is a slight decrease in size for the 10 mg/mL sample compared to the 0.1 and 1 mg/mL samples which show no concentration dependence. For NCL49-1, there is a slight increase in size for the 10 mg/mL sample compared to the 0.1 and 1 mg/mL samples, which show no concentration dependence.

For NCL48-2 and NCL49-2, there was a slight increase in size for the 25 mg/mL sample compared to the 0.25 and 2.5 mg/mL samples which show no concentration dependence.

Over certain concentration ranges, concentration can affect specific viscosity. The high concentration samples (10 mg/mL for NCL48-1 and NCL49-1 and 25 mg/mL for NCL48-2 and NCL49-2) may be more viscous than the low concentration samples and this could contribute to higher measured hydrodynamic sizes.

Thermal Stability: Hydrodynamic Size vs. Temperature in PBS

Design and Methods

The thermal stability of NCL48 and NCL49 were measured by batch-mode DLS over a temperature range of 20 – 60 ºC. Samples were diluted in PBS to give a final concentration of 1 mg/mL. Samples (1 mL) were placed into a glass cuvette and capped with a polystyrene cap. Samples were equilibrated at each temperature for 10 minutes before a minimum of ten measurements were taken.

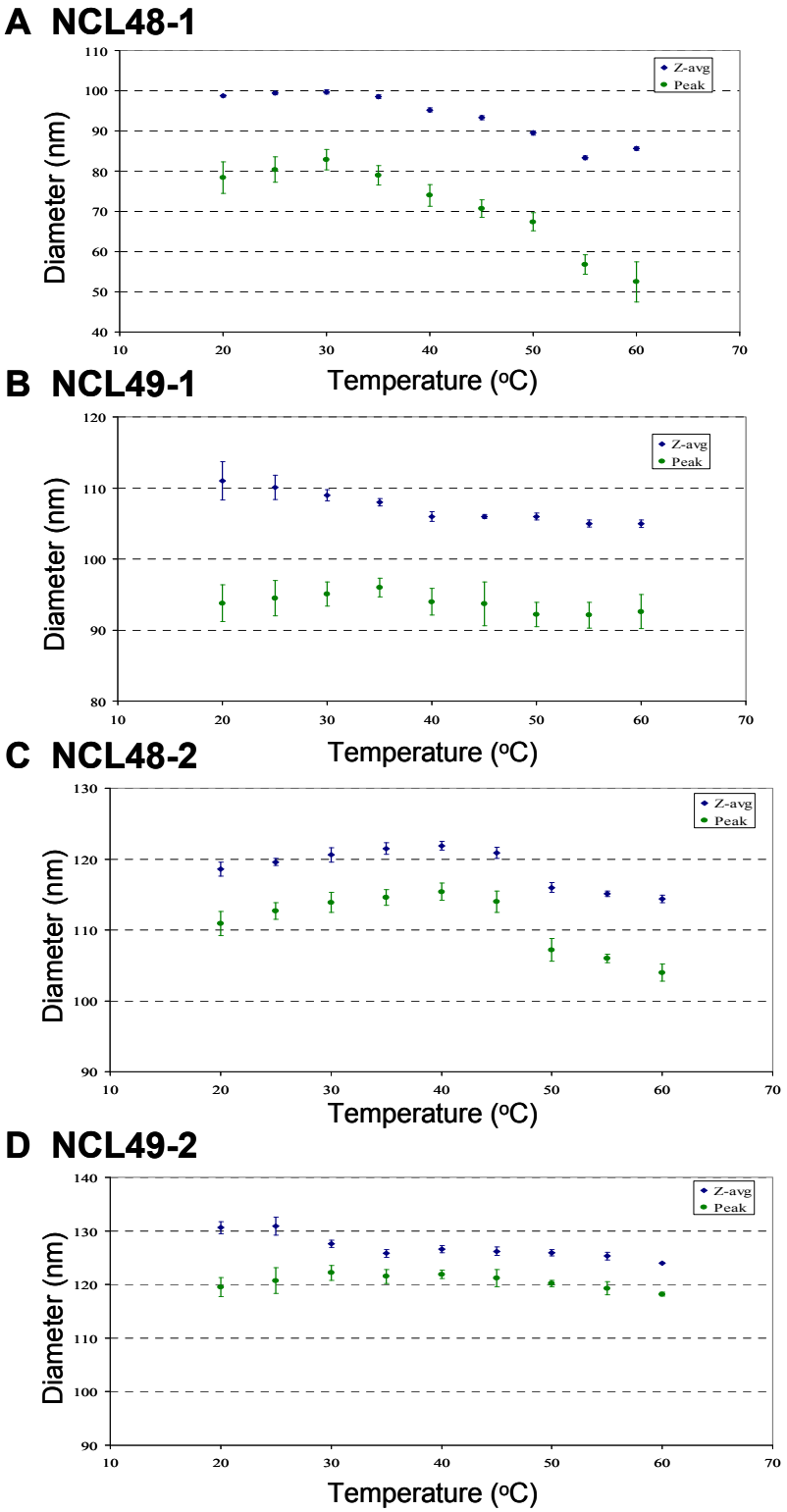

Figure 4. The hydrodynamic volume-weighted size and Z-avg size as a function of temperature. (A) NCL48-1, (B) NCL49-1, (C) NCL48-2 and (D) NCL49-2. "Peak" indicates the volume-weighted peak. Error bars are standard deviations based on at least 10 measurements per temperature.

Analysis and Conclusions

The general trend for the volume weighted peak for NCL48-1 is to remain fairly constant up to 35 ºC, after which it decreases in size up to 60 ºC (Figure 4 panel A). The Z-avg values follow a similar trend. The volume weighted peak for NCL49-1 remains fairly independent of temperature. A very slight decrease in the Z-avg values is observed for NCL49-1 in the temperature range studied (Figure 4 panel B).

The general trend for the volume-weighted peak for NCL48-2 is a slight increase up to 40 ºC followed by a decrease in size to 60 ºC (Figure 4 panel C). The Z-avg values follow a similar trend. The volume-weighted for NCL49-2 remains fairly constant. A very slight decrease in the Z-avg values is observed for NCL49-2 over the temperature range studied (Figure 4 panel D).

Long-Term Storage Stability

Design and Methods

Long-term storage stability is defined by diluting the stock solution (stored at 4 °C) periodically and measuring size. For this purpose, the stock was diluted in saline (154 mM NaCl) to give a final concentration of 1 mg/mL as described before. Sample size was measured at predetermined times and consisted of a 10 minute equilibration at 25 °C before a minimum of ten measurements were taken.

Results

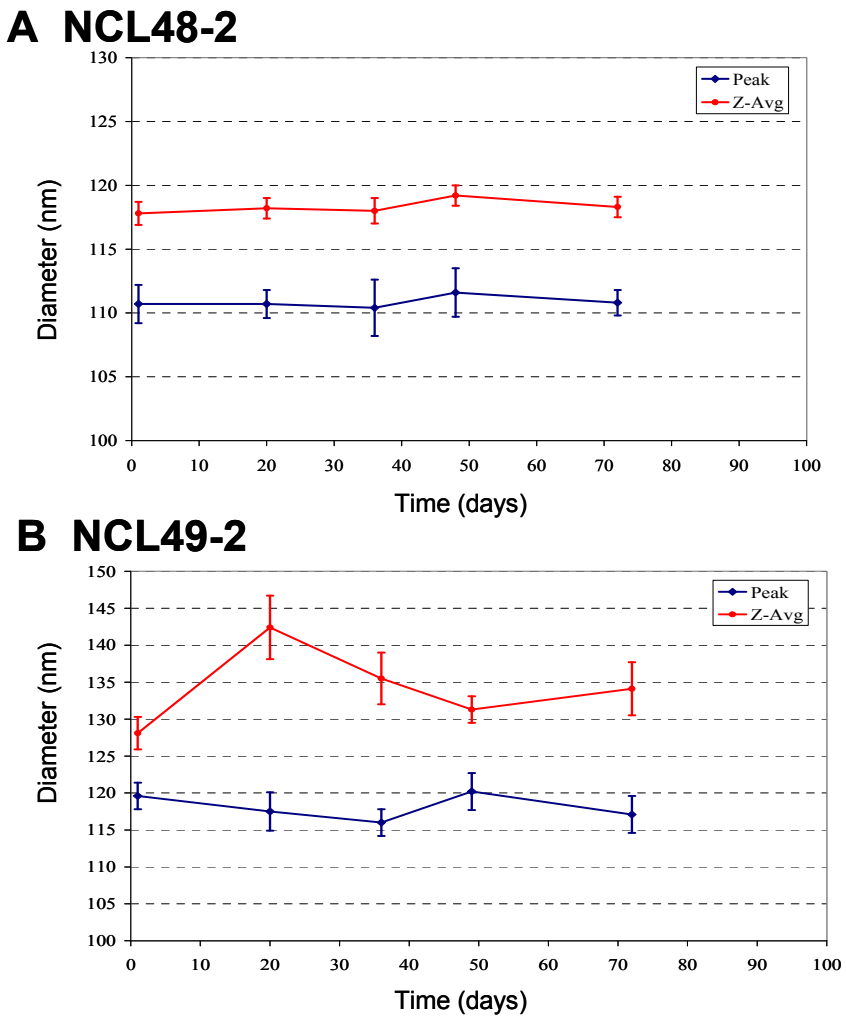

Figure 5. The long-term stability, as measured by batch-mode DLS of (A) NCL48-2 and (B) NCL49-2 in saline as a function of time.

Analysis and Conclusions

The results show that there is no appreciable change in the volume-weighted peak (denoted 'Peak' in figures) or the Z-Avg up to 70 days for NCL48-2 (Figure 5 panel A). While there is no change for the volume-weighted distribution for NCL49-2 (Figure 5 panel B), the Z-Avg size changes with time (Figure 5 panel B).

Short-Term Storage Stability

Design and Methods

Short-term storage stability is defined by diluting the stock solution (stored at 4°C) in saline (154 mM NaCl) to give a final concentration of 1 mg/mL and storing the samples (1 mL) in low volume disposable polystyrene cuvettes (capped and sealed with parafilm) at room temperature (RT), 4 °C, or 37 °C. Sample size was measured at predetermined times and consisted of a 10 minute equilibration at 25 °C before a minimum of ten measurements were taken.

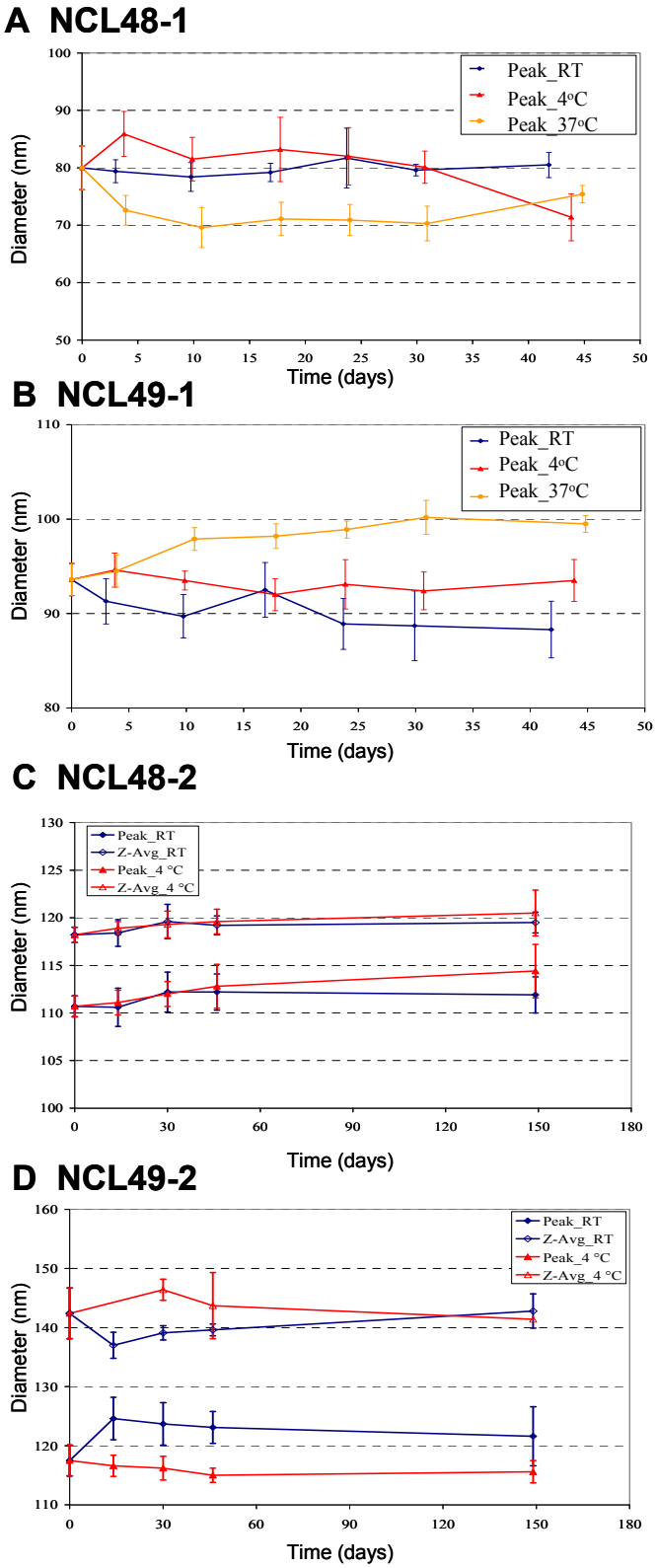

Figure 6. The short-term stability, as measured by batch-mode DLS for (A) NCL48-1, (B) NCL49-1, (C) NCL48-2, and (D) NCL49-2 in saline as a function of time.

Analysis and Conclusions

For the NCL48-1 samples diluted in saline, no appreciable change in the volume-weighted peak was observed at all temperatures studied up to 45 days (Figure 6 panel A). A similar trend was observed for the Z-Avg size (data not shown).

The NCL49-1 samples diluted in saline incubated at 4 ºC showed no significant change up to 45 days (Figure 6 panel B). The RT incubated sample diluted in saline also showed no size-dependence with time. However, a slight increase in size was observed for the 37 ºC incubated sample diluted in saline (Figure 6 panel B). A similar trend was observed for the Z-Avg size (data not shown).

The results show that there is no appreciable change in the volume-weighted peak or the Z-Avg size over a period of up to 145 days for NCL48-2 (Figure 6 panel C) and NCL49-2 (Figure 6 panel D) at both storage temperatures for these concentrations. The results also show that the size for NCL48-2 is independent of storage temperature. However, for NCL49-2, storage at room temperature leads to a larger volume-weighted peak size relative to the 4 °C stored sample.

Effect of pH on the Size Stability

Design and Methods

The pH stability NCL48-2 in saline was measured by batch-mode DLS. Two samples were prepared; one for low pH evaluation (titrated with acid) and the other for high pH evaluation (titrated with base). To keep the ionic strength constant, 0.1 M HCl and 0.1 M NaOH were prepared in saline (154 mM NaCl). Samples were prepared by diluting the stock solution in saline (154 mM NaCl) to give a final concentration of 1 mg/mL. Solution pH was adjusted and measured using an autotitrator before sample size was measured (minimum of ten measurements).

Results

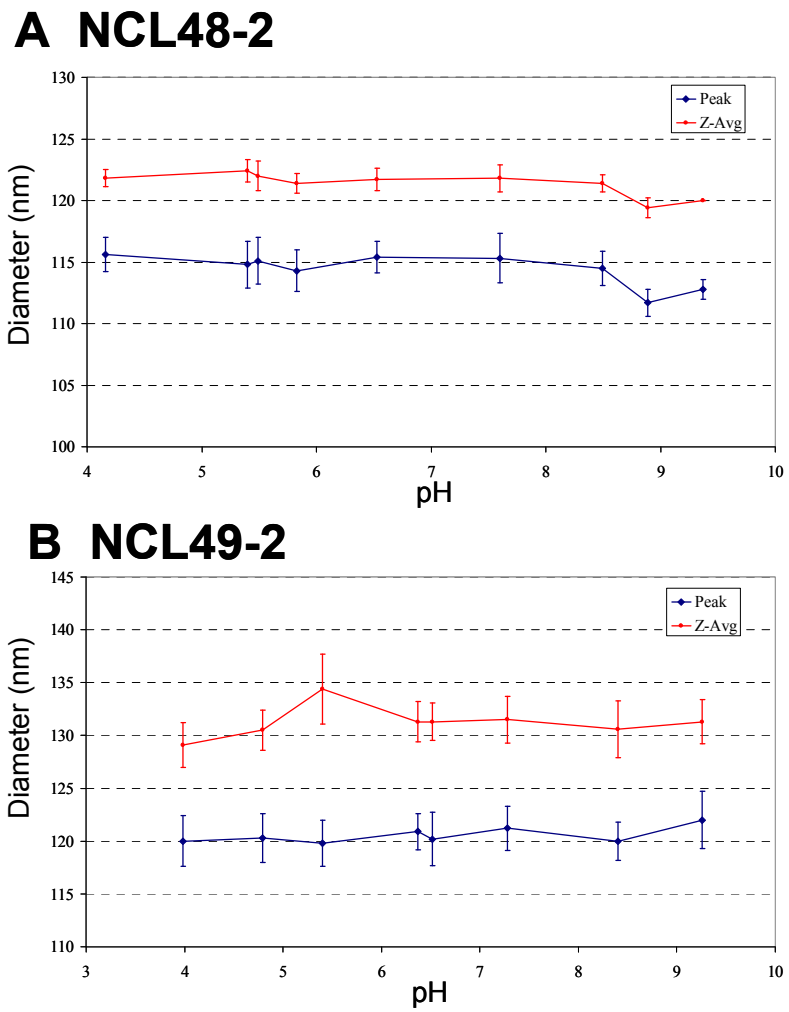

Figure 7. The pH stability, as measured by batch-mode DLS. (A) NCL48-2 and (B) NCL49-2 in saline.

Analysis and Conclusions

The results show that there is no appreciable change in the volume-weighted peak or the Z-Avg for NCL48-2 (Figure 7 panel A) and NCL49-2 (Figure 7 panel B) in the pH range studied.

Effect of DMSO on Hydrodynamic Size

Design and Methods

In vitro studies conducted contained 5 % DMSO to solubilize free ceramide and the effect of DMSO on hydrodynamic size of NCL48-1 was measured. For this purpose, samples were diluted in DMSO and in either PBS or saline to give a solution containing 1 mg/mL NCL48-1 and 5 %(v/v) DMSO. A third sample was prepared to contain 0.00625 mg/mL ceramide, 1 mg/mL NCL48-1, and 5 %(v/v) DMSO in PBS.

Results

Table 4. Summary of the comparison of size of the original samples in PBS and saline to those containing 5% DMSO and ceramide.

Sample	Z-avg (nm)	PdI	Vol-Peak (nm)	Vol-Peak %Vol
PBS	99.6 (0.4)	0.174 (0.019)	77.3 (3.3)	99.8 (0.7)
PBS, 5% DMSO	111.0 (0.6)	0.173 (0.013)	93.9 (7.9)	100 (0)
Saline	99.1 (0.5)	0.174 (0.011)	80.0 (3.8)	99.8 (0.4)
Saline, 5% DMSO	110.0 (0.3)	0.177 (0.010)	89.8 (6.7)	100 (0)
PBS, 5% DMSO, Ceramide	110.0 (0.5)	0.180 (0.009)	92.0 (5.6)	100 (0)

Note: The standard deviations (N > 7) are given in parenthesis.

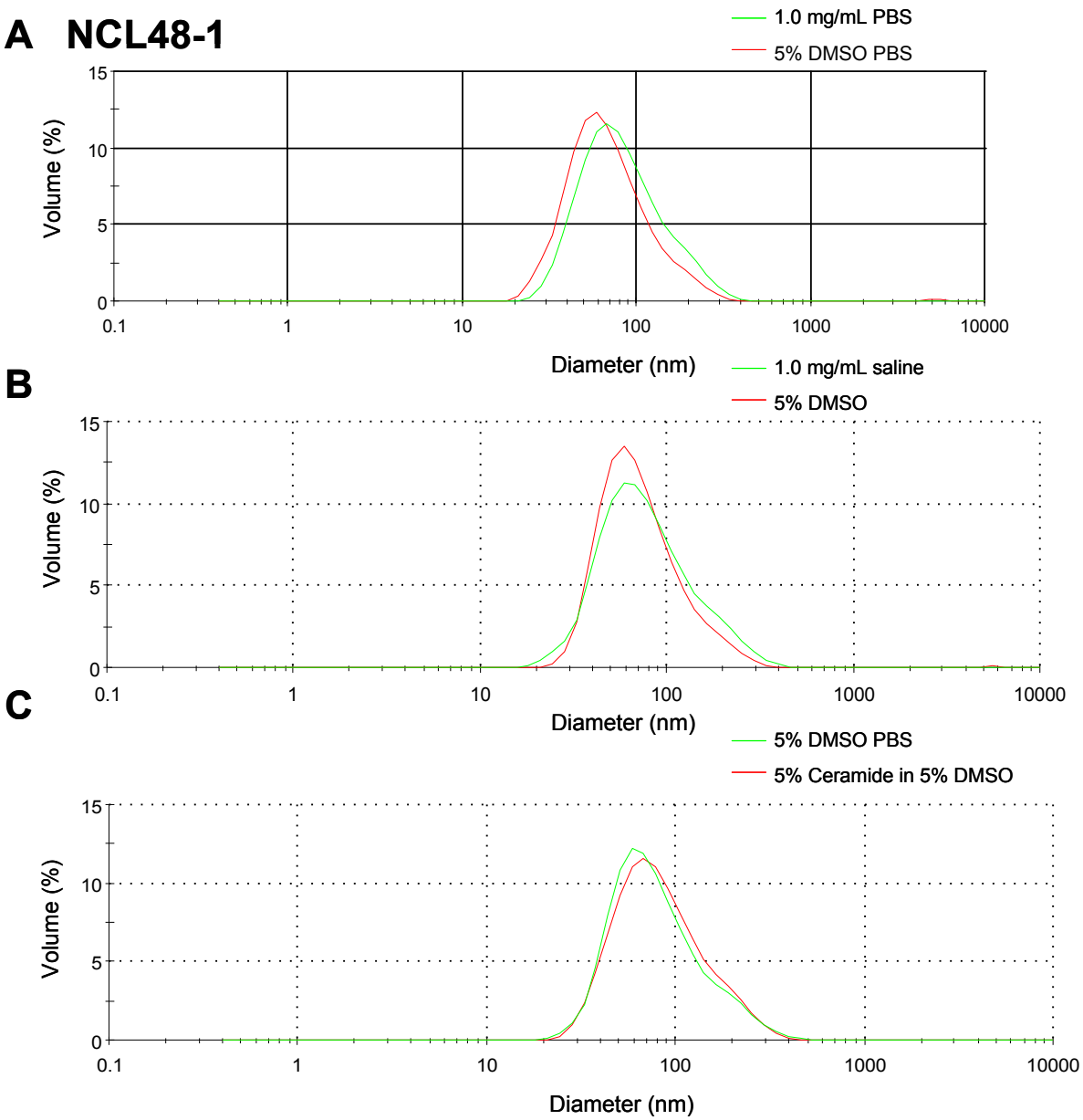

Figure 8. The Average Volume distribution plots (average of at least seven measurements per sample) for NCL48-1. Each panel shows the distribution plot with and without DMSO in (A) PBS, (B) saline, and (C) with ceramide in PBS.

Analysis and Conclusions

Regardless of media (PBS or Saline), the size increases with addition of DMSO. The extent of the increase is the same for both NCL48-1 and NCL49-1.There is no effect in size with addition of ceramide. The viscosity change due to DMSO was taken into consideration for size measurement.

Effect of Cell Culture Media on Hydrodynamic Size

Design and Methods

The effect of the cell culture media, RPMI supplemented (contains Fetal Bovine Serum (FBS)) and non-supplemented, on size for NCL48-1 and NCL49-1was studied via batch-mode DLS measurements at 25 and 37 °C. Samples were diluted in RPMI with or without FBS to a final concentration of 1 mg/mL. Samples were incubated at the appropriate temperature for 10 minutes before a minimum of ten measurements were taken for each sample.

Results

Table 5. Comparison of NCL48-1 size of the original samples in PBS to those in RPMI with and without FBS at 25 and 37 °C.

Sample	Z-avg	PdI	Vol-Peak	Vol-Peak
	(nm)		(nm)	%Vol
PBS, 25 °C	99.6 (0.4)	0.174 (0.019)	77.3 (3.3)	99.8 (0.7)
RPMI w/o FBS, 25 °C	102.0 (0.6)	0.182 (0.008)	79.2 (5.0)	100 (0)
RPMI w/ FBS, 25 °C	93.9 (1.1)	0.248 (0.007)	84.0 (3.9)	99.8 (0.5)
PBS, 35 °C	98.5 (0.5)	0.181 (0.010)	79.0 (2.4)	100 (0)
RPMI w/o FBS, 37 °C	96.5 (0.6)	0.205 (0.010)	71.2 (4.9)	100 (0)
RPMI w/ FBS, 37 °C	94.4 (0.5)	0.246 (0.006)	85.0 (3.7)	100 (0)

Note: The standard deviations (N > 7) are given in parenthesis.

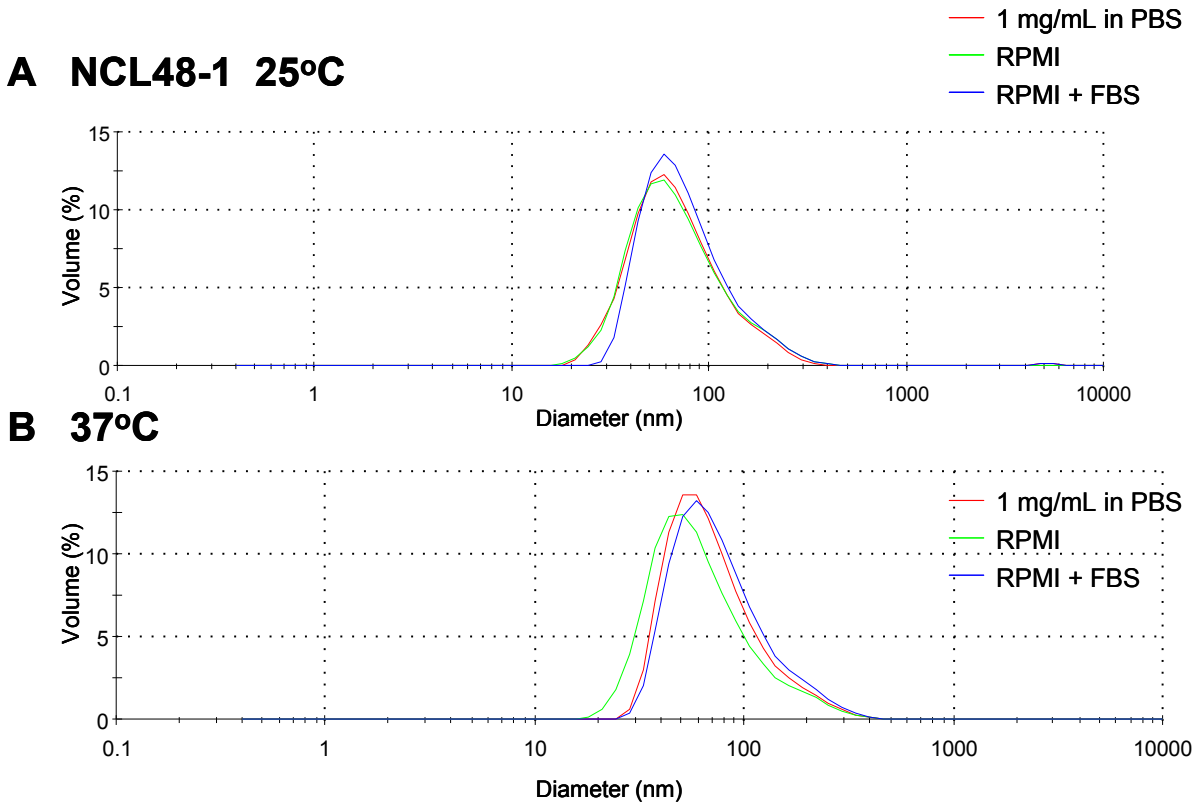

Figure 9. The average volume distribution plots for NCL48-1 in cell culture media. The average volume distribution plots (average of at least seven measurements per sample) are shown for NCL48-1 in cell culture media at (A.) 25 and (B.) 37 °C.

Table 6. Comparison of NCL49-1 size in PBS to size in RPMI with and without FBS at 25 and 37 °C.

Sample	Z-avg (nm)	PdI	Vol-Peak (nm)	Vol-Peak %Vol
PBS, 25 °C	111.0 (1.4)	0.189 (0.015)	93.6 (1.4)	98.4 (1.3)
RPMI w/o FBS, 25 °C	114.0 (1.5)	0.200 (0.016)	96.9 (2.6)	98.0 (1.1)
RPMI w/ FBS, 25 °C	108.0 (0.8)	0.225 (0.012)	97.2 (3.4)	98.6 (1.5)
PBS, 35 °C	108.0 (0.5)	0.134 (0.008)	96.0 (1.3)	100 (0)
RPMI w/o FBS, 37 °C	110.7 (0.8)	0.134 (0.006)	99.2 (1.3)	100 (0)
RPMI w/ FBS, 37 °C	104.0 (0.8)	0.197 (0.008)	96.3 (1.5)	100 (0)

Note: The standard deviations (N > 7) are given in parenthesis. Experimental details are the same as in Table 4.

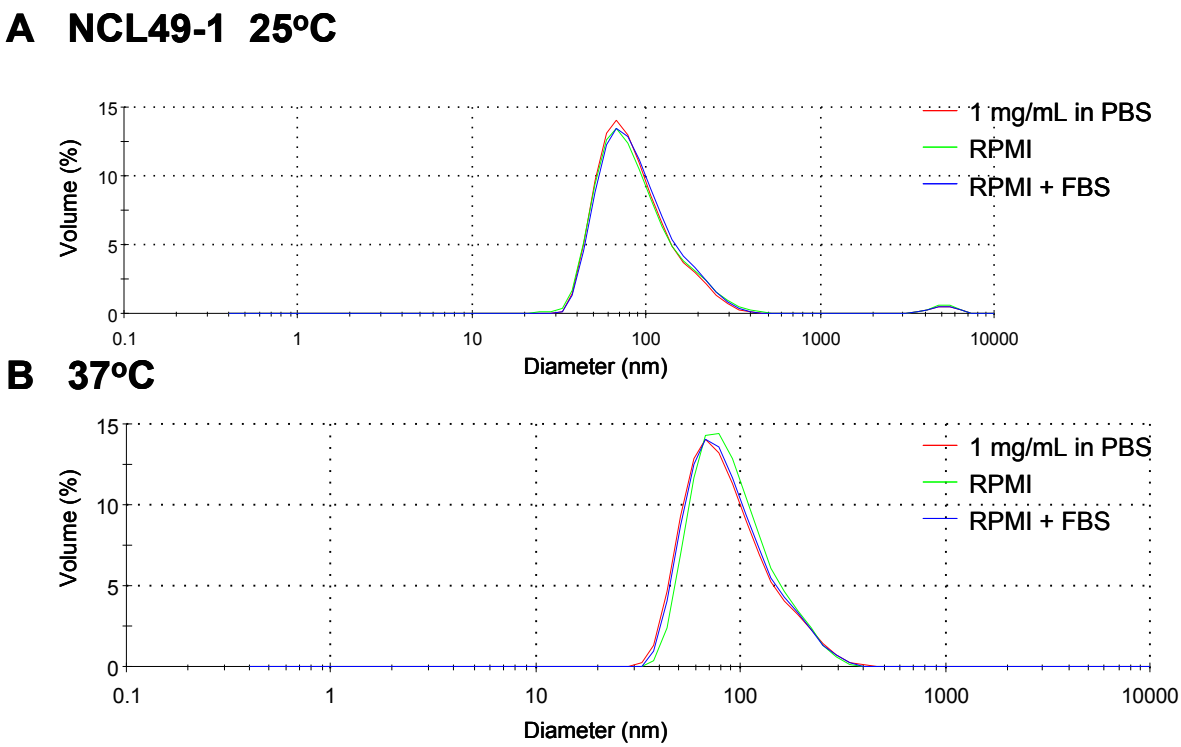

Figure 10. The average volume distribution plots for NCL49-1 in cell culture media. The average size by volume distribution plots (average of at least seven measurements per sample) are shown for NCL49-1 in cell culture media at (A) 25 and (B) 37 °C.

Analysis and Conclusions

The volume weighted peak (indicated by “Peak” in figures) and Z-avg for NCL48-1 at a given temperature, regardless of media, remains fairly constant. The PdI values increase slightly as RPMI is added followed by RPMI w/ FBS. No dependence on media at a given temperature is seen for the volume weighted peak for NCL49-1 (see Figure 10). The PdI values again increase as seen with NCL48-1 while the Z-avg values show no significant change.

Freeze-Thaw Stability

Design and Methods

The freeze-thaw stability of NCL48 and NCL49 were measured by batch-mode DLS measurements. Samples were diluted in saline to give a 1 mg/mL final concentration. Samples (1 mL total volume in 1.8 mL eppendorf tube) were then frozen at -20 ºC for a predetermined period of time, after which they were allowed to thaw at room temperature. Once thawed (~ 3 hours), the samples were transferred to a low volume disposable polystyrene cuvette, capped, and incubated at 25 ºC for 10 minutes before a minimum of ten measurements were taken. Samples were transferred back to the eppendorf tube for freezing. This cycle was repeated several times.

Results

NCL49-1

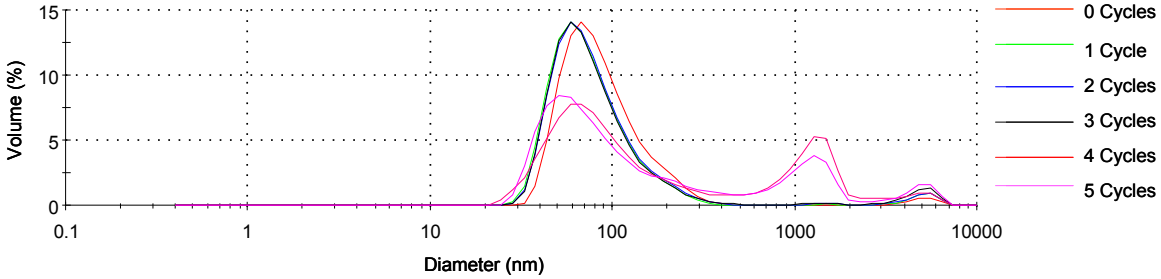

Figure 11. The averaged volume distribution plots (average of at least seven measurements per sample) for NCL49-1 thawed at room temperature Cycles are indicated in legend. The volume distribution plot shows the appearance of a larger-in-size population after the fourth and fifth cycles. This implies that the sample has become more polydispersed. The PdI (data not shown) increases slightly with the first three cycles but jumps significantly after the forth and fifth cycles. This is expected to affect the Z-avg measurement more than the volume weighted measurement.

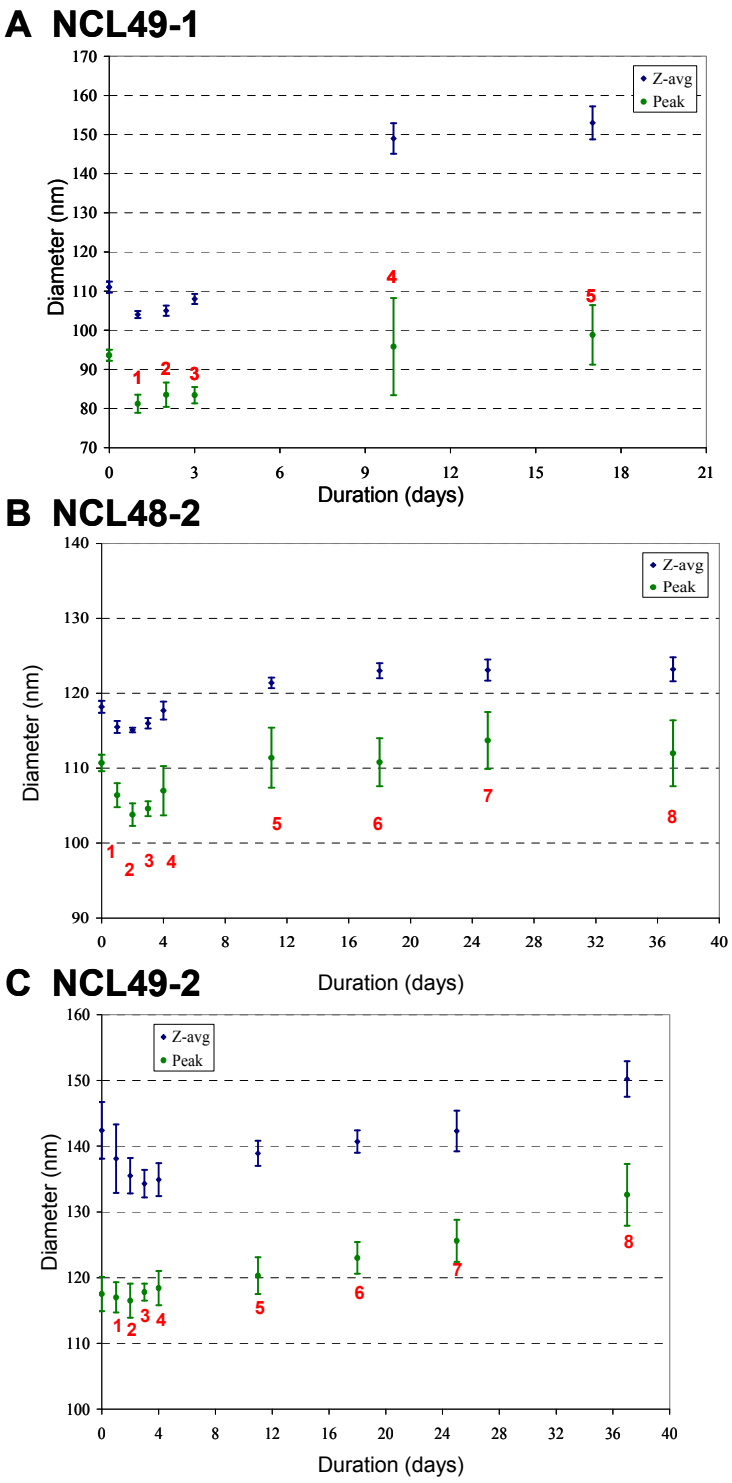

Figure 12. The freeze-thaw stability measured by batch-mode DLS. The volume-weighted diameter for (A) NCL49-1 (B) NCL48-2 and (C) NCL49-2 as a function of duration in days. Cycle number is indicated in red. Error bars are standard deviations for a minimum of ten measurements.

Analysis and Conclusions

The volume-weighted peak (indicated by “Peak” in figures) for all samples decrease from the initial value and remain approximately constant after three cycles of freezing/thawing (one day of freezing per cycle). The next four cycles correspond to a freezing period of at least 7 days between each cycle. The peak has now increased to a nominal value greater than the initial sample size. However, due to the large error bars for this measurement, it is hard to say if this increase is significant. The Z-avg values remain fairly constant after three cycles. However, a slight increase is seen after the next cycle and remains constant. This can be explained by noting that the PdI slightly increases (data not shown) after the fifth cycle and remains fairly constant.

Lyophilization Stability

Design and Methods

The stock solution of NCL49-1 has a concentration of 15 mg/mL in saline, as specified by the client. To determine the accuracy of this, 300 μL of stock NCL49-1 was dialyzed overnight to remove the salts. 220 μL of the dialyzed sample was lyophilized until a constant weight was obtained. Based on the lyophilized (dry) sample weight and the dialyzed sample volume, a concentration of 10.9 mg/mL was determined.

The lyophilized sample of NCL49-1 was re-suspended in 1 mL water and vortexed. Samples were prepared by diluting in water to give a 1 mg/mL final concentration. The sample was incubated at 25 ºC for 10 minutes before eleven measurements were taken.

Results

Table 7. Comparison of the hydrodynamic size of the original sample (un-lyophilized) in PBS to the lyophilized sample in water.

Sample	Z-avg (nm)	PdI	Vol-Peak (nm)	Peak %Vol
Original, in PBS	111.0 (1.4)	0.189 (0.015)	93.6 (1.4)	98.4 (1.3)
Lyophilized, in water	378 (5)	0.466 (0.017)	1048 (267)	84 (8)

Note: The standard deviations (N > 10) are given in parenthesis.

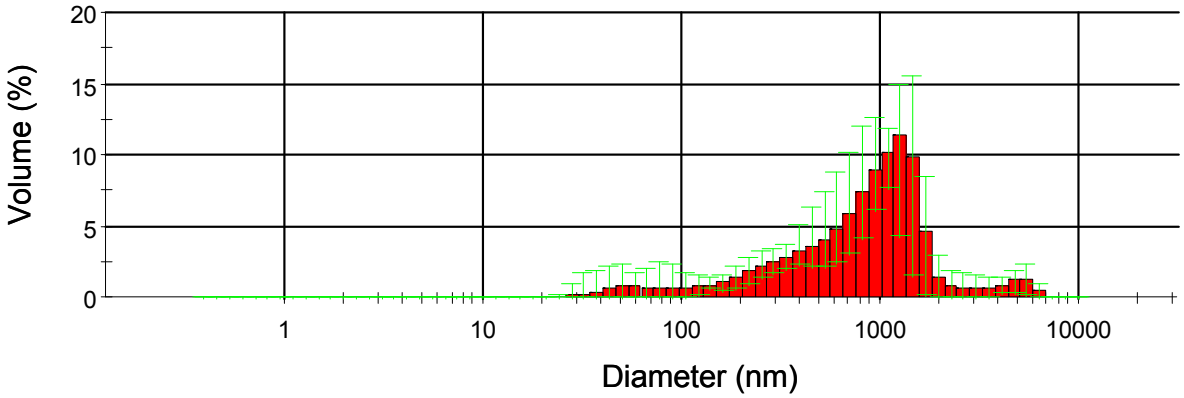

Figure 13. Effect of lyophilization on size. Volume distribution plots (11 measurements) of NCL49-1 re-suspended in water after lyophilization. Sample concentration was 1 mg/mL in water and measured at 25 ºC.

Analysis and Conclusions

As can be seen from the data, the Z-avg, PdI, and the volume weighted peak for the lyophilized sample are all substantial. The results suggest that liposomes are not stable after lyophilization *under these conditions*.

Zeta Potential

Design and Methods

A folded capillary flow cell was used for zeta potential measurement at a voltage of 100 V. The zeta potential of NCL48-1 and NCL49-1 at 25° C was measured at two different concentrations. Samples were diluted in 10 mM NaCl to give a 0.1 and 1 mg/mL final concentration. A minimum of ten measurements were taken for each sample. Samples of NCL48-2 and NCL49-2 were diluted in 10 mM NaCl to give a 1 mg/mL final concentration.

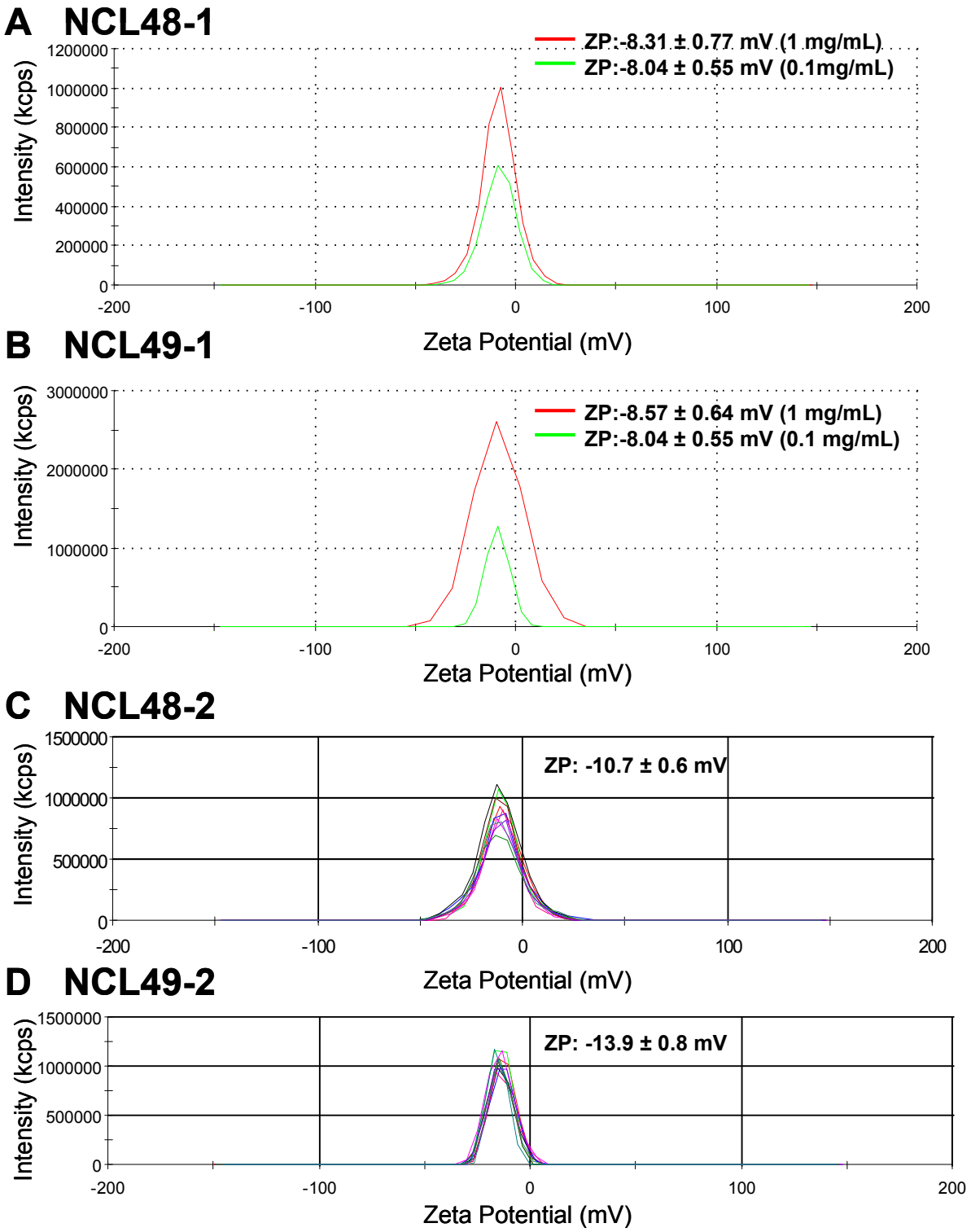

Figure 14. The zeta potential distributions. The zeta potential distributions derived from the electrophoretic mobility for (A) NCL48-1(average of at least 7 measurements), (B.) NCL49-1(average of at least 7 measurements), (C) NCL48-2, and (D) NCL49-2 in 10 mM NaCl.

Analysis and Conclusions

The zeta potentials for both NCL48-1 and NCL49-1, regardless of concentration, are similar. The measured zeta potentials are slightly negative implying a slight negative surface charge.

The zeta potentials for NCL48-2 and NCL49-2 were -10.7 mV and -13.9 mV respectively. Again, these negative zeta potential values indicated a slight net negative surface charge for the liposomes.

Size Analysis on the Fractionated Sample

Size Exclusion Chromatography (SEC) – Multiple Angle Laser Light Scattering (MALLS)

Design and Methods

Size Exclusion Chromatography (SEC) is a separation technique used for determining purity and polydispersity of a sample. A sample is fractionated based on the molecular size of its components. When SEC is coupled with a Multiple Angle Laser Light Scattering (MALLS) apparatus, the molecular weight and root mean square (rms) radius of the fractionated sample can be determined. This information about the particle size can be complementary to size information determined by DLS.

The chromatographic system used here consisted of an isocratic pump (Agilent G1310A, Palo Alto, CA) and TosoHaas TSKgel Guard PWH 06762 (7.5 mm ID x 7.5 cm, 12 μm) and TSKgel G6000PW 05765 (7.5 mm ID x 30 cm, 17 μm) columns (TosoHaas, Montgomeryville, PA). A Wyatt Injection System (Wyatt Technology, Santa Barbara, CA) was used for the first batch of liposomes and a well-plate autosampler (Agilent G1329A) was used for sample injection of the second batch of liposomes.

The size exclusion column was connected in-line to a light scattering (MALLS) detector (DAWN EOS, 690 nm laser, Wyatt Technology, Santa Barbara, CA) and a Refractive Index (RI) detector (Optilab rEX, Wyatt Technology, Santa Barbara, CA). The isocratic mobile phase was PBS (1x, pH 7.5, Sigma D1408, St. Louis, MO) at a flow rate of 1 mL/min.

Sample concentrations of NCL48-1 and NCL49-1 were 1 and 10 μg/mL in PBS. Sample concentrations of NCL48-2 and NCL49-2 were 25 and 100 μg/mL in PBS. Samples of 100 μL were injected.

Molecular weights were determined using Astra V 5.1.9.1 (Wyatt Technology, Santa Barbara, CA).

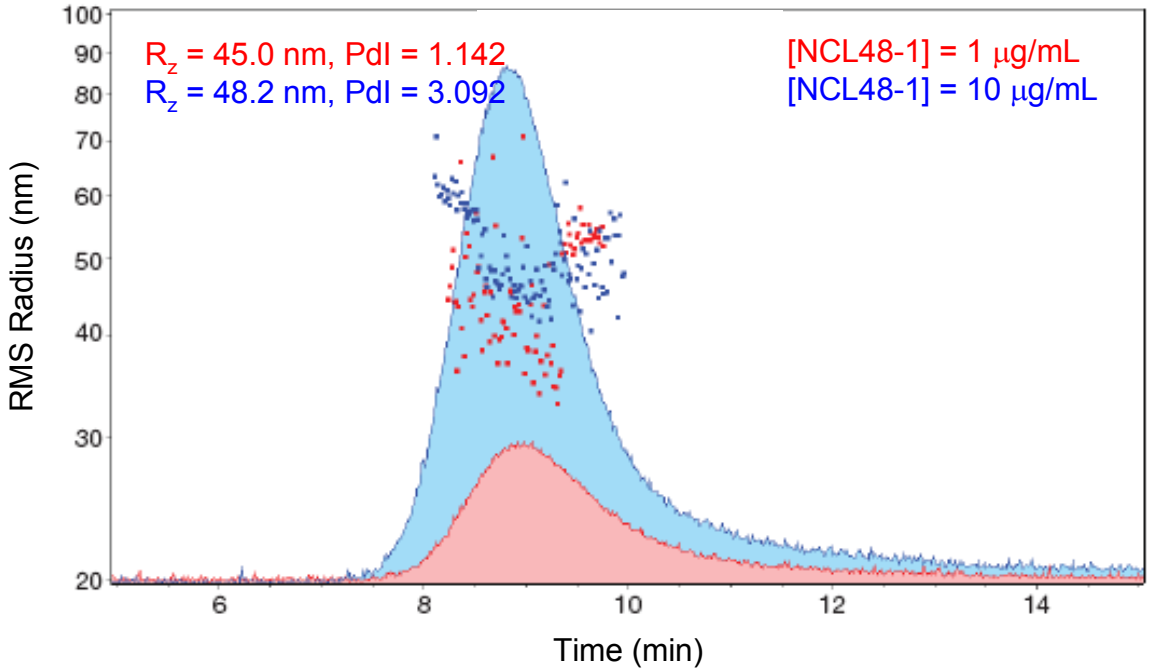

Figure 15. SEC chromatograms of NCL48-1 at two concentrations. The calculated rms radius (R_z) for NCL48-1 was 45.0 nm and 48.2 nm at 1 and 10 μg/mL, respectively.

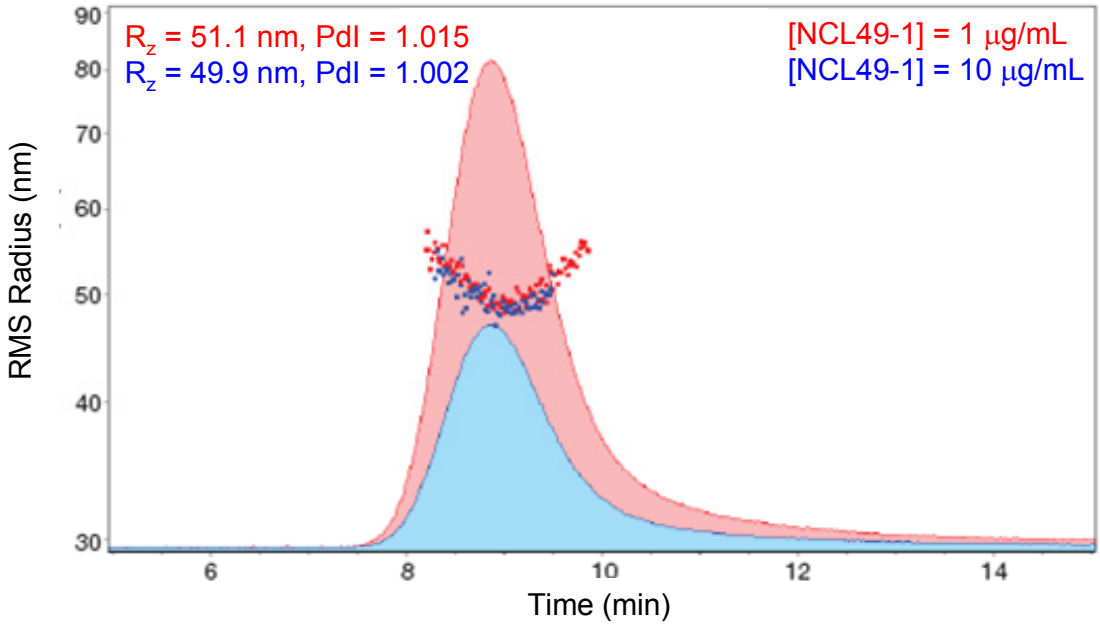

Figure 16. SEC chromatograms of NCL49-1 at two concentrations. The calculated rms radius (R_z) for NCL49-1 was 51.1 nm and 49.9 nm at 1 and 10 μg/mL, respectively.

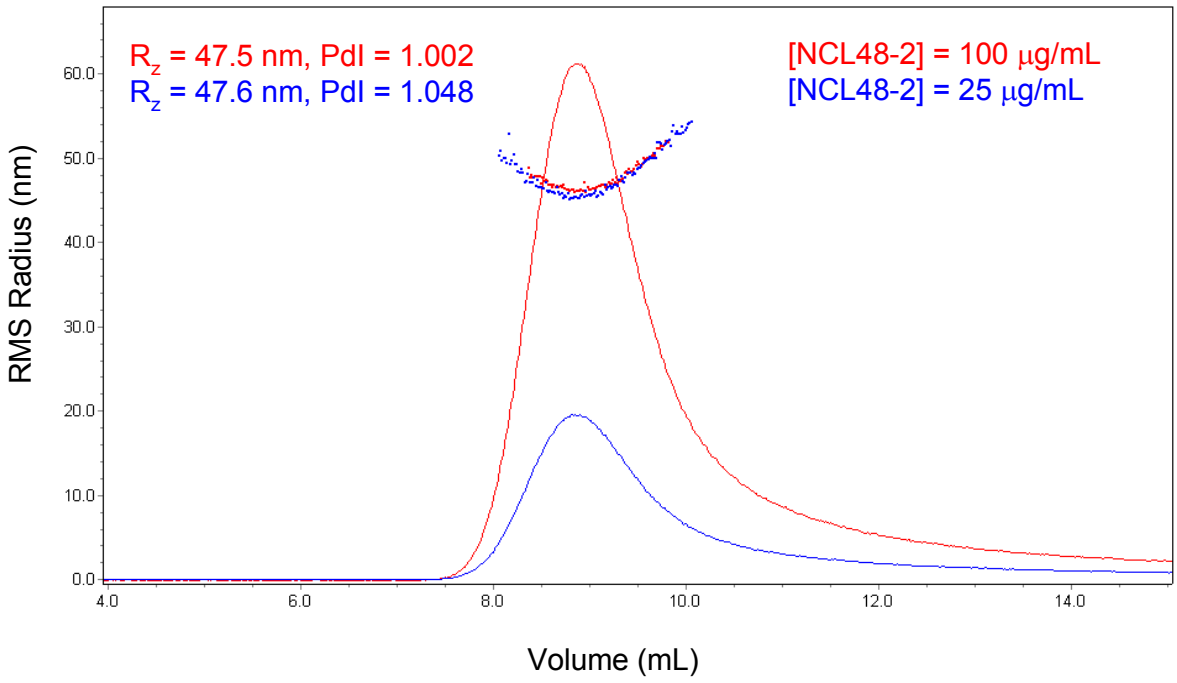

Figure 17. SEC chromatograms of NCL48-2 at two concentrations. The calculated rms radius (R_z) for NCL48-2 was 47.5 nm and 47.6 nm at 25 and 100 μg/mL, respectively.

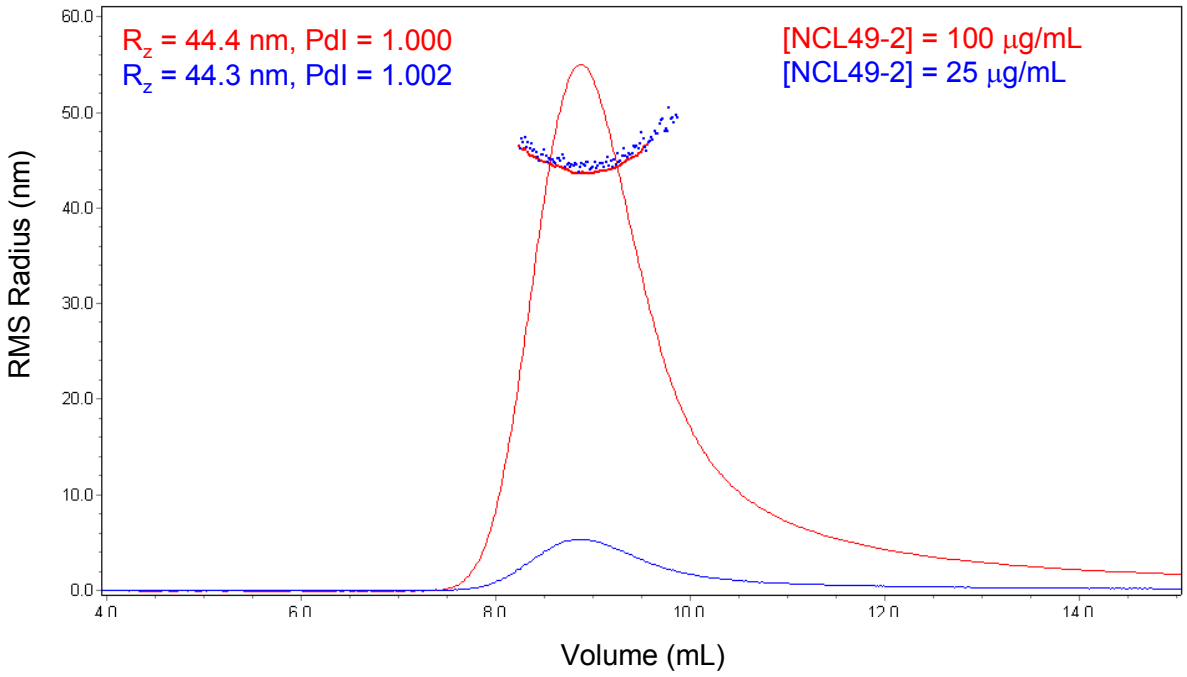

Figure 18. SEC chromatograms of NCL49-2 at two concentrations. The calculated rms radius (R_z) for NCL49-2 was 44.4 nm and 44.3 nm at 25 and 100 μg/mL, respectively.

Table 8. Comparison of the SEC-MALLS-measured sizes (rms radii) of the liposome samples.

Sample	Conc. (μg/mL)	R_z (nm)	PdI
NCL48-1	1	45.0	1.142
NCL48-1	10	48.2	3.092
NCL49-1	1	51.1	1.002
NCL49-1	10	49.9	1.105
NCL48-2	25	47.5	1.048
NCL48-2	100	47.6	1.002
NCL49-2	25	44.4	1.002
NCL49-2	100	44.3	1.000

Analysis and Conclusions

The rms radius distribution plots for NCL48-1, NCL49-1, NCL48-2, and NCL49-2, each at two concentrations, are tabulated in Table 8. The calculated rms radius for NCL48-2 and NCL49-2 is independent of concentration. A slight difference (~3 nm) is observed for the first batch of liposomes. Based on these results alone, it appears that both batches of NCL48 are consistent in size, while the second batch of NCL49 is only slightly smaller (~5 nm) than the first batch. The data also suggests that NCL49-1 is larger than NCL48-1, but NCL48-2 is slightly larger than NCL49-2.

Asymmetrical Flow Field-Flow Fractionation (AFFF)-Multiple Angle Light Scattering (MALLS)

Design and Methods

AFFF is a column-free fractionation system for the efficient separation and characterization of nanoparticles, polymers, and proteins in a fast and gentle way. When coupled with a Multiple Angle Light Scattering (MALLS) system, the rms radius can be obtained for the fractionated sample. Here the cross flow was 1 mL/min, the channel flow was 1 mL/min, and the sample concentration was 0.1 mg/mL in isotonic saline. The membrane was made of 10 kDa regenerated cellulose.

Results

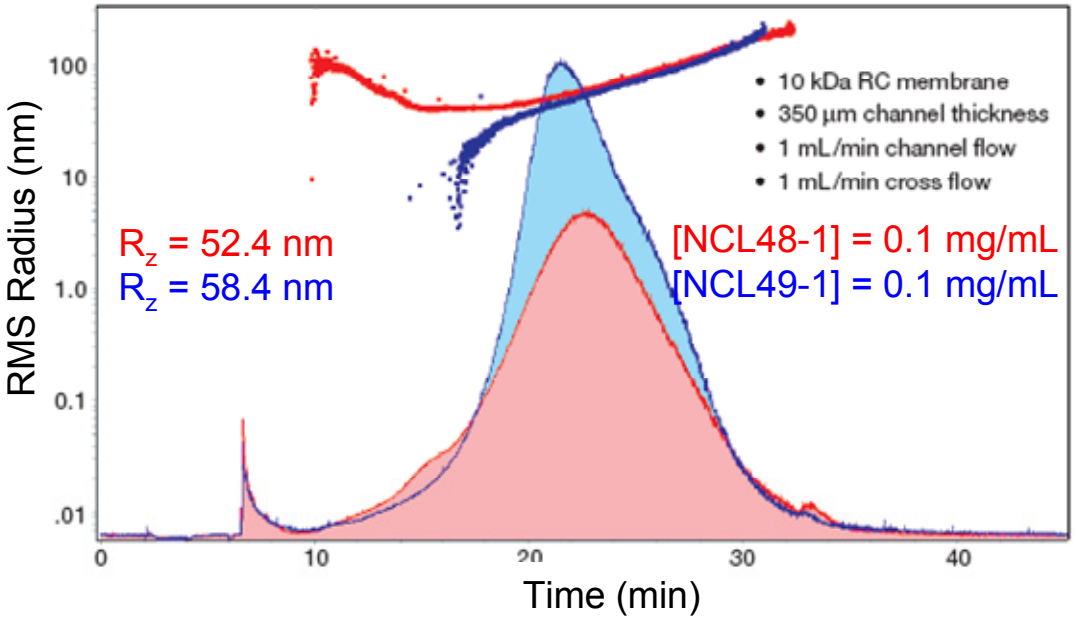

Figure 19. The rms radius distribution versus elution time for NCL48-1 (red) and NCL49-1 (blue) by AFFF-MALLS. The multiple peaks suggest the polydisperse size distribution of NCL48-1 and NCL49-1. The calculated rms radius (R_z) of NCL48-1 and NCL49-1 are 52.4 nm, and 58.4 nm, respectively.

Analysis and Conclusions

The multiple peaks suggest the polydisperse size distribution of NCL48-1 and NCL49-1. The calculated rms radius (R_z) of NCL48-1 and NCL49-1 are 52.4 nm, and 58.4 nm, respectively.

Atomic Force Microscopy (AFM)

Design and Methods

A tapping mode AFM measurement can be carried out in either air mode or liquid mode. For air mode AFM imaging the sample is prepared by dropping the particle solution on a solid support (typically mica, Au (111) or silicon are used) and then blown dry with a nitrogen stream and the subsequent AFM imaging takes place in air. This method is relatively easy and robust for “hard” particles such as metallic, semi-conductive particles. For liquid mode, the particle solution is loaded in a liquid cell mounted onto a solid support and then AFM imaged. There is no drying process involved in liquid mode so the particles remain in the same solution conditions. Additionally, the AFM tip generates a less lateral force to the particles when operated in liquid mode so that there is less shape deformation during imaging. Most soft materials (such as DNA, protein, or liposomal particles) are imaged in liquid mode to minimize shape deformation. Here we used AFM liquid mode measurement to avoid dehydration of the liposomes which may occur in dry mode.

The AFM measurement was performed on a PicoPlus SPM II (Molecular Imaging, AZ, USA) with magnetic AC (MAC) mode in liquid. Type II MACLever silicon tip (Molecular Imaging, spring constant 2.8 N/m) was used at a driving frequency of 30 kHz in liquid throughout all experiments. A 1.5 x 1.5 cm^2 mica (Ted Pella) is freshly cleaved and pre-treated with 10 mM $MgCl_2$ solution to make surface slightly positively charged. The liposomal samples (0.04 mg/mL in PBS of each of NCL48-1 and NCL49-1) were prepared by adding 250 µL liposome solutions on the mica surface, which is covered with a fluid cell (Molecular Imaging) and incubated for 1 minute before imaging. The electrostatic interaction between the mica surface (which is slightly positive after the salt treatment) and the liposomal particles (which are slightly negative, see zeta potential data above) may cause the particle to adhere to the mica surface.

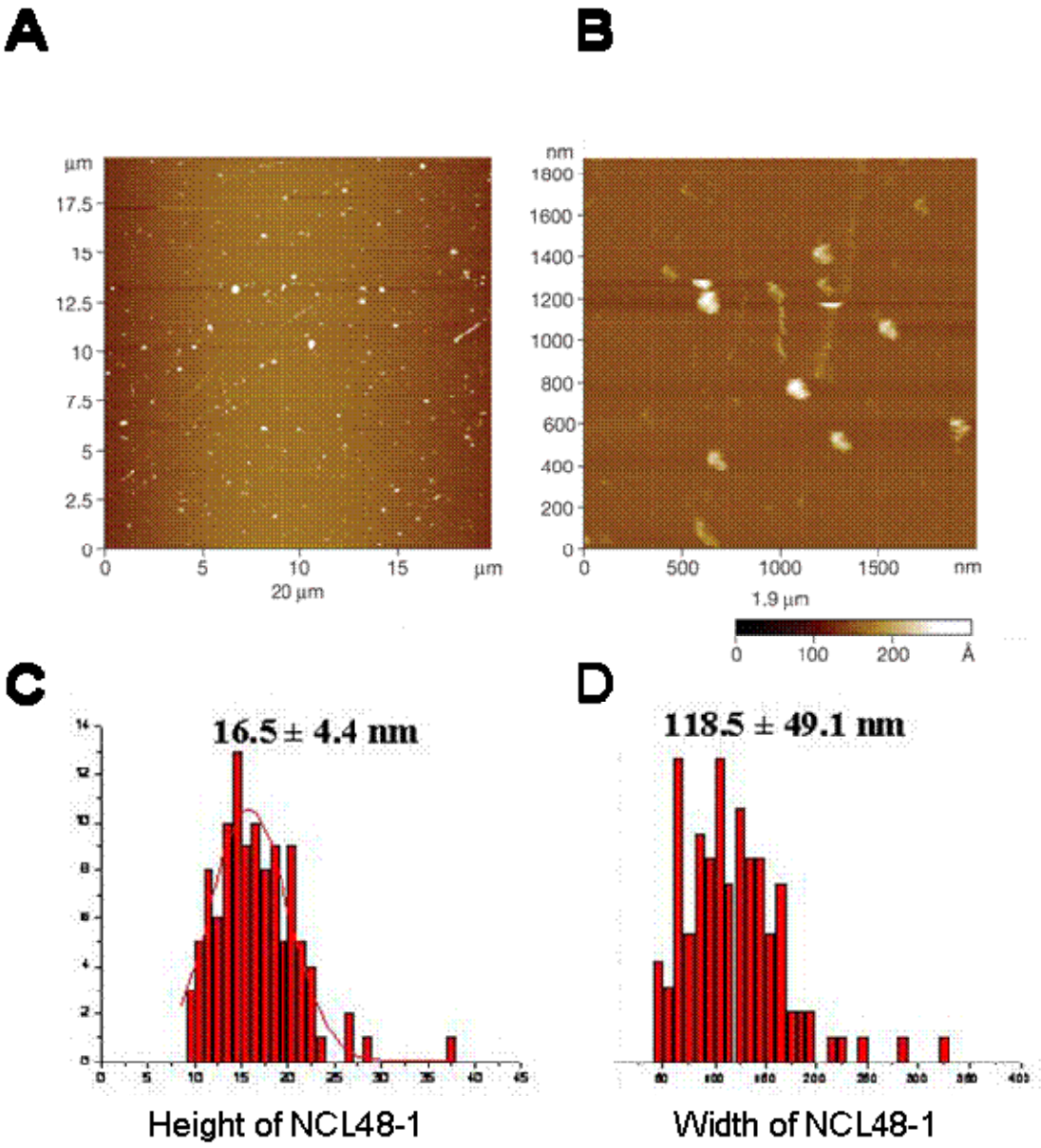

Figure 20. Typical topographic AFM images (A-B) and size distributions (C-D) of NCL48-1 obtained by tapping in saline solvent (liquid mode). The average height of NCL48-1 is 16.5 nm and the average width (full width half maximum, FWHM) is 118.5 nm.

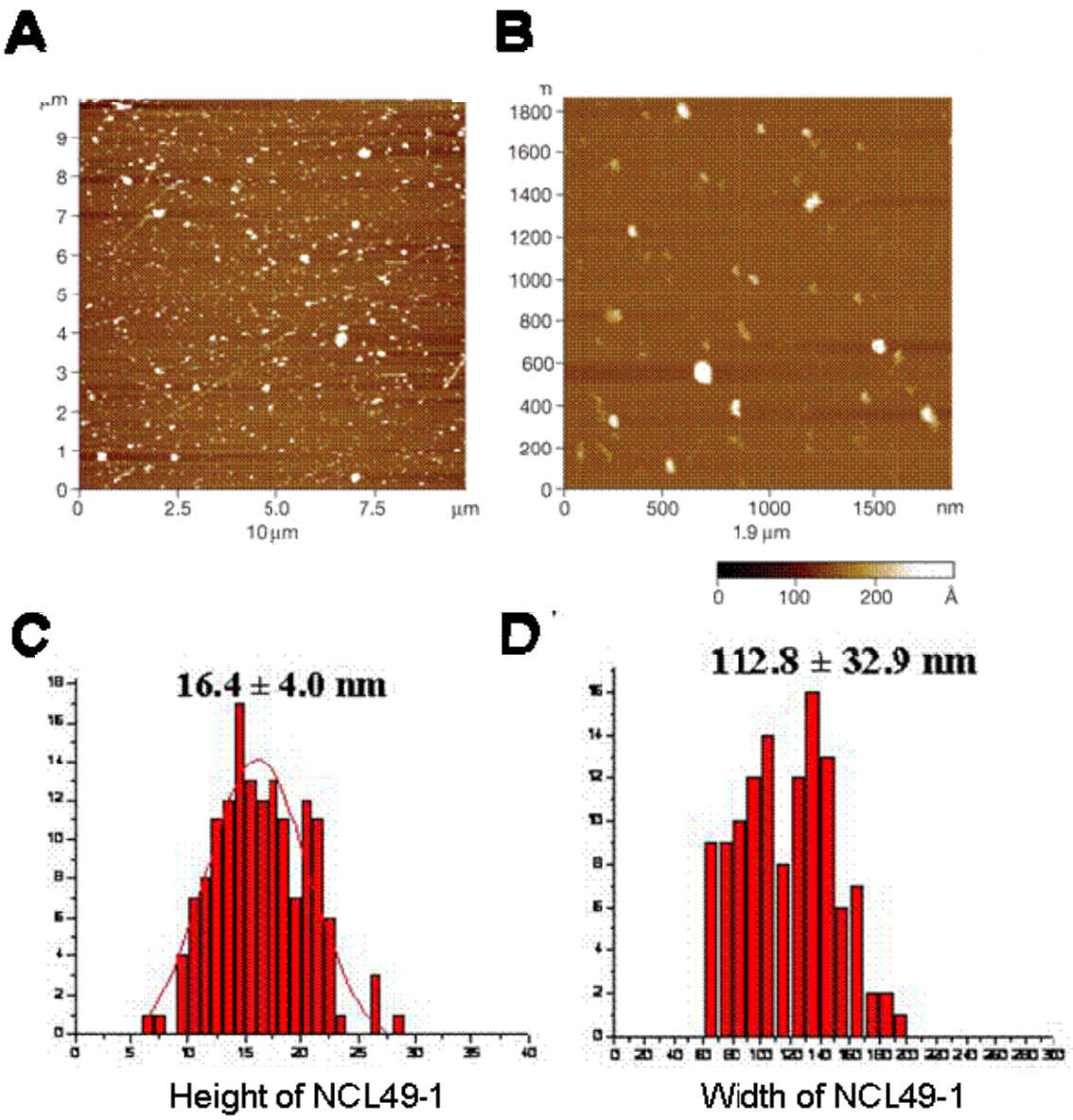

Figure 21. Typical Topographic AFM images (A-B) and size distribution (C-D) of NCL49-1 obtained by tapping in saline solvent (Liquid mode). The average height of NCL49-1 is 16.4 nm and the average width (full width half maximum, FWHM) is 112.8 nm.

Analysis and Conclusions

The mean heights of NCL48-1 and NCL49-1 are 16.5 nm and 16.4 nm, respectively, which are both significant smaller than the DLS-measured diameters (77.3 nm for NCL48-1 and 93.6 nm for NCL49-1) and SEC-MALLS-measured diameters (90 nm for NCL48-1 and 102.2 nm for NCL49-1). This indicates the liposomal particle was deformed when it was in contact with mica surface or by tip-particle interaction, though the force applied to particles by the tip was minimized through optimization of the setpoint setting. Due to the well-known AFM convolution effect in the X and Y dimension, the height (Z dimension) of particles is normally used to as a measure of particle size, rather than the width (X and Y dimensions) in AFM data analysis, especially for “hard” particles. This is not applicable to “soft” (e.g. liposomal)

particles. So the width of particles is also reported here. The average width (full width half maximum, FWHM) of NCL48-1 and NCL49-1 are 118.5 nm and 112.8 nm respectively.

Sterility

Prior to initiation of *in vitro* studies all formulations were tested for potential microbial and endotoxin contamination according to the NCL protocols STE-1, STE-2 and STE-3. These sterility tests did not reveal the presence of bacterial, yeast, mold, or mycoplasma contamination in either batch of NCL48 and NCL49. NCL48-1, 48-2 and 49-2 interfered with the LAL (*Limulus* Amoebocyte Lysate) test (STE-1) at concentration 1mg/mL, therefore endotoxin content reported for these materials was determined at a liposome concentration of 0.2mg/mL, for which IEC (inhibition enhancement control) demonstrated acceptable performance. NCL49-1 was tested at a concentration 1mg/mL. The observed endotoxin content was as follows (EU stands for Endotoxin Unit): NCL48-1: < 0.1EU/mL; NCL49-1: 0.136 EU/mL; NCL48-2: < 0.25 EU/mL, and NCL49-2: < 0.25 EU/mL.

In Vitro Toxicology

Section Summary

Ceramide, an endogenous shingolipid derived membrane component, has been shown to have antiproliferative and proapoptotic properties in cancer cell lines (Padron, 2006). Ceramide has also been reported to have additive anticancer effects when combined with current chemotherapeutics *in vitro* (Metha *et al.*, 2000). Liposomal formulation of ceramide was shown to enhance ceramide's potency against cancer cells *in vitro*, and liposomal ceramide has proven anticancer activity in murine breast adenocarcinoma models (Stover and Kester, 2003; Stover *et al.*, 2005). The present studies examined ceramide liposome, NCL49-1, biocompatibility and mechanism of action *in vitro*.

The ghost liposome, NCL48-1, was determined to be nontoxic to the Hep G2 cell line, by MTT and LDH cytotoxicity assays, up to the maximum test concentration of 1 mg/mL (Figure 22). NCL49-1, the ceramide loaded liposome, was determined to be moderately toxic to the Hep G2 cells, by both MTT and LDH assays (Figure 23). The 48 hour IC_{50} values for NCL49-1 in Hep G2 cells, was estimated to be 0.14 (0.11 – 0.18, 95% CI) mg liposome/mL by LDH assay, and 0.13 (0.11 – 0.15, 95% CI) mg liposome/mL by the MTT assay; this corresponds to an approximate 48 hour IC_{50} value of 40 μg /mL for the active ceramide component, assuming a 30% loading (Figure 24).

NCL49-1 cytotoxicity in porcine renal proximal tubule (LLC-PK1) cells was associated with caspase 3 dependent apoptosis, while cytotoxicity in the human hepatocarcinoma cell line, Hep G2, appears to be caspase 3 independent. Previous studies in rat hepatocytes have demonstrated that ceramide can induce apoptosis in rat hepatocytes by caspase independent mechanisms (Jones *et al.*, 1999). Future studies will further examine the mechanism of ceramide induced apoptosis.

Hep G2 LDH and MTT Cytotoxicity Assays

Design and Methods

The objective of this study was to determine the cytotoxicity of the ghost liposome (NCL48-1) and ceramide liposome (NCL49-1) in human hepatocarcinoma (Hep G2) cells.

Cytotoxicity was determined as described in the NCL method, Hep G2 Hepatocarcinoma Assay (GTA-2). Briefly, test materials were diluted to the desired assay concentrations in cell culture media (0.004-1.0 mg/mL). Cells were plated in 96-well, microtiter plate format. Cells were preincubated for 24h prior to test material addition, reaching an approximate confluence of 80%. Cells were then exposed to test material for 6, 24, and 48h in the dark, and cytotoxicity was determined using the MTT cell viability and LDH membrane integrity assays. In order to estimate IC_{50} values, the MTT and LDH cytotoxicity assay dose-response curves were fit to a sigmoidal Hill equation, $E=Emax\ C^{\gamma}/C^{\gamma}+IC_{50}^{\gamma}$), using nonlinear regression analysis (WinNonlin, Pharsight Corp., Mountain View, CA).

Results

The maximum concentration of NCL48-1 and 49 tested in the Hep G2 cytotoxicity study was 1.0 mg/mL. Treatment of cells with NCL48-1 did not produce any measurable loss of cell viability, as determined by the MTT assay, or loss of membrane integrity, as determined by the LDH cytotoxicity assay at the concentrations tested (Figure 22). Treatment of cells with NCL49-1, however, resulted in a dose-responsive loss of cell viability (Figure 23), as measured by MTT assay, and a minor, non-dose responsive loss of membrane integrity (Figure 24), as measured by LDH leakage. The IC_{50} value, estimated from nonlinear regression analysis of the 48 hour MTT assay dose-response curves, was 0.14 (0.11 – 0.18, 95% CI) mg liposome/mL corresponding to 0.042 mg ceramide/mL at 30% loading (Figure 24). The IC_{50} value, estimated from the nonlinear regression analysis of the 48 hour LDH assay dose-response curves, was 0.13 (0.11 – 0.15, 95% CI) mg liposome/mL, corresponding to 0.039 mg ceramide/mL at 30% loading (Figure 24).

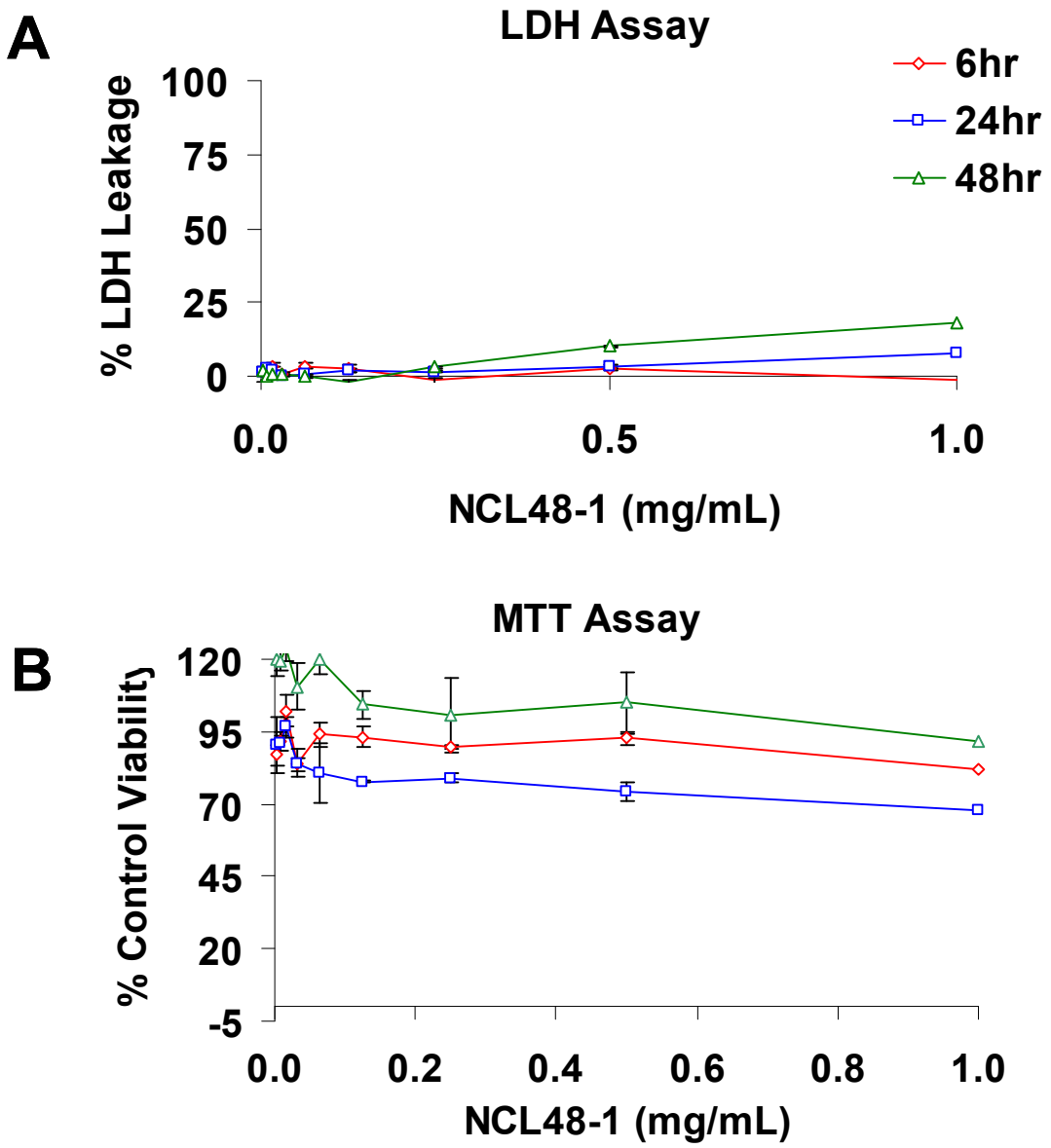

Figure 22. NCL48-1 cytotoxicity assay in Hep G2 cells. Porcine renal proximal tubule cells were treated for 6, 24, and 48 hour with 0.004-1.0 mg/mL of test sample. Cytotoxicity was determined at each time point by the LDH (A) and MTT (B) assays, as described in the Hep G2 Hepatocarcinoma Assay (GTA-2). Data represents the mean ± SE, *N*=3.

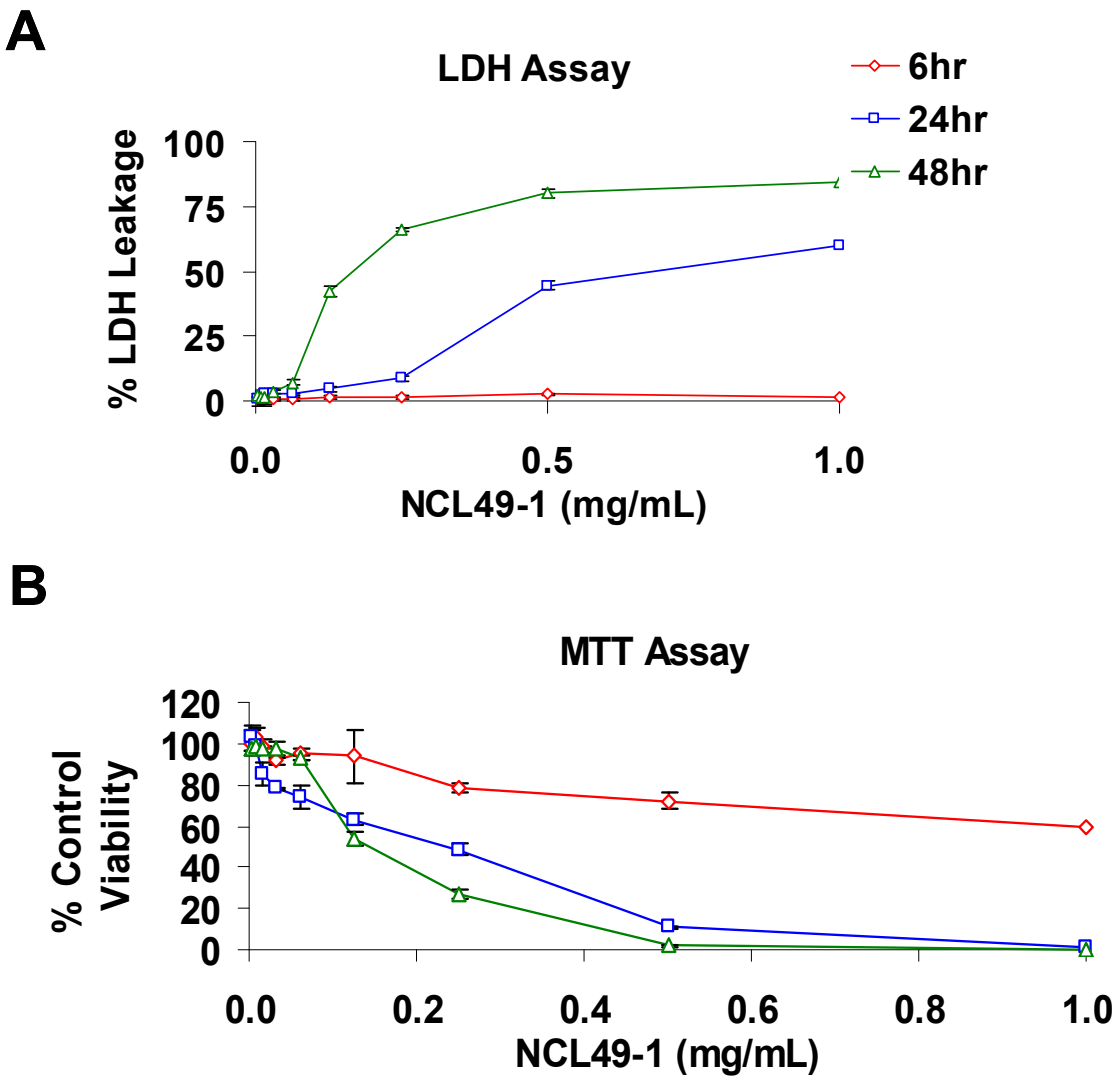

Figure 23. NCL49-1 cytotoxicity assay in Hep G2 cells. Porcine renal proximal tubule cells were treated for 6, 24, and 48 hour with 0.004-1.0 mg/mL of test sample. Cytotoxicity was determined at each time point by the LDH (A) and MTT (B) assays, as described in the Hep G2 Hepatocarcinoma Assay (GTA-2). Data represents the mean ± SE, *N*=3.

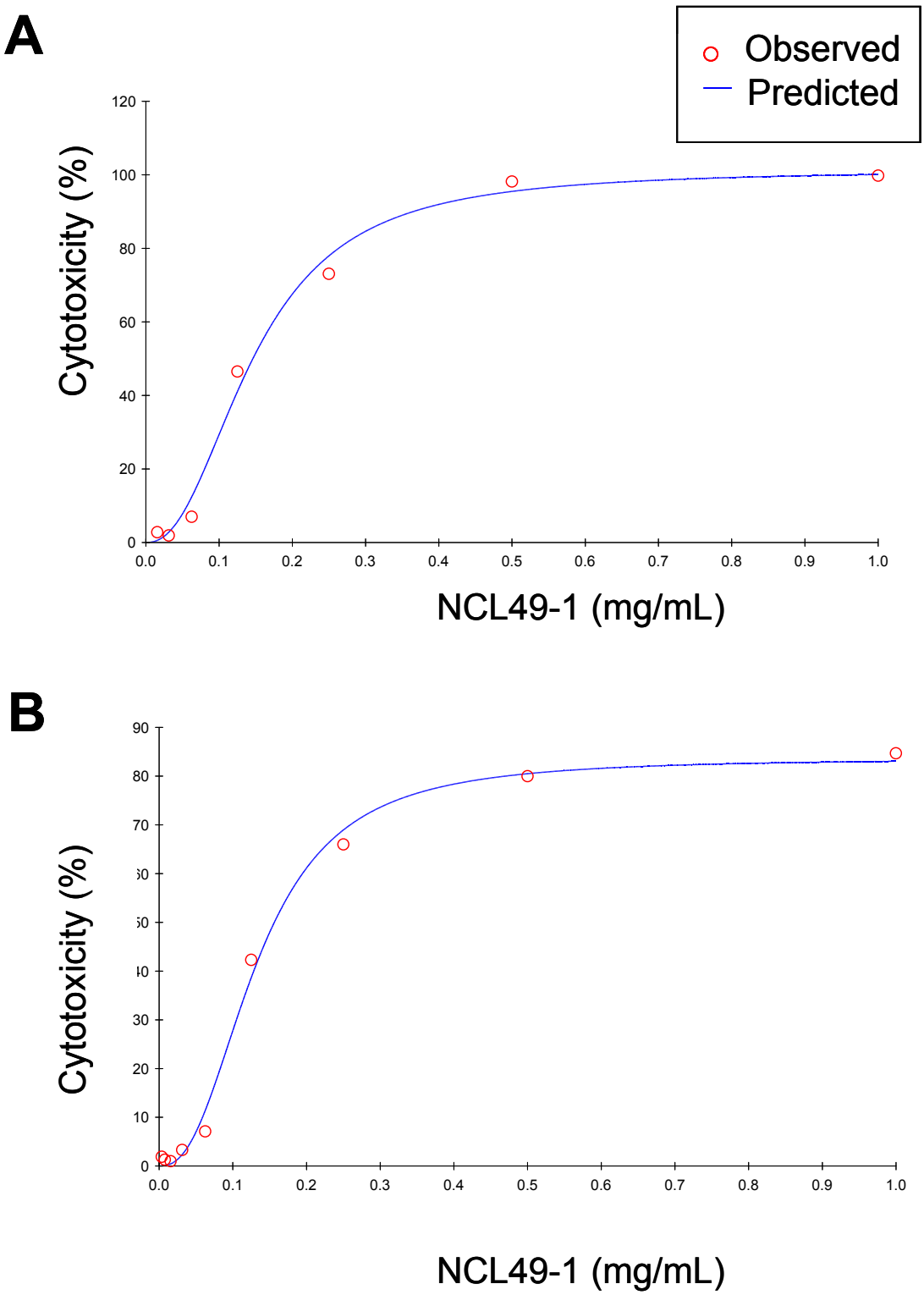

Figure 24. Nonlinear Regression Analysis. This graph displays the nonlinear fit of the 48h **NCL49-1** (**A**) MTT data and (**B**) LDH data to a sigmoidal Hill equation**.** Data is presented as cytotoxicity vs. NCL49-1 concentration.

Analysis and Conclusions

NCL48-1 was found to be nontoxic to the Hep G2 cells, under these assay conditions. NCL49-1 was determined to be moderatly toxic to Hep G2 cells, by both MTT and LDH assays.

Apoptosis Induction by NCL49-1 in LLC-PK1 and Hep G2

Design and Methods

The objective of this study was to determine if NCL49-1 cytotoxicity in porcine renal proximal tubule (LLC-PK1) cells and human hepatocarcinoma (Hep G2) cells is associated with induction of apoptosis, as measured by caspase 3 activation.

In this study, caspase 3 activation was used as a measure of apoptosis. Caspase 3 activity was measured as described in the LLC-PK1 Kidney Apoptosis and Hepatocarcinoma Apoptosis Assays (GTA-5 and 6). Briefly, test materials were diluted to the 0.125 mg/mL test concentration in cell culture media. LLC-PK1 and Hep G2 cells were plated in 35 mM, 6-well plate format. Cells were pre-incubated for 24h prior to addition of test sample, reaching an approximate confluence of 80%. Cells were treated with test sample, media control or 10 mM acetaminophen positive control in the dark for 2, 6 or 24h. Following the designated treatment period, the cells were imaged under a light microscope and prepared for caspase 3 activity measurement according to the protocol. Caspase 3 activity was measured using a microtiter plate spectrophotometer at excitation 415 nm and emission 505 nm.

Results

Treatment of LL-PK1 cells with 0.125 mg NCL49-1/mL resulted in loss of adherent cell density and morphological changes (Figure 25), that were associated with increased caspase 3 activation (Figure 26). Treatment of the Hep-G2 cells with 0.125 mg NCL49-1/mL , on the other hand, resulted in changes in adherent cell density and cell morphology (Figure 25), that were not associated with caspase 3 activation (Figure 26).

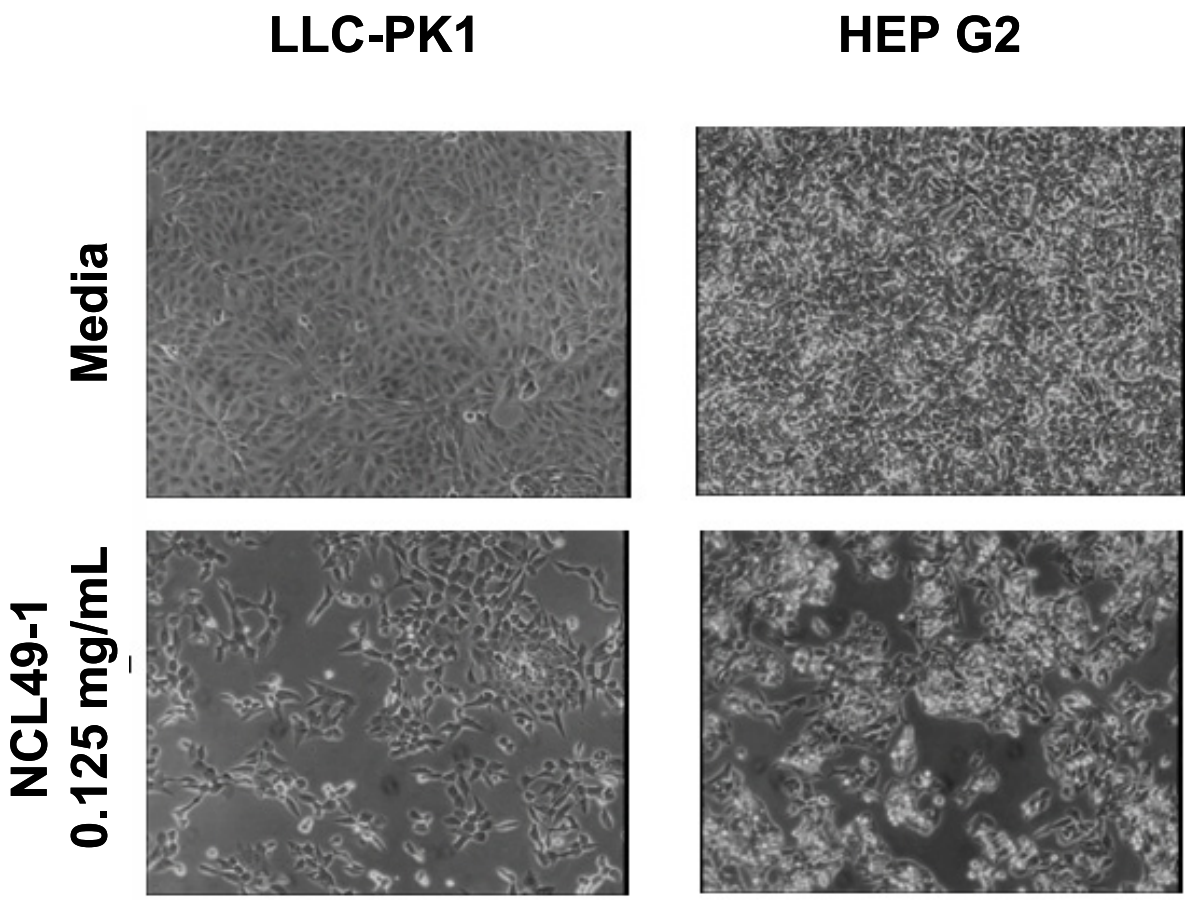

Figure 25. Effect of NCL49-1 on LLC-PK1 and Hep G2 morphology. Photomicrographs show representative phase contrast images (x225) of cells treated for 24 hour with 0.125 mg NCL49-1/mL, or control media.

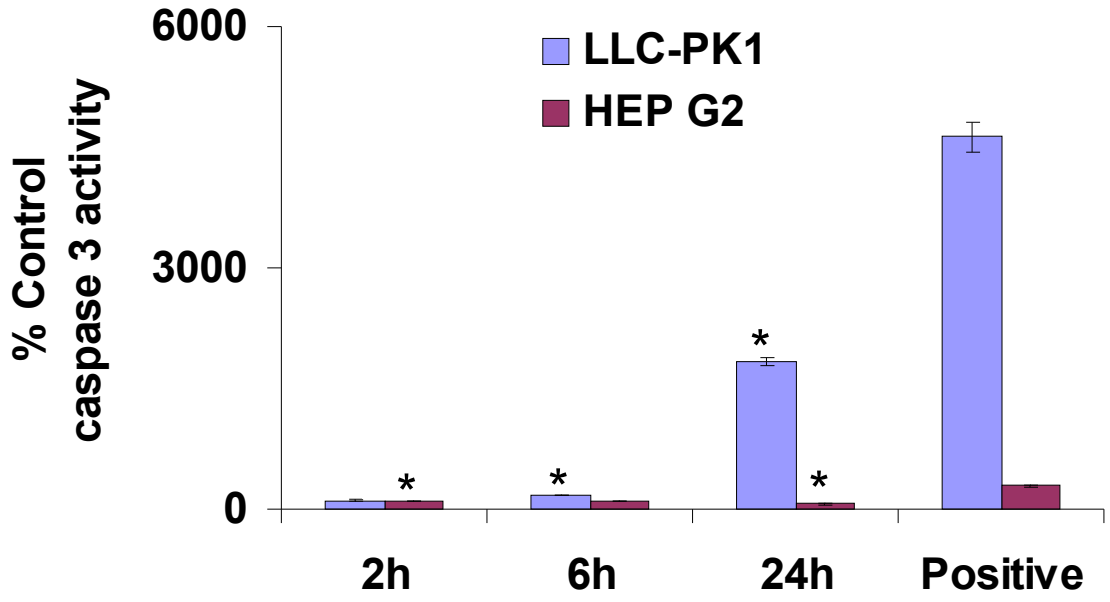

Figure 26. Effect of NCL49-1 treatment on 24 hour caspase-3 activity in LLC-PK1 and Hep G2 cells. Cells were treated for 2, 6, and 24h with 0.125 mg NCL49-1/mL, control media or positive controls (10 mM acetaminophen for Hep G2, and 50 μM cisplatin for LLC-PK1). Data are presented as % control caspase 3 activity normalized to total cellular protein. Bars correspond to the mean ± SE of six individual samples. * P<0.05 *versus* media control by Student's *t* –test.

Analysis and Conclusions

NCL49-1 cytotoxicity in LLC-PK1 cells involves caspase 3 dependent apoptosis, while cytotoxicity in Hep G2 cells appears to be caspase 3 independent.

In Vitro Immunological Characterization

Section Summary

The blood contact properties of the first batch of materials, referred to as NCL48-1 and NCL49-1, were evaluated in three assays designed for *in vitro* study of potential nanoparticle effects on the integrity of blood cellular components and coagulation pathways. Potential hemolytic properties, effects on platelet aggregation and blood coagulation were studied in the NCL protocols ITA-1, ITA-2 and ITA-12**.** Both nanoparticle formulations were tested at two concentrations: high (1mg/mL) and low (0.2 mg/mL for NCL48-2 and 0.0625 mg/mL for NCL49-2). These concentrations were selected based on the results of general toxicity assay (GTA-2, Figures 22 and 23).

The same protocols were then performed on the second lot of NCL48 and NCL49, referred to as NCL48-2 and NCL49-2. Both nanoparticle formulations were tested for blood contact properties in hemolysis (NCL protocol ITA-1), platelet aggregation (ITA-2), complement activation (ITA-5) and coagulation assays (ITA-12). Hemolysis and platelet aggregation assays were repeated for both NCL48-2 and NCL49-2 to test for potential batch-to-batch variability. NCL48-2 and NCL49-2 were also analyzed in cell-based assays: CFU-GM (ITA-3), leukocyte proliferation (ITA-6), oxidative burst (ITA-7), chemotaxis (ITA-8) and phagocytosis (ITA-9).

Main findings *in vitro* include potential complement activation, suppression of CFU-GM formation and PHA-M-induced leukocyte proliferation, as well as slight reduction of zymosan uptake in the presence of nanoparticle formulations. Inter-lot variability in test results was observed for NCL48-2 in the hemolysis assay. No adverse particle effects were seen *in vitro* in coagulation, platelet aggregation and nitric oxide secretion tests.

Nanoparticle Hemolytic Properties (ITA-1)

Design and Methods

The objective of this experiment was to evaluate liposome effects on integrity of red blood cells. NCL protocol ITA-1 was followed**.** Both nanoparticle formulations were tested at two concentrations: high (1mg/mL) and low (0.2 mg/mL for NCL48 and 0.0625 mg/mL for NCL49).

Results

Batch 1: At high concentration (1 mg/ml) both NCL48-1 and NCL49-1 disturbed the integrity of red blood cells as manifest by percent hemolysis at or above 5% (Figure 27). Low concentrations of NCL48-1 (0.2mg/mL) and NCL49-1 (0.0625 mg/mL) were not hemolytic (Figure 27).

Batch 2: No hemolytic activity was observed for both concentrations of NCL48-2 or for low concentration of NCL49-2. At high concentration, NCL49-2 is hemolytic (% hemolysis >5) (Figure 28).

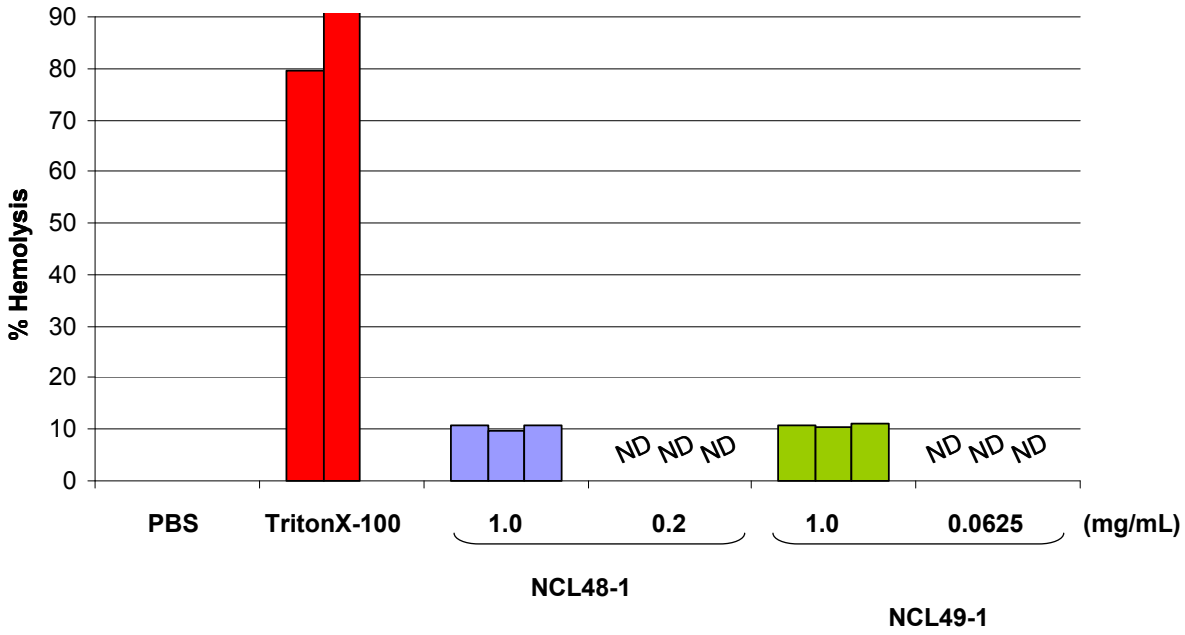

Figure 27. Analysis of nanoparticle hemolytic properties (ITA-1). NCL48-1 and NCL49-1 at high (1 mg/mL) and low (0.2 and 0.0625 mg/mL, respectively) concentration were used to evaluate potential particle effects on the integrity of red blood cells. Three independent samples were prepared for each nanoparticle concentration and analyzed in duplicate (%CV<25). Each bar represents the mean of duplicate results. ND indicates there were no detectable results. Triton X-100 was used as a positive control. PBS was used to reconstitute nanoparticles and represented the negative control. At high concentration (1 mg/ml) both NCL48-1 and NCL49-1 disturbed the integrity of red blood cells as manifest by percent hemolysis at or above 5%. Low concentrations of NCL48-1 (0.2mg/mL) and NCL49-1 (0.0625 mg/mL) were not hemolytic.

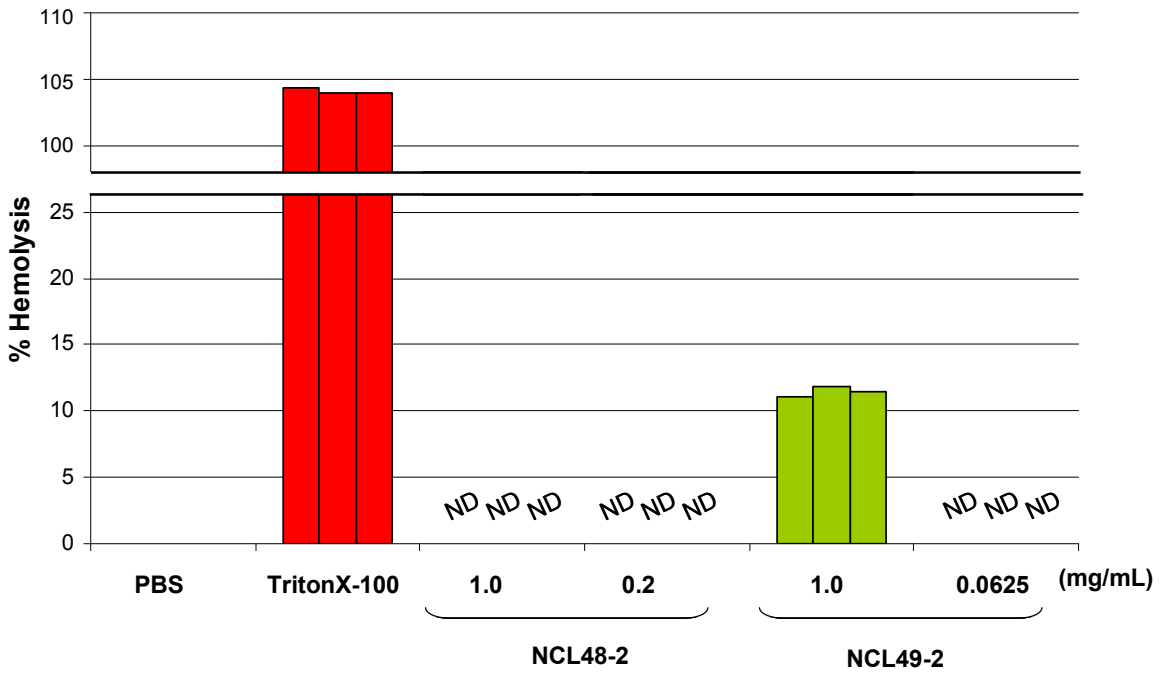

Figure 28. Analysis of nanoparticle hemolytic properties (ITA-1). NCL48-2 and NCL49-2 at high (1 mg/mL) and low (0.2 and 0.0625 mg/mL, respectively) concentration were used to evaluate potential particle effects on the integrity of red blood cells. Three independent samples were prepared for each nanoparticle concentration and analyzed in duplicate (%CV<25). Each bar represents the mean of duplicate results. ND indicates there were no detectable results. Triton X-100 was used as a positive control. PBS was used to reconstitute nanoparticles and represented the negative control. NCL49-2 at high concentration was hemolytic (% hemolosis>5). Low concentration of NCL49-2 and both low and high concentrations of NCL48 did not disturb the integrity of red blood cells.

Analysis and Conclusions

None of the formulations were hemolytic at low concentration (0.2 mg/mL for NCL48-2 and 0.0625 mg/mL for NCL49-2). Both NCL49-1 and NCL49-2 were hemolytic at high concentration (1 mg/mL). NCL48-1is hemolytic at high concentration (1mg/mL) while NCL48-2 is not. This batch-to-batch difference is possibly due to the batch-to-batch difference in particle size between NCL48-1 and NCL48-2 (see physico-chemical characterization section).

Nanoparticle Effects on Platelet Aggregation (ITA-2)

Design and Methods

The objective of this experiment was to evaluate liposome effects on human platelets *in vitro*. NCL protocol ITA-2 was followed**.** Both nanoparticle formulations were tested at two concentrations: high (1mg/mL) and low (0.2 mg/mL for NCL48 and 0.0625 mg/mL for NCL49).

Results

Batch 1: At both concentrations, NCL48-1 and NCL49-1 did not induce platelet aggregation and did not interfere with platelet aggregation caused by collagen (Figure 29).

Batch 2: At both concentrations NCL48-2 and NCL49-2 did not induce platelet aggregation and did not interfere with platelet aggregation caused by collagen (Figure 30).

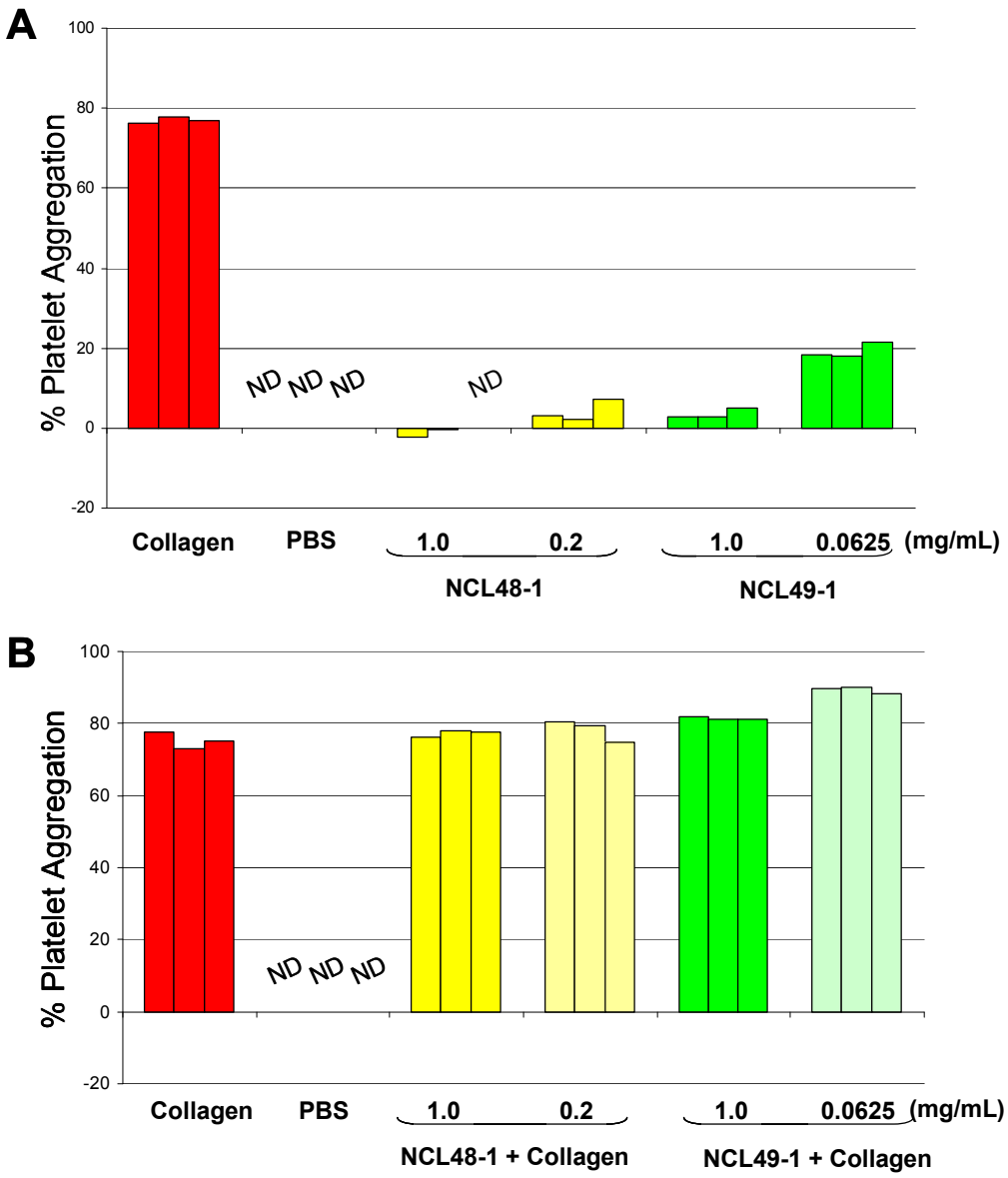

Figure 29. NCL48-1 and NCL49-1 evaluated for their potential effects on the cellular component of the blood coagulation cascade. For each nanoparticle concentration, three independent samples were prepared and analyzed in duplicate (%CV < 20). Each bar represents the mean of duplicate results. ND indicates there were no detectable results. (A) Nanoparticle formulations alone.The results demonstrate that none of tested nanoparticle formulations is capable of inducing significant platelet aggregation (%aggregation<20). Collagen and PBS were used as positive and negative controls, respectively. (B) Nanoparticle treatments were combined with collagen. The results demonstrate that NCL48-1 and NCL49-1 did not interfere with collagen-induced platelet aggregation.

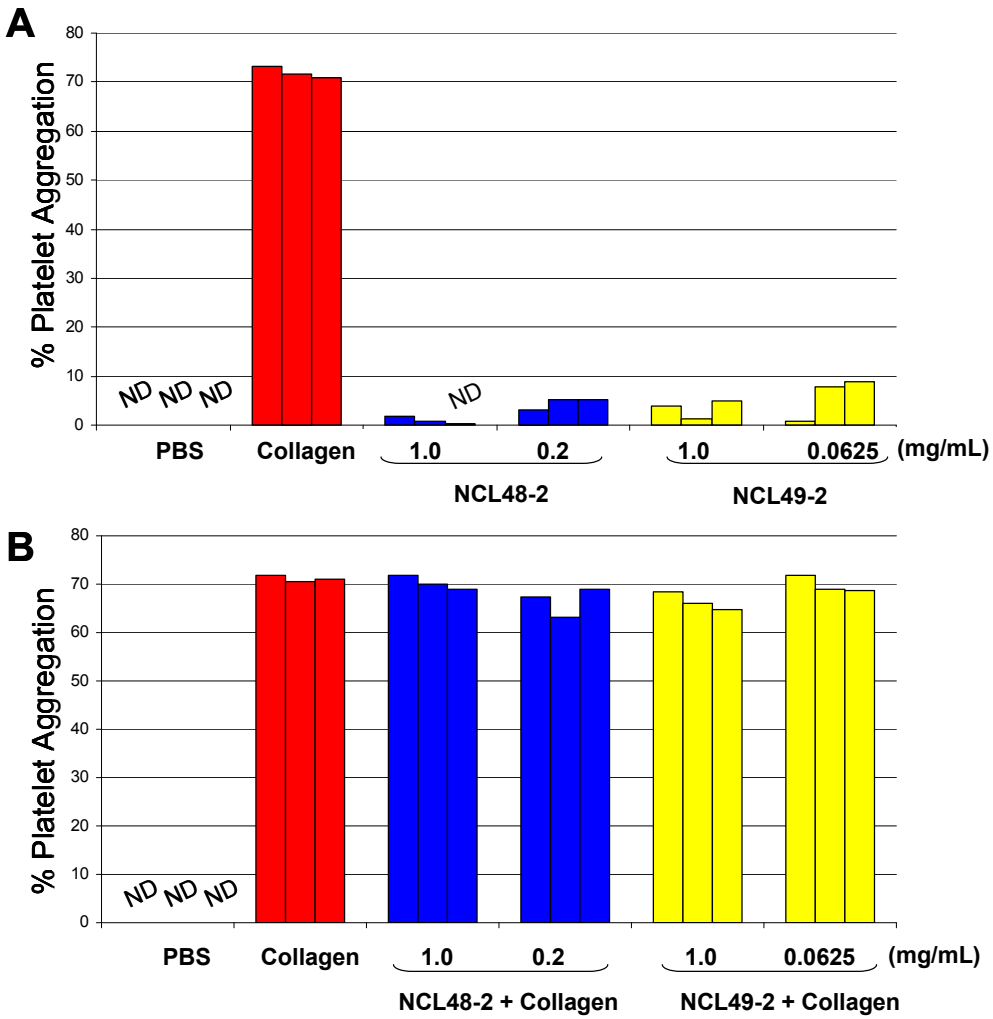

Figure 30. Analysis of nanoparticle effects on platelet aggregation (ITA-2). (A) NCL48-2 and NCL49-2 were evaluated for their potential effects on the cellular component of the blood coagulation cascade. For each nanoparticle concentration, three independent samples were prepared and analyzed in duplicate (%CV < 20). Each bar represents the mean of duplicate results. ND indicates there were no detectable results. The results demonstrate that none of tested nanoparticle formulations is capable of inducing significant platelet aggregation (%aggregation < 20). Collagen and PBS were used as positive and negative controls, respectively. (B) Nanoparticle treatments were combined with collagen. The results demonstrate that NCL48-2 and NCL49-2 did not interfere with collagen-induced platelet aggregation.

Analysis and Conclusions

In our platelet aggregation study, both high and low concentrations of NCL48-1 and high concentration of NCL49-1 did not induce platelet activation (i.e. percent platelet aggregation was less than 20), while low concentration of the NCL49-1 slightly induced platelet aggregation. That is, a reverse dose response was also observed in this assay (Figure 29A). Neither nanoparticle formulation interfered with the collagen-induced platelet aggregation (Figures 29 and 30B).

NCL48-2 and NCL49-2 do not induce platelet aggregation and do not interfere with collagen-induced platelet aggregation *in vitro.*

Nanoparticle Effect on Coagulation (ITA-12)

Design and Methods

The objective of this experiment was to evaluate liposome effects on human plasma coagulation *in vitro*. NCL protocol ITA-12 was followed**.** Both nanoparticle formulations were tested at two concentrations: high (1mg/mL) and low (0.2 mg/mL for NCL48 and 0.0625 mg/mL for NCL49)

Results

Batch 1: NCL48-1 and NCL49-1 at both high and low concentrations did not interfere with plasma coagulation as indicated by undisturbed prothrombin time (PT), activated partial thromboplastin time (APTT), thrombin and reptilase time when compared to untreated plasma and normal coagulation control standard (Figure 31).

Batch 2: At both concentrations NCL48-2 and NCL49-2 did not interfere with plasma coagulation in PT, APTT, Thrombin and reptilase time *in vitro* (Figure 32).

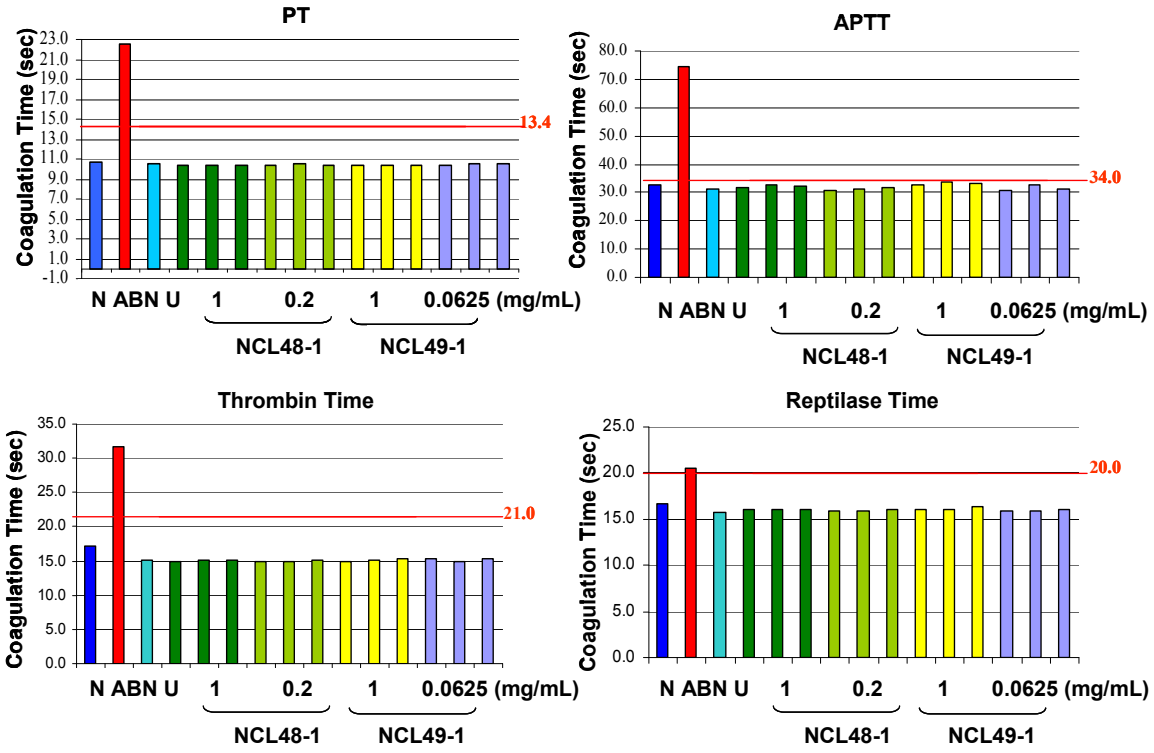

Figure 31. Analysis of nanoparticle effect on coagulation (ITA-12) – batch 1, donor group 1A. This figure presents potential particle effects on the biochemical component of the blood coagulation cascade. For each nanoparticle, three independent samples were prepared and analyzed in duplicate (%CV < 5%). Each bar represents the mean of duplicate results. Normal plasma standard (N) and abnormal plasma standard (ABN) were used for the instrument control. Plasma pooled from at least three donors was either untreated (Unt.) or treated with nanoparticle preparations NCL48-1 or NCL49-1. The dotted red line indicates the clinical standard cut-off for normal coagulation time for each of the tests. NCL48-1 and NCL49-1 at both high (1mg/mL) and low (0.2 and 0.0625mg/mL, respectively) do not interfere with plasma coagulation in prothrombin time (PT), activated partial thromboplastin time (APTT), thrombin and reptilase time tests.

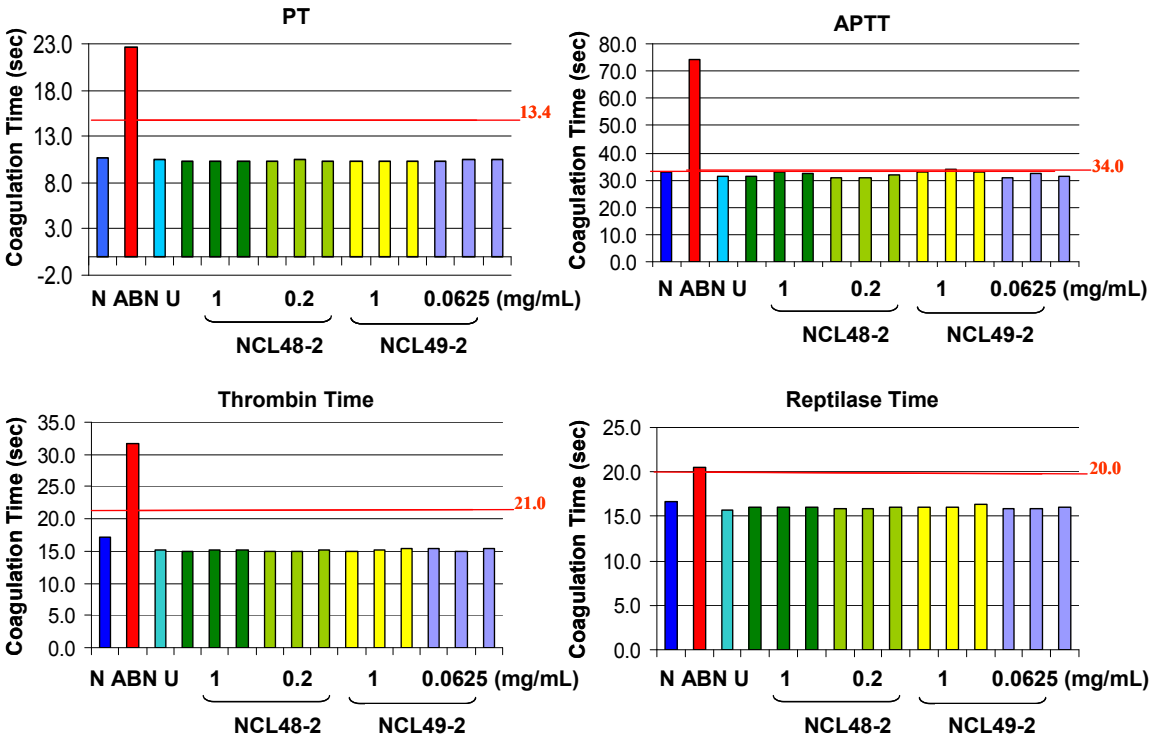

Figure 32. Analysis of nanoparticle effect on coagulation – batch 2, donor group 1B (ITA-12). This figure presents potential particle effects on the biochemical component of the blood coagulation cascade. For each nanoparticle, three independent samples were prepared and analyzed in duplicate (%CV < 5%). Each bar represents the mean of duplicate results. Normal plasma standard (N) and abnormal plasma standard (ABN) were used for the instrument control. Plasma pooled from at least three donors was either untreated (Unt.) or treated with nanoparticle preparations NCL48-2 or NCL49-2. The dotted red line indicates the clinical standard cut-off for normal coagulation time for each of the tests. NCL48-2 and NCL49-2 at both high (1mg/mL) and low (0.2 and 0.0625mg/mL, respectively) do not interfere with plasma coagulation in prothrombin time (PT), activated partial thromboplastin time (APTT), thrombin and reptilase time tests.

Analysis and Conclusions

None of NCL48-1, NCL49-1, NCL48-2, and NCL49-2 interfere with plasma coagulation *in vitro*.

Nanoparticle Effects on CFU-GM Formation (ITA-3)

Design and Methods

The objective of this experiment was to evaluate liposome effects on CFU-GM formation *in vitro*. NCL protocol ITA-3 was followed**.** Both nanoparticle formulations were tested at two concentrations: high (1mg/mL) and low (0.2 mg/mL for NCL48-2 and 0.0625 mg/mL for NCL49-2)

Results

Batch 2: Low concentrations of NCL48-2 and NCL49-2, and high concentration of NCL48-2 result in ~2-fold reduction in number of CFU-GM, while high concentration of NCL49-2 is as myelosuppressive as cisplatin ($p<0.05$) (Figure 28).

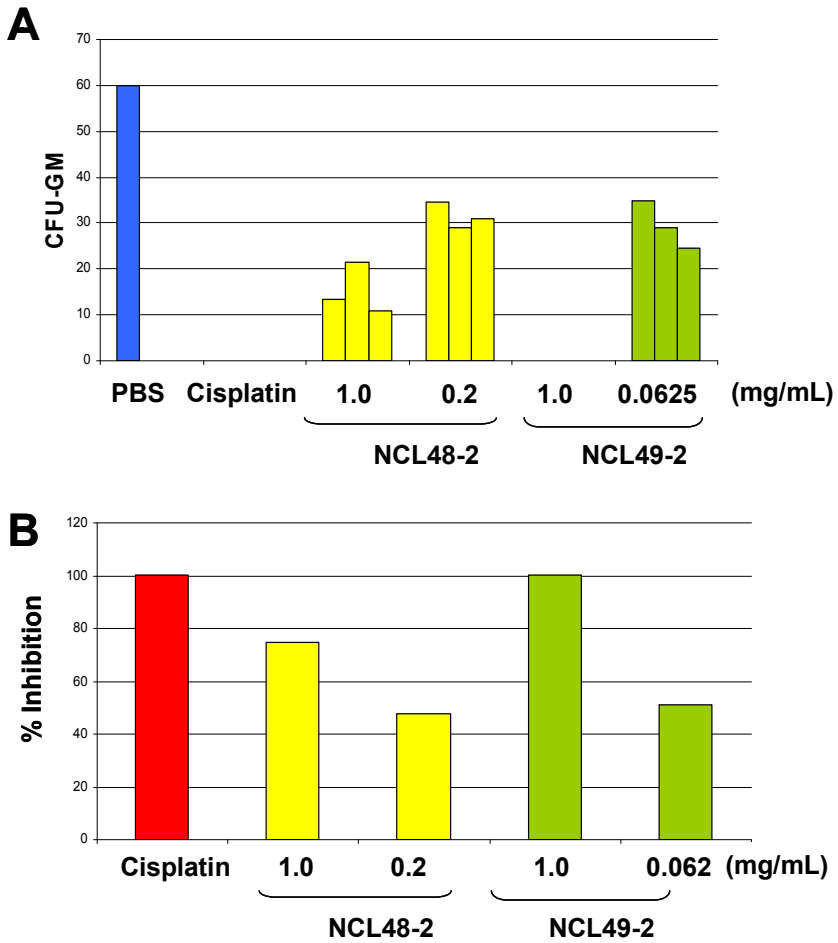

Figure 33. Analysis of nanoparticle effects on CFU-GM formation (ITA-3). NCL48-2 and NCL49-2, at either high (1 mg/mL) or low (0.2 and 0.0625 mg/mL, respectively) concentration, were used to evaluate potential particle effects on the formation of granulocyte-macrophage colonies from bone marrow precursors. For each nanoparticle concentration, three independent samples were prepared and analyzed in duplicate (%CV < 20%). Each bar represents the mean of duplicate results. Cisplatin and PBS were used as a positive and negative control, respectively: (A) This graph shows number of CFU-GM for each sample. (B) This graph summaries % CFU-GM inhibition calculated by comparing number of GM colonies in each treatment with that in negative control sample.

Analysis and Conclusions

Under *in vitro* conditions NCL48-2 at both concentrations and NCL49 at low concentration reduced number of GM colonies. NCL49-2 at high concentration completely suppressed CFU-GM formati on *in vitro*. Analysis of bone marrow precursors *in vivo* is required to prove this finding.

Complement Activation (ITA-5)

Design and Methods

The objective of this experiment was to evaluate liposome effects on human complement system. NCL protocol ITA-5 was followed**.** Both nanoparticle formulations were tested at two concentrations: high (1mg/mL) and low (0.2 mg/mL for NCL48-2 and 0.0625 mg/mL for NCL49-2).

Results

Batch 2: A qualitative test for complement activation demonstrated that both formulations may induce activation of human complement system as evident by appearance of an extra band corresponding to C3 split product (Figure 34).

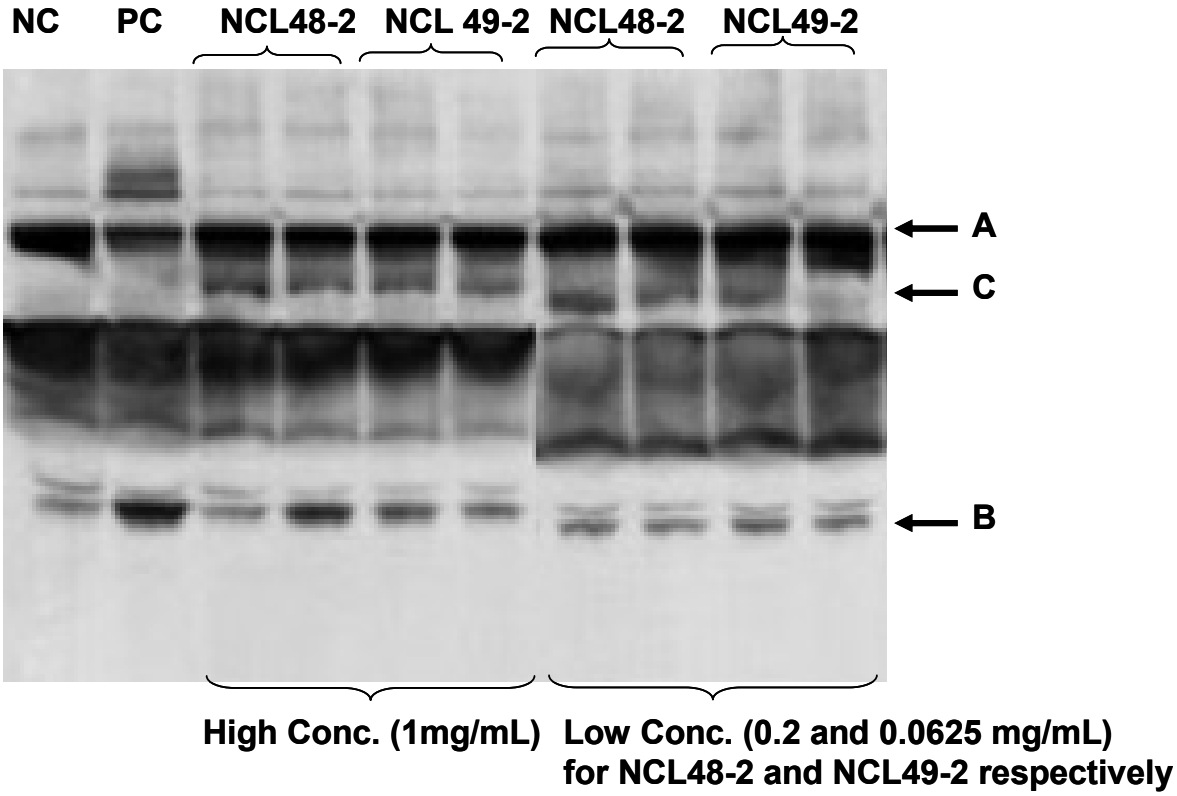

Figure 34. Analysis of complement activation (ITA-5). NCL48-2 and NCL49-2 were tested for their ability to activate a complement at high (1mg/mL) and low concentrations (0.2 and 0.0625 mg/mL for NCL48-2 and NCL49-2, respectively). Two independent samples were prepared for each formulation and each sample was analyzed in duplicate. PBS and cobra venom factor (CVF) were used as the negative and positive control, respectively. At both concentrations NCL48-2 and NCL49-2 induced complement activation, evidenced by the appearance of split product (bands C). Band A is the full length C3, and band B is the final C3 split product

Analysis and Conclusions

More sensitive quantitative assay is needed to prove the finding that NCL48-2 and NCL49-2 may induce complement activation *in vitro*. Analysis of complement activation by quantitative assay is on hold until inter-lot variability in size is addressed by vendor.

Nanoparticle Effect on Leukocyte Proliferation (ITA-6)

Design and Methods

The objective of this experiment was to evaluate liposome effects on proliferation of human leukocytes *in vitro*. NCL protocol ITA-6 was followed**.** Both nanoparticle formulations were tested at two concentrations: high (1mg/mL) and low (0.2 mg/mL for NCL48-2 and 0.0625 mg/mL for NCL49-2)

Results

Batch 2: NCL48-2 and NCL49-2 at both concentrations did not induce leukocyte proliferation. NCL49-2 was toxic to leukocytes at both concentrations. High concentration NCL48-2 and NCL49-2 resulted in ~70 and ~90% inhibition of proliferation induced by PHA-M, respectively. At low concentrations NCL48-2 was less toxic (% proliferation inhibition ~40), while NCL49-2 resulted in ~80% inhibition of PHA-M induced proliferation (Figure 35).

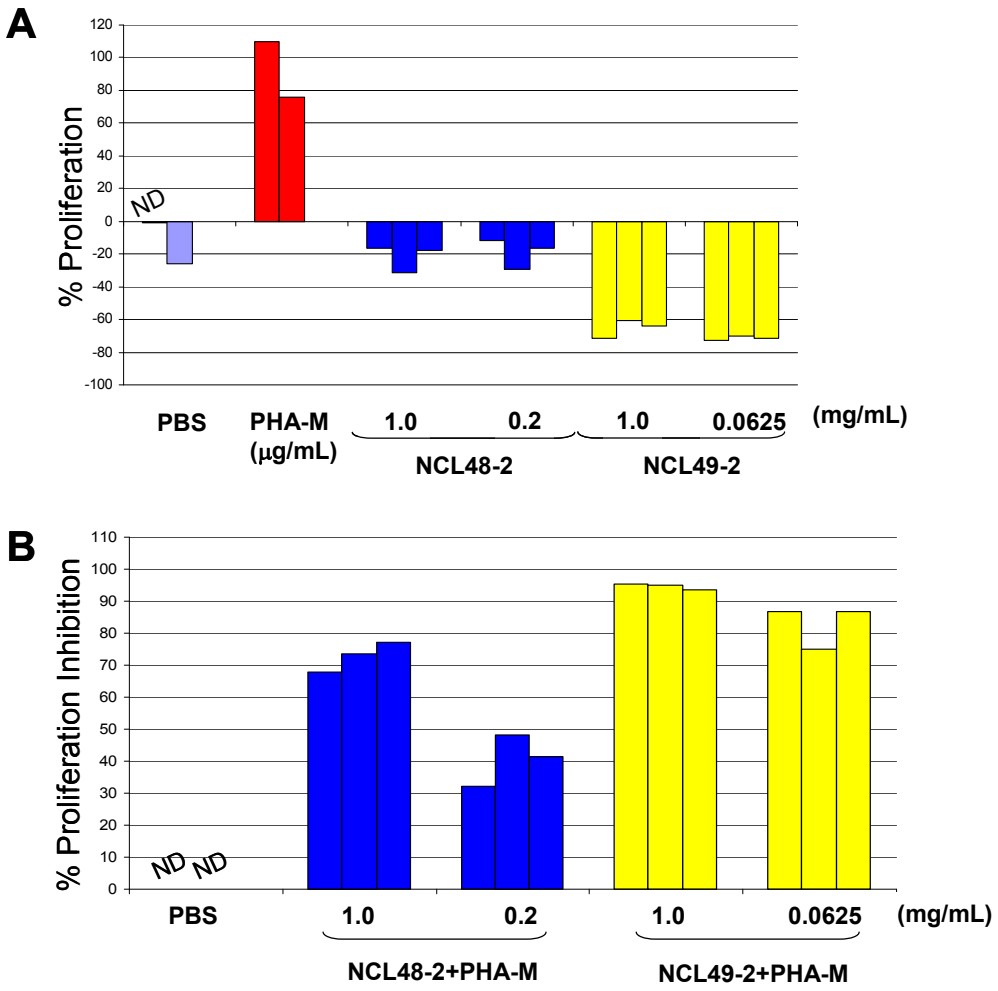

Figure 35. Analysis of nanoparticle effect on leukocyte proliferation (ITA-6). NCL48-2, and NCL49-2 at high (1mg/mL) and low (0.2 and 0.0625 mg/mL, respectively) were evaluated in leukocyte proliferation test. Three independent samples were prepared for each formulation and analyzed in duplicate (%CV<25%). Phytohemaglutinin-M (PHA-M) was used as a positive control for proliferation induction. PBS was used as a negative control. Each bar represents the mean of duplicate results. ND indicates no detectable result. A) Both formulation did not induced proliferation and were toxic to PBMC cultures (toxicity is evident by MTT values lower that that of untreated cells). B) PHA-M treatment was combined with nanoparticles to test for potential particles' interference with known proliferation stimulus. At high concentration NCL48-2 and NCL49-2 resulted in ~70 and ~90% proliferation inhibition, respectively. At low concentrations NCL48-2 was less toxic (% proliferation inhibition ~40), while NCL49-2 resulted in ~80% inhibition of PHA-M induced proliferation.

Analysis and Conclusions

At both concentrations NCL48-2 and NCL49-2 did not induce proliferation of human leukocytes *in vitro*. NCL49-2 at both concentrations and NCL48-2 at high concentration suppressed leukocyte proliferation induced by PHA-M. NCL48-2 at low concentration slightly inhibited proliferation of human leukocytes treated with PHA-M.

Nitric Oxide Production by Macrophages (ITA-7)

Design and Methods

The objective of this experiment was to evaluate liposome effects on oxidative burst of macrophages *in vitro*. NCL protocol ITA-7 was followed**.** Both nanoparticle formulations were tested at two concentrations: high (1mg/mL) and low (0.2 mg/mL for NCL48-2 and 0.0625 mg/mL for NCL49-2)

Results

Batch 2: Treatment of RAW264.7 macrophage cell line with either high or low concentration of NCL48-2 and NCL49-2 did not induce oxidative burst as evident by lack of nitric oxide secretion into culture medium (Figure 36).

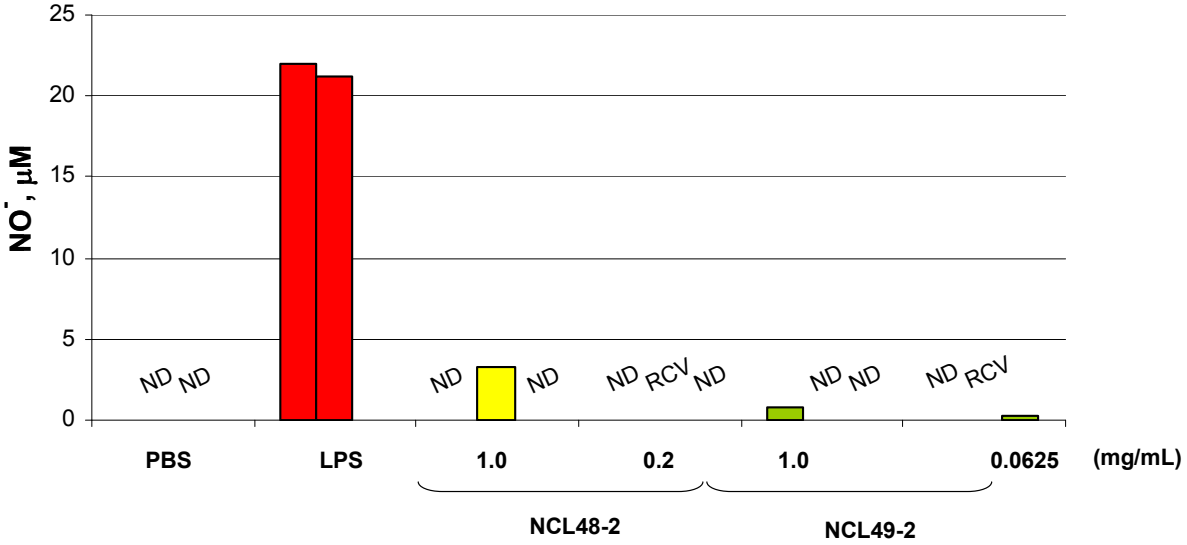

Figure 36. Analysis of nitric oxide (NO^-) production by macrophages (ITA-7). NCL48-2 and NCL49-2 were analyzed at high (1 mg/mL) and low (0.2 and 0.0625 mg/mL respectively) concentrations. For each concentration, three independent samples were prepared and analyzed in duplicate (%CV < 25%). Each bar represents the mean of duplicate results. NCL48-2 and NCL49-2 did not induce NO^- production. PBS and bacterial LPS were used as a negative and positive control, respectively. RCV indicates that the %CV>25%, data were not accepted for these samples.

Analysis and Conclusions

NCL48-2 and NCL49-2 did not induce nitric oxide production by macrophages *in vitro.*

Nanoparticle Effect on Chemotaxis (ITA-8)

Design and Methods

The objective of this experiment was to evaluate liposome effects on chemotactic mobility of macrophages. NCL protocol ITA-8 was followed**.** Both nanoparticle formulations were tested at two concentrations: high (1mg/mL) and low (0.2 mg/mL for NCL48-2 and 0.0625 mg/mL for NCL49-2)

Results

Batch 2: At high concentration both NCL48-2 and NCL49-2 induced chemotaxis of macrophage like cell line HL-60. No chemotaxis was seen in cells when low concentrations of both formulations were used (Figure 37).

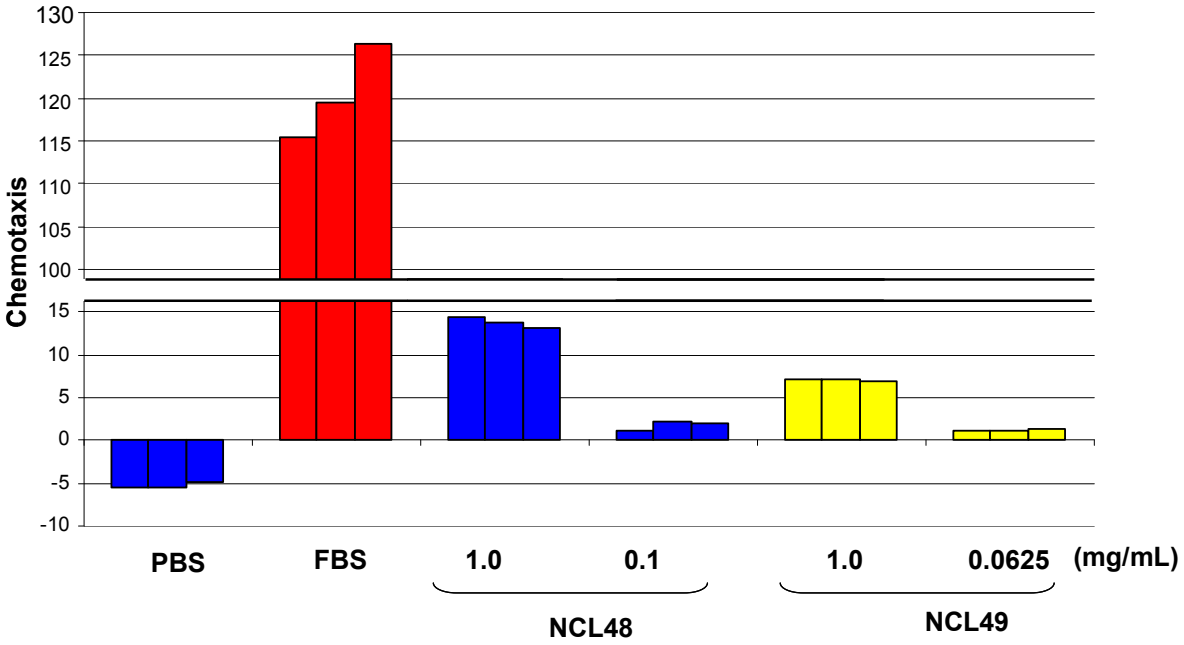

Figure 37. Analysis of nanoparticle effect on chemotaxis (ITA-8). NCL48-2 and NCL49-2 at high and low concentrations were used to test chemotaxis of HL-60 macrophage-like cells. PBS and FBS were used as negative and positive controls, respectively. Three independent samples were prepared for each formulation and analyzed in triplicate (%CV<25). Shown is the mean of triplicate results for each sample. Results demonstrate that at high concentration both NCL48-2 and NCL49-2 acted as chemoattractants. Low chemotaxis rate by NCL49-2 may be attributed to ceramide toxicity to migrated macrophages.

Analysis and Conclusions

NCL49-2 and NCL49-2 are capable of including macrophage chemotaxis *in vitro*.

Phagocytosis Assay (ITA-9)

Design and Methods

The objective of this experiment was to evaluate liposome effects on phagocytosis of zymosan A and their phagocytic uptake *in vitro*. NCL protocol ITA-9 was followed**.** Both nanoparticle formulations were tested at a concentration of 0.5 mg/mL

Results

Batch 2: Neither NCL48-2 nor NCL49-2 were internalized by macrophages via phagocytosis, however both formulations slightly reduced uptake of zymosan A (Figure 38).

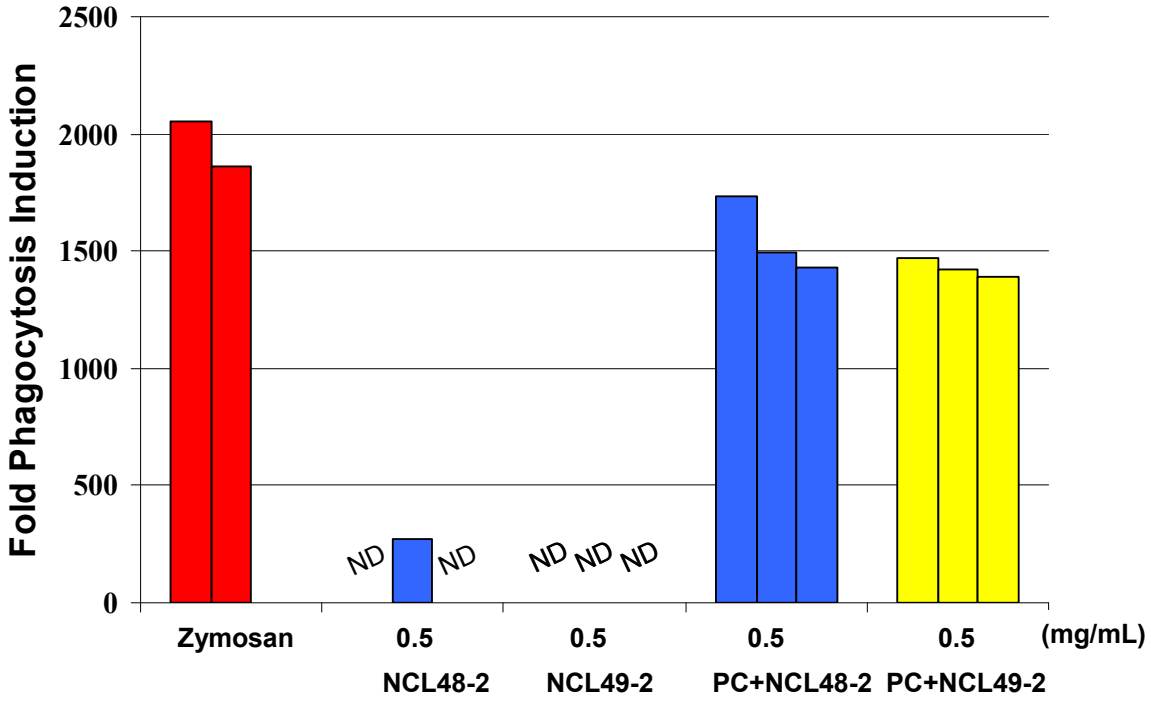

Figure 38. Phagocytosis assay (ITA-9). NCL48-2 and NCL49-2 were analyzed 0.5 mg/mL concentration. For each preparation, three independent samples were prepared and analyzed in duplicate (%CV < 25%). Each bar represents the mean of duplicate results. ND indicates no detectable result. Zymosan A was used as positive control. NCL48-2 and NCL49-2 were not internalized via phagocytosis by macrophages. Both formulations slightly reduced uptake of zymosan A.

Analysis and Conclusions

In vitro indirect phagocytosis assay did not reveal liposome uptake via phagocytosis. This assay is not sensitive to other mechanisms of uptake, such as for example liposome fusion with the macrophage membrane. This indirect assay demonstrated a reduction in phagocytosis of yeast particle zymosan A by macrophages *in vitro*.

In Vivo ADME Toxicology

Section Summary

Ceramide, an endogenous sphingolipid derived membrane component, has been shown to have antiproliferative and proapoptotic properties in cancer cell lines (Padron, 2006). Ceramide has also been reported to have additive anticancer effects when combined with current chemotherapeutics *in vitro* (Mehta et al., 2000). The use of ceramide as a chemotherapeutic agent is limited due to its low solubility. For this reason, a liposomal delivery system has been developed to increase ceramide solubility and achieve therapeutic doses. Liposomal formulation of ceramide was shown to enhance ceramide's potency against cancer cells *in vitro*, and liposomal ceramide has proven anticancer activity in murine breast adenocarcinoma models (Stover and Kester, 2003; Stover et al., 2005). Other advantages of the liposomal delivery system includes the ability to shield the ceramide from metabolism, and vary size, charge and surface properties during formulation to optimize biocompatibility and disposition, e.g. biocompatible polymers, such as polyethylene glycol (PEG), have been incorporated to prevent elimination by the reticulo-endothelial system (RES) and increase plasma half-life.

Expanded acute toxicology studies in rats for the ceramide liposome were negative for all signs of systemic toxicity, at the maximum intravenous dose achievable. No biologically significant changes in mortality, body weight, organ weight, clinical chemistry, hematology, gross pathology, or histology were observed between control and treatment groups.

14-Day Acute Toxicity Study in Rats

Design and Methods

The purpose of this study was to identify any acute toxicities resulting from intravenous administration of ceramide liposome (NCL49-2) to rats. A dose of 50 mg NCL49-2/kg, corresponding to 15 mg ceramide /kg at 30% (w/w) ceramide liposome loading, was administered to rats by tail vein injection at a dosing volume of 2 mL/kg. This 50 mg NCL49-2/kg dose represents the maximum ceramide liposome dose achievable in this animal model, due to constraints regarding ceramide loading, liposome stability, and dosing volume. Toxicological endpoints were evaluated at 2 and 14 days post dose. No biologically significant changes in body weight, organ weight, clinical chemistry, hematology, gross pathology or histology were observed at this dose level in this animal model.

The animal model utilized was 10-week-old Sprague Dawley rats, three animals per treatment group per sex. The study included both a 2-day interim and 14-day main study, with a 50 mg/kg NCL59 treatment group and a 50 mg/kg NCL 58 vehicle control group (Table 13). Drug or vehicle control was administered by tail vein at 2 mL/ kg body weight. Animals were monitored daily for mortality and signs of pharmacologic or toxicologic effects. Body weights were measured previous to dosing, on study days 3 and 7, and at study termination. The animals were sacrificed by CO_2 asphyxiation 14 days post dose, and blood was removed by cardiac puncture for hematology and clinical chemistry. Necropsy consisted of organ weights, gross organ description and histopathology.

Table 13. Dose Groups

TEST GROUP	DOSE TO ANIMALS (mg/kg body-weight, tail vein)	VOLUME (mL/kg BW)	NUMBER OF MALES	NUMBER OF FEMALES
2- DAY INTERIM NCL48-2	50 mg/kg	**2**	**3**	**3**
2- DAY INTERIM NCL49-2	50 mg/kg	**2**	**3**	**3**
14- DAY MAIN NCL48-2	50 mg/kg	**2**	**3**	**3**
14- DAY MAIN NCL49-2	50 mg/kg	**2**	**3**	**3**

Husbandry

Animals were acclimated to the study environment for two weeks prior to study initiation. Animal rooms were kept at 50% relative humidity, 68-72 F with 12 hour light/dark cycles. Rats were housed by treatment group, with two animals/cage (Rat polycarbonate cage type), with ¼" corncob bedding. Animals were allowed *ad libitum* access to Purina 18% NIH Block and Chlorinated tap water.

Statistical Methods

Statistical analysis was conducted separately for each sex and study time point, using the software program Statistica version 7.1 (StatSoft, Inc., Tulsa, OK.). Statistical differences for parametric data were determined by Student's t-test. Statistical differences for nonparametric data were determined by the Mann-Whitney U Test.

In-Life Results

Clinical Observations: No abnormal clinical observations were noted for any of the animals in any of the treatment groups. All animals, in all treatment groups, survived to the scheduled study termination.

Body Weight Change: The animals in all treatment groups gained weight during the 14-day study period (Table 14). No significant difference in body weight change from control values were noted for any of the in-life body weight measurement periods.

Table 14. Body Weight Change for NCL59 Acute Toxicology Study.

A. Interim Study Body Weight

Day	Male Vehicle Interim Mean, g	SD	Male NCl 48 Interim Mean, g	SD	Female Vehicle Interim Mean, g	SD	Female NCL 48 Interim Mean, g	SD
3	5	5	2	4	4	9	1	4

B. Main Study Body Weight

Day	Male Vehicle Interim Mean, g	SD	Male NCL 48 Interim Mean, g	SD	Female Vehicle Interim Mean, g	SD	Female NCL 48 Interim Mean, g	SD
3	-2	2	-4	6	-1	7	-2	2
7	10	3	17	5	5	9	5	1
15	33	21	33	21	15	25	36	28

Note:The change in animal body weight from pre-treatment values is displayed by treatment group for the interim (**A**) and main (**B**) study. Data is presented as the Mean ± SD (*N*=3).

Necropsy Results

Organ Weights: In the interim study, female kidney absolute weight and female spleen % brain weight values for the NCL48-2 control and NCL49-2 treated rats were significantly different from each other (Table 15 A). In the main study, male kidney % body weight, male spleen absolute weight, female liver % body weight and female spleen % body weight values for the NCL48-2 control and NCL49-2 treated rats were significantly different from each other (Table 15 B). No significant differences in the remaining organ weights (absolute, % body weight or % brain weight) or terminal body weight were observed between the two treatment groups (Table 15 A and B).

Table 15. Organ Weights for NCL49-2 Acute Toxicology Study.

A. Interim Study Organ Weights and Terminal Body Weights

SEX		MALE		FEMALE	
DOSE GROUP		**NCL48-2 CONTROL**	**NCL49-2**	**NCL48-2 CONTROL**	**NCL49-2**
NUMBER OF ANIMALS		3	3	3	3
BODY WEIGHT (gram)[a]		327 ± 25	346 ± 15	209 ± 10	219 ± 14
BRAIN					
Absolute Weight	gram	1.95± 0.10	1.94 ± 0.05	1.83 ± 0.10	1.93 ± 0.24
Per Body Weight	%	0.60± 0.07	0.56 ± 0.04	0.87 ± 0.00	0.89 ± 0.09
HEART					
Absolute Weight	gram	1.30± 0.09	1.40 ± 0.15	0.93 ± 0.15	0.97 ± 0.07
Per Body Weight	%	0.40± 0.05	0.40 ± 0.04	0.45 ± 0.09	0.44 ± 0.04
Per Brain Weight	%	67.04± 6.02	72.11 ± 7.27	51.20 ± 11.05	50.19 ± 3.32
KIDNEYS					
Absolute Weight	gram	2.73± 0.07	2.87 ± 0.18	1.52 ± 0.08	1.76 ± 0.09*
Per Body Weight	%	0.84± 0.08	0.83 ± 0.03	0.73 ± 0.03	0.80 ± 0.08
Per Brain Weight	%	140± 5	148 ± 12	83 ± 4	91 ± 6
LIVER					
Absolute Weight	gram	14.93± 1.04	15.05 ± 0.89	8.30 ± 1.26	8.43 ± 1.13
Per Body Weight	%	4.57± 0.04	4.35 ± 0.30	3.96 ± 0.40	3.94 ± 0.28
Per Brain Weight	%	770± 91	777 ± 45	452 ± 52	438 ± 75
SPLEEN					
Absolute Weight	gram	0.62± 0.01	0.71 ± 0.08	0.43 ± 0.02	0.43 ± 0.03
Per Body Weight	%	0.19± 0.02	0.20 ± 0.03	0.21 ± 0.00	0.20 ± 0.02
Per Brain Weight	%	32.03± 1.32	36.44 ± 3.28	23.51 ± 0.42	22.41 ± 0.42*
LUNG					
Absolute Weight	gram	1.67± 0.15	2.21 ± 0.47	1.33 ± 0.10	1.29 ± 0.08
Per Body Weight	%	0.52± 0.08	0.64 ± 0.14	0.64 ± 0.02	0.59 ± 0.03
Per Brain Weight	%	85± 7	114 ± 23	73 ± 2	67 ± 7

B. Main Study Organ Weights and Terminal Body Weights

SEX		MALE		FEMALE	
DOSE GROUP		**NCL48-2 CONTROL**	**NCL49-2**	**NCL48-2 CONTROL**	**NCL49-2**
NUMBER OF ANIMALS		3	3	3	3
BODY WEIGHT (gram)[a]		330± 53	321 ± 73	237 ± 31	271 ± 81
BRAIN					
Absolute Weight	gram	1.95± 0.10	1.94 ± 0.05	1.83 ± 0.10	1.93 ± 0.24
Per Body Weight	%	0.60± 0.07	0.56 ± 0.04	0.87 ± 0.00	0.89 ± 0.09
HEART					
Absolute Weight	gram	1.30± 0.21	1.08 ± 0.19	0.94 ± 0.19	0.89 ± 0.09
Per Body Weight	%	0.41± 0.09	0.34 ± 0.03	0.39 ± 0.05	0.34 ± 0.06
Per Brain Weight	%	68.32± 11.42	56.55 ± 8.79	51.02 ± 8.31	53.67 ± 12.42
KIDNEYS					
Absolute Weight	gram	2.96± 0.47	2.18 ± 0.65	1.66 ± 0.21	1.83 ± 0.47
Per Body Weight	%	0.90± 0.11	0.68 ± 0.08*	0.70 ± 0.04	0.68 ± 0.04
Per Brain Weight	%	152± 24	114 ± 28	90 ± 7	113 ± 44
LIVER					
Absolute Weight	gram	16.05± 2.58	12.61 ± 3.07	8.11 ± 1.36	10.99 ± 3.02
Per Body Weight	%	4.94± 1.08	3.93 ± 0.25	3.41 ± 0.17	4.08 ± 0.10*
Per Brain Weight	%	825± 141	661 ± 139	441 ± 48	676 ± 279
SPLEEN					
Absolute Weight	gram	0.71± 0.09	0.51 ± 0.05*	0.42 ± 0.10	0.57 ± 0.15
Per Body Weight	%	0.22± 0.04	0.16 ± 0.04	0.18 ± 0.02	0.21 ± 0.01*
Per Brain Weight	%	36.46± 5.12	27.01 ± 4.66	22.97 ± 3.90	35.01 ± 14.19
LUNG					
Absolute Weight	gram	1.72± 0.50	1.45 ± 0.14	1.30 ± 0.18	1.33 ± 0.10
Per Body Weight	%	0.54± 0.22	0.46 ± 0.08	0.55 ± 0.06	0.52 ± 0.12
Per Brain Weight	%	88± 27	76.± 11	71 ± 7	80 ± 14

Note:The organ weights for the interim (**A**) and main (**B**) studies are displayed both as absolute values, % body weight, and % brain weight. Data is presented as the Mean ± SD (*N*=3).
***Significantly different from control, p<0.05 (Student's t-test)**

Clinical Chemistry Parameters: In the interim study, statistically significant differences were observed between the NCL48-2 control and NCL49-2 treated female rats for phosphate, urea nitrogen, albumin and total protein values (Table 16 A). Of note, alkaline phosphatase values for both the male and female NCL49-2 treated rats were approximately 50% of NCL48-2 control values. No statistically significant differences in the remaining clinical chemistry parameters were observed for this study period.

In the main study, statistically significant differences were observed between the NCL48-2 control and NCL49-2 treated female rats for sodium, amylase, alkaline phosphatase, albumin and total protein values (Table 16 B). No statistically significant differences in the remaining clinical chemistry parameters were noted for this study period.

Table 16. Clinical Chemistry Parameters for NCL59 Acute Toxicology Study.

A. Interim Study Clinical Chemistry

SEX		MALE		FEMALE	
DOSE GROUP		NCL48-2 CONTROL	NCL49-2	NCL48-2 CONTROL	NCL49-2
NUMBER OF ANIMALS		3	3	3	3
ELECTROLYTE BALANCE					
Calcium	mmol/L	12.27±0.23	12.50±0.75	12.53±0.72	12.70±0.46
Phosphate	mmol/L	10.57±1.91	9.47±0.23	12.37±0.50	9.50±0.98*
Potassium	mmol/L	6.60±0.20	6.40±0.17	7.03±0.47	6.63±0.85
Sodium	mmol/L	157.00±2.00	155.67±3.06	157.67±3.06	154.67±2.08
CARBOHYDRATE METABOLISM					
Glucose	mmol/L	167.67±10.79	160.67±23.50	191.33±32.32	141.67±19.86
PANCREATIC FUNCTION					
Amylase	U/L	872±66	820±81	897±62	756±168
LIVER FUNCTION: A) HEPATOBILIARY					
Total Bilirubin	mg/dL	0.3±0.0	0.3±0.1	0.3±0.0	0.3±0.0
LIVER FUNCTION: B) HEPATOCELLULAR					
Alanine Aminotransferase (ALT or SGPT)	U/L	61±22	43±2	56±5	41±10
KIDNEY FUNCTION					
Creatinine	μmol/L	<0.2	<0.2	<0.2	<0.2
Urea Nitrogen	mg/dL	11±1	10±1	13±1	11±1*
OTHERS					
Albumin (A)	g/L	4.43±0.32	5.20±0.61	4.37±0.06	5.40±0.10*
Alkaline Phosphatase (ALP)	U/L	203±8	118±13*	263±83	119±21*
Globulin (G, calculated)	g/L	2.00±0.10	2.13±0.06	1.97±0.42	1.97±0.15
A/G Ratio		2.22±0.18	2.13±0.06	1.97±0.42	1.97±0.16
Total protein	g/L	2.22±0.18	2.44±0.33	2.30±0.55	2.76±0.27*

B. Main Study Clinical Chemistry

SEX		MALE		FEMALE	
DOSE GROUP		NCL48-2 CONTROL	NCL49-2	NCL48-2 CONTROL	NCL49-2
NUMBER OF ANIMALS		3	2	3	3
ELECTROLYTE BALANCE					
Calcium	mmol/L	13.67±1.22	12.90±0.42	12.50±0.75	12.67±0.50
Phosphate	mmol/L	13.27±0.50	10.95±2.62	10.97±0.45	10.53±1.15
Potassium	mmol/L	7.17±1.00	5.85±0.78	6.70±0.78	6.13±1.35
Sodium	mmol/L	159±3	154±0.00	160±4	153±2*
CARBOHYDRATE METABOLISM					
Glucose	mmol/L	263±162	189±84	140±31	157±3
PANCREATIC FUNCTION					
Amylase	U/L	978±136	713±98	1008±68	668±43*
LIVER FUNCTION: A) HEPATOBILIARY					
Total Bilirubin	mg/dL	0.40±0.00	0.35±0.07	0.30±0.00	0.30±0.00
LIVER FUNCTION: B) HEPATOCELLULAR					
Alanine Aminotransferase (ALT or SGPT)	U/L	53±6	54±7	63±21	42±6
KIDNEY FUNCTION					
Creatinine	μmol/L	<0.2	<0.2	<0.2	<0.2
Urea Nitrogen	mg/dL	13±2	13±1	10±3	10±1
OTHERS					
Albumin (A)	g/L	4.57±0.21	4.85±0.49	4.53±0.06	5.10±0.26*
Alkaline Phosphatase (ALP)	U/L	380±103	170±31	303±34	200±53*
Globulin (G, calculated)	g/L	2.00±0.10	2.13±0.06	1.97±0.42	1.97±0.15
A/G Ratio		2.22±0.18	2.44±0.33	1.97±0.42	1.97±0.15
Total protein	g/L	6.40±0.40	7.33±0.58	6.33±0.40	7.37±0.06*

Note: Data is presented as the Mean ± SD, for both the interim (**A**) and main (**B**) studies.
***Significantly different from control, p<0.05 (Student's t-test)**

Hematology Parameters: In the interim study, statistically significant differences were observed between the NCL48-2 control and NCL49-2 treated male rats for total erythrocyte count and red cell distribution width values (Table 17 A). No statistically significant differences in the remaining hematology parameters were noted for this study period.

In the main study, statistically significant differences from control were observed for the granulocyte count in male rats and red cell distribution width in female rats (Table 17 B). No statistically significant differences in the remaining hematology parameters were noted for this study period.

Table 17. Hematology Parameters for NCL59 Acute Toxicology Study.

A. Interim Study Hematology

SEX		MALE		FEMALE	
DOSE GROUP		**NCL48-2 CONTROL**	**NCL49-2**	**NCL48-2 CONTROL**	**NCL49-2**
NUMBER OF ANIMALS		3	3	3	3
Red Blood Cells					
Hematocrit (Hct)	%	46.60±1.27	44.88±0.59	43.18±2.44	43.80±1.25
Hemoglobin Conc. (Hb)	g/dL	15.7±0.4	15.2±0.1	14.7±0.6	15.4±0.2
Mean Corp. Hb. (MCH)	pg	20.7±0.5	21.2±0.1	20.7±0.4	20.87±0.45
Mean Corp. Hb. Conc. (MCHC)	g/dL	33.73±0.81	23.87±17.38	34.2±1.0	35.2±0.61
Mean Corp. Volume (MCV)	fL	61±2	63±1	60±2	59±3
Total Erythrocyte Count (RBC)	M/µL	7.61±0.06	7.17±0.08*	7.13±0.41	7.39±0.15
Red Cell Distribution Width	%	18.0±0.5	16.3±0.6*	17.4±0.5	17±0.26
White Blood Cells					
Lymphocytes	10^3/µL	7.61±1.54	6.9±2.7	5.9±2.0	3.46±1.45
Macrophage/ Monocytes	10^3/µL	0.23±0.19	0.57±0.68	0.33±0.17	0.10±0.10
Granulocytes	10^3/µL	1.76±0.31	1.15±0.36	0.96±0.36	1.23±0.31
Total Leukocytes (WBC)	10^3/µL	9.60±1.77	8.64±3.70	7.17±2.29	4.78±1.41
Clotting Potential					
Platelet Count (PLT)	10^3/µL	807±136	925±75	645±165	249±411
Mean Platelet Volume (MPV)	fL	8.1±0.2	7.6±0.4	7.67±0.84	7.83±0.40
Platelet Distribution Width (PDW)	%	34.1±1.2	34.5±1.6	34.07±2.97	34.13±0.70
Plateletcrit (PLT)	%	0.66±0.11	0.7±0.03	0.49±0.14	0.75±0.13

B. Main Study Hematology

SEX		MALE		FEMALE	
DOSE GROUP		MALE NCL48-2 CONTROL	MALE NCL49-2	NCL48-2 CONTROL	NCL49-2
NUMBER OF ANIMALS		3	3	3	3
Red Blood Cells					
Hematocrit (Hct)	%	45.05±0.95	43.56±1.64	30.55±22.78	45.46±0.47
Hemoglobin Conc. (Hb)	g/dL	15.2±0.3	15.1±0.7	14.9±0.7	15.4±0.2
Mean Corp. Hb. (MCH)	pg	20.2±0.8	20.0±0.7	19.9±0.7	20.9±0.3
Mean Corp. Hb. Conc. (MCHC)	g/dL	33.90±0.26	34.53±0.35	33.3±0.6	33.8±0.7
Mean Corp. Volume (MCV)	fL	59.67±2.31	58.00±1.73	60±2	59±0
Total Erythrocyte Count (RBC)	M/µL	7.58±0.43	7.50±0.33	7.53±0.49	7.68±0.06
Red Cell Distribution Width	%	18.2±0.4	16.5±0.5	18.1±0.3	16.7±0.5*
White Blood Cells					
Lymphocytes	10^3/µL	6.58±3.49	8.86±5.00	8.01±4.29	9.19±1.90
Macrophage/ Monocytes	10^3/µL	0.60±0.81	0.50±0.81	0.67±0.57	0.57±0.16
Granulocytes	10^3/µL	0.18±0.27	1.11±0.60**	1.12±0.44	1.26±0.70
Total Leukocytes (WBC)	10^3/µL	7.36±4.08	10.47±5.47	9.87±5.29	11.33±6.35
Clotting Potential					
Platelet Count (PLT)	10^3/µL	ND	815±52	993±185	721±51
Mean Platelet Volume (MPV)	fL	ND	7.1±0.4	8.4±7.6	7.37±0.32
Platelet Distribution Width (PDW)	%	ND	33.1±0.8	34.5±1.6	33.4±1.1
Plateletcrit (PLT)	%	ND	0.57±0.02	0.79±0.09	0.53±0.06

Note: Hematology parameters are displayed by treatment group for the interim (**A**) and main (**B**) studies. Data is presented as Mean ± SD.
ND= Data is not available due to sample clotting
***Significantly different from control, p<0.05 (Student's t-test)**
****Significantly different from control, p<0.05 (Mann-Whitney U Test)**

Gross Pathology: Gross lesions were observed in a small number of animals in both the interim and main studies, in both male and female rats, and in both control and NCL49-2 groups. (Table 18).

Table 18. Gross Pathology Findings.

		A. Interim Study Gross Pathology NUMBER OF ANIMALS WITH GROSS LESIONS			
	SEX	FEMALES		MALES	
	DOSE GROUP	NCL48-2 CONTROL	DOSE GROUP	NCL48-2 CONTROL	DOSE GROUP
	NUMBER OF ANIMALS EXAMINED	3	3	3	3
ORGAN/TISSUE	LESIONS				
LIVER	ALL LOBES, RETICULAR PATTERN	0	1	0	0
LYMPH NODE, MANDIBULAR	BOTH DISCOLORED	0	0	1	0
LUNG	ALL LOBES DISCOLORED, MOTTLED	1	2	0	0
UTERUS	BOTH HORNS ENLARGED	1	1		

		B. Main Study Gross Pathology NUMBER OF ANIMALS WITH GROSS LESIONS			
	SEX	FEMALES		MALES	
	DOSE GROUP	NCL48-2 CONTROL	DOSE GROUP	NCL48-2 CONTROL	DOSE GROUP
	NUMBER OF ANIMALS EXAMINED	3	3	3	3
ORGAN/TISSUE	LESIONS				
LIVER	ALL LOBES, RETICULAR PATTERN	0	0	2	1
LUNG	ALL LOBES DISCOLORED, MOTTLED	0	0	1	0
	FOCI	0	1	1	0
SPLEEN	GRANULAR	1	1	0	1

Note: Gross pathology findings are displayed by treatment group for the interim (**A**) and main (**B**) studies.

Histopathology: All lesions tabulated below are typical of background, spontaneous findings in this stock of rat (Table 19). The severity of these lesions were minimal to mild, and of no clinical significance. A significant difference in eosinophil infiltration in the stomach glandular

tissue was identified between NCL48-2 control and NCL49-2 treated male rats in the main study, as determined by Mann-Whitney U Test. No significant differences in lesion severity between the control NCL48-2 and NCL49-2 treated animals were identified for the remainder of the lesions, for both sexes and both timepoints (3 and 15 days post exposure).

Table 19. Histopathology Findings.

		A. Interim Study Histopathology NUMBER OF ANIMALS WITH HISTOPATHOLGICAL LESIONS			
	SEX	FEMALES		MALES	
	DOSE GROUP	NCL48-2 CONTROL	DOSE GROUP	NCL48-2 CONTROL	DOSE GROUP
	NUMBER OF ANIMALS EXAMINED	3	3	3	3
ORGAN/TISSUE	LESIONS				
ADRENAL	NONE				
BRAIN	NONE				
CECUM	HYPERPLASIA, GALT	0	0	1	0
CLITORAL GLAND	NONE				
COAGULATING GLAND	NONE				
COLON	HYPERPLASIA, GALT	1	0	0	0
DUODENUM	HYPERPLASIA, GALT	0	1	0	0
EPIDIDYMIS	NONE				
ESOPHAGUS	NONE				
EYE	INFLAMMATION, CHRONIC	0	0	1	1
	RUPTURE, LENS	0	0	1	0
FEMUR	NONE				
FEMUR, MARROW	NONE				
HARDERIAN GLAND	INFLAMMATION, SUBACUTE	0	1	0	0
	LYMPHOCYTIC INFILTRATE	1	0	0	0
	NECROSIS	0	1	0	0
HEART	LYMPHOCYTIC INFILTRATE	1	0	0	0
ILEUM	HYPERPLASIA, GALT	0	0	1	0
JEJUNUM	NONE				
KIDNEY	CYST				
	DEGENERATION, TUBULE	0	1	0	0
	LYMPHOCYTE INFILTRATE	0	0	2	1

		A. Interim Study Histopathology NUMBER OF ANIMALS WITH HISTOPATHOLGICAL LESIONS			
	SEX	FEMALES		MALES	
	DOSE GROUP	NCL48-2 CONTROL	DOSE GROUP	NCL48-2 CONTROL	DOSE GROUP
	NUMBER OF ANIMALS EXAMINED	3	3	3	3
ORGAN/TISSUE	LESIONS				
	MINERALIZATION	2	1	0	0

		A. Interim Study Histopathology NUMBER OF ANIMALS WITH HISTOPATHOLGICAL LESIONS			
	SEX	FEMALES		MALES	
	DOSE GROUP	NCL48-2 CONTROL	DOSE GROUP	NCL48-2 CONTROL	DOSE GROUP
	NUMBER OF ANIMALS EXAMINED	3	3	3	3
ORGAN/TISSUE	LESIONS				
LIVER	EXTRAMEDULLARY HEMATOPOIESIS	1	2	2	1
	INFLAMMATION, SUBACUTE	1	1	0	1
LYMPH NODE, MANDIBULAR	HEMORAGE	0	0	1	0
	HYPERPLASIA, LYMPHOID	3	3	2	3
	PLASMACYTOSIS	2	1	0	2
LYMPH NODE, MESNTERIC	DILATION, SINUSOIDS	1	0	1	0
	HYPERPLASIA, LYMPHOID	2	1	3	3
LUNG	HISTIOCYTOSIS, ALVEOLAR	1	1	2	0
	LYMPHOCYTIC INFILTRATE	2	3	2	1
	METAPLASIA, OSSEOUS	0	0	1	0
	MINERLAIZATION	2	2	1	3
	PNEUMOIA, CHRONIC ACTIVE	0	0	2	0
	VACULITIS, EOSINOPHILIC	1	1	1	1
MAMMARY GLAND	NONE				
NASAL SECTIONS	FOREIGN MATERIAL, LUMEN	1	0	0	0
	HYALINOSIS	1	0	0	0
	INFLAMMATION ACUTE	1	0	0	0
OVARY	NONE				
PANCREAS	LYMPHOCYTIC INFLITRATION	1	0	0	0
PARATHYROID	ECTOPIC THYMUS	2	0	0	1
PITUITARY	NONE				
PREPUTIAL GLAND	NONE				
PROSTATE	LYMPHOCYTIC INFLITRATION			1	0
RECTUM	NONE				
SALIVARY GLAND	BQASOPHILIC FOCUS, PAROTID	2	1	2	1
SEMINAL VESICLE	NONE				
SKIN/ SUBCUTIS	NONE				
SPINAL CORD	NONE				
SPLEEN	NONE				

		A. Interim Study Histopathology NUMBER OF ANIMALS WITH HISTOPATHOLGICAL LESIONS			
	SEX	FEMALES		MALES	
	DOSE GROUP	NCL48-2 CONTROL	DOSE GROUP	NCL48-2 CONTROL	DOSE GROUP
	NUMBER OF ANIMALS EXAMINED	3	3	3	3
ORGAN/TISSUE	LESIONS				
STOMACH, GLANDULAR	EOSINOPHILS	1	2	0	1
STOMACH, NONGLANDULAR	EOSINOPHILS	3	3	2	3
	HYPERPLASIA, SQUAMOS EPITHELIUM	0	2	0	0
TAIL	NONE				
TESTIS	NONE				
THYMUS	HEMMORAGE			0	1
THYROID	CYST, ULTIMOBRACHIAL	1	2	0	0
TONGUE	NONE				
TRACHEA	HYALINOSIS	3	3	2	3
	LUMPHOCYTIC INFILTRATE	1	0	1	0
URINARY BLADDER	COAGULUM, LUMEN	0	0	1	1
UTERUS	DILATION	1	2		
VERTEBRA	NONE				

		B. Main Study Histopathology NUMBER OF ANIMALS WITH HISTOPATHOLGICAL LESIONS			
	SEX	FEMALES		MALES	
	DOSE GROUP	NCL48-2 CONTROL	NCL49-2	NCL48-2 CONTROL	NCL49-2
	NUMBER OF ANIMALS EXAMINED	3	3	3	3
ORGAN/TISSUE	LESIONS				
ADRENAL	HYPERPLASIA CORTEX	0	0	1	0
BRAIN	NONE				
CECUM	HYPERPLASIA, GALT	0	1	0	0
	HYPERPLASIA, GOBLET CELLS	0	1	0	0
CLITORAL GLAND	NONE				
COAGULATING GLAND	NONE				
COLON	NONE				
DUODENUM	NONE				
EPIDIDYMIS	NONE				
ESOPHAGUS	NONE				
EYE	NONE				
FEMUR	NONE				
FEMUR, MARROW	NONE				
HARDERIAN GLAND	NONE				
HEART	METAPLASIA, CARTILAGENOUS	1	2	1	1
ILEUM	HYPERPLASIA, GALT	0	1	0	1
JEJUNUM	NONE				
KIDNEY	LYMPHOCYTE INFILTRATE	0	1	0	0
	MINERALIZATION	3	1	0	0
	NEPHROPATHY, CHRONIC	0	1	0	0

		B. Main Study Histopathology NUMBER OF ANIMALS WITH HISTOPATHOLGICAL LESIONS			
	SEX	FEMALES		MALES	
	DOSE GROUP	NCL48-2 CONTROL	NCL49-2	NCL48-2 CONTROL	NCL49-2
	NUMBER OF ANIMALS EXAMINED	3	3	3	3
ORGAN/TISSUE	LESIONS				
LIVER	EXTRAMEDULLARY HEMATOPOIESIS	1	1	2	1
	INFLAMMATION, SUBACUTE	1	1	0	1
	VACUOLATION, HEPATOCELLULAR	0	0	1	0
LYMPH NODE, MANDIBULAR	HYPERPLASIA, LYMPHOID	3	2	3	3
	PLASMACYTOSIS	2	1	0	2
LYMPH NODE, MESNTERIC	HYPERPLASIA, LYMPHOID	3	3	2	2
	PLASMACYTOSIS	1	0	1	0
LUNG	FOREIGN MATERIAL, ALVEOLAR LUMEN	0	0	1	0
	HEMMORRHAGE	1	2	2	0
	HISTIOCYTOSIS, ALVEOLAR	0	1	0	1
	INFLAMMATION, GRANULOMATOUS	0	0	0	1
	LYMPHOCYTIC INFILTRATE	1	2	1	0
	MINERALIZATION	1	2	2	2
	PNEUMOIA, CHRONIC ACTIVE	0	0	0	1
	VACULITIS, EOSINOPHILIC	1	2	0	1
MAMMARY GLAND	NONE				
NASAL SECTIONS	EXUDATE, NASOLACRIMAL DUCT	0	0	2	1
OVARY	HYPERPLASIA, SERTOLI CELL	1	0		
PANCREAS	ACCESSORY SPLEEN	0	0	1	0
	INFLAMMATION, CHRONIC	1	1	0	0
PARATHYROID	NONE				
PITUITARY	CYST	0	0	0	1
PREPUTIAL GLAND	NONE				
PROSTATE	LYMPHOCYTIC INFLITRATION			2	2
RECTUM	NONE				
SALIVARY GLAND	BQASOPHILIC FOCUS, PAROTID	1	2	2	3
	LYMPHOCYTIC INFILTRATE	0	0	1	0

		B. Main Study Histopathology NUMBER OF ANIMALS WITH HISTOPATHOLGICAL LESIONS			
	SEX	FEMALES		MALES	
	DOSE GROUP	NCL48-2 CONTROL	NCL49-2	NCL48-2 CONTROL	NCL49-2
	NUMBER OF ANIMALS EXAMINED	3	3	3	3
ORGAN/TISSUE	LESIONS				
	METAPLASIA, MUCINOUS, PAROTID	0	1	0	0
SEMINAL VESICLE	NONE				
SKIN/ SUBCUTIS	NONE				
SPINAL CORD	NONE				
SPLEEN	NONE				
STOMACH, GLANDULAR	EOSINOPHILS	3	3	3	0*
STOMACH, NONGLANDULAR	EOSINOPHILS	3	3	3	3
	HYPERPLASIA, SQUAMOS EPITHELIUM	0	0	0	2
TAIL	NONE				
TESTIS	NONE				
THYMUS	NONE				
THYROID	CYST, ULTIMOBRACHIAL	0	1	1	2
TONGUE	NONE				
TRACHEA	HYALINOSIS	3	3	3	2
	INFLAMMATION, SUBACUTE	0	0	0	1
	LUMPHOCYTIC INFILTRATE	0	2	0	0
URINARY BLADDER	COAGULUM, LUMEN	0	0	1	0
UTERUS	DILATION	1	1		
VERTEBRA	NONE				

Note: Hematology pathology findings are displayed by treatment group for the interim (**A**) and main (**B**) studies.
***Significantly different from control, p<0.05 (Mann-Whitney U Test)**

Analysis and Conclusion

There were no mortalities observed over the interim and main study periods, with all the animals, in all treatment groups, surviving to the scheduled study termination. Additionally, no abnormal clinical observations were noted for any of the animals. All animals in the NCL49-2 treatment groups gained weight over the study period, and no significant differences in body weight change compared to control were noted for any of the measurement periods (Table 14). Statistically significant differences in organ weights identified between the control NCL48-2 and NCL49-2 treated animals were not considered biological significant and were likely due to the small sample size (Table 15 A and B). Likewise, statistically significant differences in clinical chemistry and hematology parameters

were also likely due to small sample size, and were not indicative of a pattern of toxicity (Table 16 and 17). Though not considered biologically significant, the consistant finding of increased total protein and albumin in the NCL49-2 treated female animals, in both the interim and main study, was noteworthy. Additionally, the consistant finding of decreased alkaline phosphatase values in NCL49-2 treated animals, in both sexes in the interim and main study groups was curious, and may indicate assay interference by ceramide or increased stabilization of membrane bound alkaline phosphatase by ceramide. In support of a ceramide interaction with alkaline phosphatatse, ceramide has been shown to directly bind alkaline phosphates *in vitro* (Lingwood and Ballantyne, 2006). Gross pathology and histopathology lesions were typical of background, spontaneous findings in this stock of rat and not considered clinically significant (Table 18 and 19).

In conclusion, under these study conditions, at the doses administered, NCL48-2 and NCL49-2 were negative for all signs of systemic toxicity . Future studies will likely necessitate the use of a different animal model in order to access safety at higher, more clinically relevant, doses.

Contributors

Nanotechnology Characterization Laboratory Staff:

Scott E. McNeil, Ph.D., Director
Anil K. Patri, Ph.D., Senior Scientist
Stephan T. Stern, Ph.D., Scientist
Marina Dobrovolskaia, Ph.D., Scientist
Jiwen Zheng, Ph.D., Scientist
Jeffrey Clogston, Ph.D., Scientist
Banu S. Zolnik, Ph.D., Postdoctoral Fellow
Chris McLeland, Senior Research Associate
Timothy M. Potter, Research Associate
Barry W. Neun, Research Assistant
Sarah Skoczen, M.S., Research Assistant

Abbreviations

ABN Abnormal Plasma Standard
ADME Absorption Distribution Metabolism and Excretion
AFFF Asymmetrical Field Flow Fractionation
AFM Atomic Force Microscopy
APTT Activated Partial Thromboplastin Time
AUC Area Under the Curve
CFU-GM Colony Forming Units-Granulocyte Macrophage
CV Coefficient of Variation
CVF Cobra Venom Factor
DLS Dynamic Light Scattering
DMSO Dimethylsulfoxide
EDX Energy Dispersive X-ray spectroscopy
EU Endotoxin Unit
FBS Fetal Bovine Serum
GTA General Toxicity Assay
HEP-G2 Human Hepatocarcinoma Cells
HPLC High Performance Liquid Chromatography
IC Inhibition Concentration
ITA Immunotoxicity Assay
kDa Kilodalton
kV KiloVolt
LAL Limulus Activation Lysate
LC Lethal Concentration
LDH Lactate Dehydrogenase
LLC-PK1 Porcine Renal Proximal Tubule Cells
LPS Lipopolysaccharide
mg Milligram
mL Milliliter
mm Millimeter
MTT 3-(4,5-dimethyl-2-thiazolyl)-2,5-diphenyl-2H-tetrazolium bromide
N Normal plasma standard
NCI National Cancer Institute
NCL Nanotechnology Characterization Laboratory
ND Not Detected
NO Nitrous Oxide
PBMC Peripheral Blood Mononuclear Cells
PBS Phosphate Buffered Saline
PdI Polydispersity Index
PHA-M Phytohemaglutinin-M
PT Prothrombin Time
RCV Random Coeficient of Variation
ROS Reactive Oxygen Species
RPMI Roswell Park Memorial Institute
SAIC Science Applications International Corporation
SEC Size Exclusion Chromatography
STE Sterility
Unt Untreated

UV-Vis Ultra Violet- Visible
v/v volume/volume
w/w weight/weight

References

Duncan, R. (1999). Polymer conjugates for tumor targeting and intracytoplasmic delivery. The EPR effect as a common gateway Pharm. Sci. Technol. Today **2**, 441-49.

Hinderling, P.H.. Red blood cells: a neglected compartment in pharmacokinetics and pharmacodynamics. Pharmacol Rev **49**: 279-95 (1997).

Jones B.E., Lo C.R., Srinivasan A., Valentino K.L., Czaja M.J. (1999). Ceramide induces caspase-independent apoptosis in rat hepatocytes sensitized by inhibition of RNA synthesis. *Hepatology* **30**, 215-22.

Lingwood, D. and Ballantyne, J.S. (2006). Alkaline phosphatase-immunoglobulin conjugate binds to lipids *in vitro*, independent of antibody selectivity. *J Immunol Methods.* **311**:174-7.

Mehta S, Blackinton D, Omar I, Kouttab N, Myrick D, Klostergaard J, Wanebo H. (2000) Combined cytotoxic action of paclitaxel and ceramide against the human Tu138 head and neck squamous carcinoma cell line. *Cancer Chemother Pharmacol* **46**, 85-92.

Pass, D. and Freeth, G. (1993). The rat. *ANZCCART* **6**, 1993.

Padron, J.M. (2006), Sphingolipids in anticancer therapy. *Curr Med Chem* **13**, 755-70.

Shabbits, J.A. and Mayer, L.D. (2003). Intracellular delivery of ceramide lipids via liposomes enhances apoptosis *in vitro*. *Biochim. Biophys. Acta* **1612**: 98-106.

Stover, T. and Kester, M. (2003). Liposomal delivery enhances short-chain ceramide-induced apoptosis of breast cancer cells. *J Pharmacol Exp Ther*. **2**, 468-75.

Stover TC, Sharma A, Robertson GP, Kester M. (2005) Systemic delivery of liposomal short-chain ceramide limits solid tumor growth in murine models of breast adenocarcinoma. *Clin Cancer Res* **11**, 3465-74.